Aspects of finite temperature corrections in string theory

Calo, Vincenzo

Queen Mary University of London
Centre for Research in String Theory
Mile End Road
E1 4NS London

PhD Thesis

Aspects of Finite Temperature Corrections in String Theory

Vincenzo Calò

December 21, 2010

Advisor Prof. Steven Thomas

To my parents
Who have taught me to love

Abstract

In this thesis some aspects of temperature corrections in string theory are analyzed: in particular, we study the thermal contributions to the 4 dimensional effective potential arising from string theory compactifications.

String theory predicts that the spacetime has more than 4 dimensions; in particular, supersymmetric string theories are consistent only if the spacetime has 10 dimensions, 1 time plus 9 space directions. In order to describe the physics of our Universe with string theory we make 6 spatial directions very small, namely, we curl them into a 6-dimensional space. The resulting 4-dimensional theory depends on a large number of parameters which are massless scalar fields called moduli. The different values that the moduli can take represent both the possible deformations of the 6-dimensional compact space and the values of the coupling constants and masses in the 4-dimensional spacetime. Allowing them to have arbitrary values leads to a lack of predictability of various 4D physical quantities, to a huge vacuum degeneracy and to unobserved long range fifth forces.

In the thesis we review some methods established in the literature in order to fix the moduli values and hence to fix a particular geometry and we investigate how the inclusion of temperature corrections alter their values and affect the geometry of the compact space. The analysis seems to suggest that at least in the specific compactification scenarios considered in this thesis, temperature corrections do no alter substantially the zero temperature results.

In the final part of this work, we analyze instead an example in which the inclusion of temperature corrections alters dramatically the picture at zero temperature. In particular, we study an unstable system constituted by a pair of Dirichlet (D) and anti-D brane that, although being unstable at zero temperature, it can become stable once finite temperature corrections are switched on.

Declaration

This dissertation is the result of my own work and no part of it has previously been submitted for a degree or other qualification at this or any other university. Much of the original research presented in this thesis has appeared in the following publications by the author together with L. Anguelova, M. Cicoli and S. Thomas.

- L. Anguelova and V. Calò, *O'KKLT at Finite Temperature*, *Nucl. Phys.* **B801** (2008) 45–69 [0708.4159].
- L. Anguelova and V. Calò, *Finite Temperature Behaviour of O'KKLT Model*, *Fortsch. Phys.* **56** (2008) 901–907 [0804.0770].
- L. Anguelova, V. Calò and M. Cicoli, *LARGE Volume String Compactifications at Finite Temperature*, *JCAP* **10** (2009) 025 [0904.0051].
- V. Calò and S. Thomas, *Phase Transitions in Separated D_{p-1} and anti-D_{p-1} Branes at Finite Temperature*, *JHEP* **06** (2008) 093 [0802.2453].

These papers are referenced [1–4] in the bibliography.

Additionally during the course of the preparation of this thesis, I published the following other articles together with G. Tallarita and S. Thomas the results of which are not included in this thesis.

- V. Calò, G. Tallarita and S. Thomas, *Non Abelian Tachyon Kinks*, *JHEP* **08** (2009) 094 [0904.0601].
- V. Calò, G. Tallarita and S. Thomas, *Dirac-Born-Infeld actions and Tachyon Monopoles*, *Phys. Rev.* **D81** (2010) 086007 [0908.3379].
- V. Calò, G. Tallarita and S. Thomas, *Non Abelian Geometrical Tachyon*, 1003.6063.

Contents

List of Tables

List of Figures

1 Foreword

We live in a very cold Universe. Away from stars and galaxies, the average temperature of the radiation has a thermal black body spectrum with a temperature of about 2.7 degrees Kelvin above the absolute zero temperature. Called the cosmic microwave background (CMB), this relict radiation released by the expansion and cooling of the early Universe is constant in all directions to within 1 part in 100,000. This radiation was emitted by the hot plasma that filled the Universe a mere 380,000 years after the big bang, which took place an estimated 13.7 billion years ago.

In fact, one of the profound observations of the 20th century is that the Universe is expanding. This expansion implies the Universe was smaller, denser and hotter in the distant past. When the visible Universe was one hundred millionth its present size, its temperature was 273 million degrees above absolute zero and the density of matter as comparable to the density of air at the Earth's surface. It seems natural then to address the issue of temperature corrections in every model, scenario or theory that attempts to describe the physics of the early Universe.

In this thesis, we do so by analyzing the consequences of the inclusion of temperature effects in two different aspects of string theory: moduli stabilization and tachyon condensation.

String theory is one of the most studied candidates as a theory of quantum gravity and of high-energy physics. It should be viewed, therefore, as a natural framework to study the physics of the early Universe. Furthermore, it could represent for cosmology the underlying theory it needs to approach the basic questions such as the initial singularity, (if there was any), the origin of inflation and of the density perturbations in the CMB. It has an extremely rich structure both from the mathematical, and the theoretical point of view. In fact, the attempt to try to understand it in depth, has led to many profound results, like the discovery of mirror symmetry [5, 6] an exact microscopic calculation of the Bekenstein-Hawking black hole entropy [7], a smooth description of space-time topology change [8–11] and the AdS/CFT correspondence [12]. Despite these successes, it has to be said that, at present, the theory still lacks any experimental evidence and a decisive low-energy test of string theory does not

seem possible. However, there is hope in the community, as the forthcoming years are expected to be characterised by a new set of experimental data coming from two crucial experiments for fundamental physics: the PLANCK satellite, which was launched by the European Space Agency in May 2009, and the Large Hadron Collider at CERN in Geneva which started operation in September 2009.

The work presented in this thesis is not at all exhaustive and much more work needs to be done to understand the inclusion of temperature corrections in string theory models. Different approaches could have also been taken or will probably be taken in the future once that more light is shed on the theory.[1]

I have tried to make it as much as self-contained as possible, however, I have decided not to include too much review material because that would go beyond the scope of the present work. The review material which I have consulted the most is [13, 14] for flux compactification, [15, 16] for the large volume scenarios and finally [17] for tachyon condensation.

As for the references, I have tried to cite all the relevant works where appropriate, but it is inevitable that there are omissions: apologises in advance to the authors of those papers. The work contained in this thesis is based on the papers [1] (chapter 2 and 3), [3] (chapter 2 and 4) and [4] (chapter 5). Once again, I would like to express my gratitude to my collaborators: Lilia Anguelova, Michele Cicoli and Steven Thomas.

Vincenzo Calò
December 21, 2010

[1] For example, in the case of moduli stabilization, one would like to understand corrections, that are due to taking into account higher derivative terms appearing in effective supergravity actions or even better, the case of thermal corrections in a moduli stabilization setup that requires going beyond the supergravity approximation so that one has to use string theory at finite temperature.

2 Moduli stabilization with thermal corrections

2.1 Introduction

Moduli stabilization is a major problem on the road to relating string theory compactifications with phenomenology. It stems from the fact that the internal geometry of the compactified extra-dimensions of higher dimensional theories[1] can have various deformations, which manifest themselves as scalar fields with effective gravitational coupling but without a potential energy in the four extended dimensions. These scalar fields are called *moduli*. Since the four dimensional (4D) effective action depends on those moduli, allowing them to have arbitrary values leads to a lack of predictability of various 4D *coupling constants* and *masses*, to a huge vacuum degeneracy and to unobserved long range fifth forces[2].

The problem of moduli stabilization is hence intertwined with the existence of *extra dimensions*, an old idea that dates back to the works of Kaluza and Klein [20,21] at the beginning of the last century. Their generalization of Einstein's General Relativity to five dimensions is a good starting point to understand the problem of moduli stabilization. To this purpose, consider the Einstein-Hilbert action in five dimensions:

$$S = \frac{1}{2k_0^2} \int d^5x \sqrt{-\det g_5}\ \mathbf{R}_5\ . \tag{2.1}$$

Now wrap the fifth dimension on a circle of radius R. The five dimensional metric g_{mn}, with $m = 0, \dots 4$, regarded as a field in four dimensions, has new non-metric degrees of freedoms: in particular, it has four components labeled as $g_{\mu 4}$ with $\mu = 0, \dots 3$, which transform as a vector field and one additional degree of freedom g_{44} which parametrize the radius of the extra-dimensional circle. This can be shown explicitly

[1] Theories with more than 3 spatial directions. Superstring theories have 9 spatial extended directions, 6 of which must be compactified.

[2] For a review on fifth force phenomenology see [18], for more recent experimental bounds see [19].

by writing the five dimensional metric g_{mn} in the following way

$$ds^2 \;=\; g_{mn}dx^m dx^n = g_{\mu\nu}dx^\mu dx^\nu + e^{2\sigma}\left(dx^4 + A_\mu dx^\mu\right)^2 \tag{2.2}$$

where we defined $g_{44} = e^{2\sigma}$. In four dimensions the previous action becomes

$$S = \frac{\pi R}{k_0^2}\int d^4x\sqrt{-\det g_4}\; e^{\sigma}\left(\mathbf{R}_4 - \frac{1}{4}e^{2\sigma}F_{\mu\nu}F^{\mu\nu}\right). \tag{2.3}$$

This theoretical result is of fundamental importance since it shows that the unification of the fundamental forces, in this case gravitation and electromagnetism, may be related to the existence of extra dimensions of spacetime. However, the problem of moduli stabilization is already present at this level: in order to disentangle the graviton kinetic term from the scalar field σ, we should perform a Weyl rescaling. If we set $g_{\mu\nu} = e^{-\frac{1}{2}(\sigma-\sigma_0)}g_{\star\mu\nu}$ and define $\tilde{\sigma} = \sigma - \sigma_0$ which has zero vacuum expectation value, by expanding around σ_0 the previous action becomes

$$S \sim \frac{\pi R e^{\sigma_0}}{k_0^2}\int d^4x\sqrt{-\det g_4}\;\left(\mathbf{R}_{\star 4} - \frac{3}{2}\partial_\mu\tilde{\sigma}\partial^{\star\mu}\tilde{\sigma} - \frac{1}{4}e^{8\sigma_0}F_{\mu\nu}F^{\star\mu\nu}\right) \tag{2.4}$$

where $\star$ have been inserted to remind that indices are raised with $g^{\star\mu\nu}$, for example $\partial^{\star\mu} = g^{\star\mu\nu}\partial_\nu$. The Weyl transformation has given a kinetic term to the field $\tilde{\sigma}$ which obeys the equation of motion of a scalar field without potential energy, hence the field $\tilde{\sigma}$ is a modulus of the theory. The invariant radius $\rho = Re^{\sigma_0}$ depends on the vacuum expectation value σ_0 and since there is no potential energy, the field equations do not determine the radius of the compact dimensions, namely, there is no preferred value of σ_0. Notice that also the U(1) gauge coupling depends on σ_0 and again since there is no preferred value for it, there is no preferred value for the gauge coupling and the theory lacks of predictability. The different values of σ_0 label degenerate configurations or states in the quantum theory. *Moduli stabilization* consists therefore in the process of finding a potential for the moduli of the theory and thus selecting a preferred state in the quantum theory as a minimum of the potential.

In superstring theory, the last decade has seen a lot of progress towards the resolution of this problem. A major ingredient in these developments was the realization that non-zero *background fluxes* induce a potential for some of the moduli [22–24]. Roughly speaking, background fluxes are gauge fields in higher dimensional theories which depend on the coordinates of the compactified internal space. At this point, another simple example can be useful to understand better the principles of moduli

stabilization with fluxes. The following one is based on the model by Freund and Rubin [25]. Consider a six dimensional Einstein-Maxwell theory: the Einstein and the Maxwell field equations admit as a solution a factorized spacetime $\mathcal{M}^4 \times \mathcal{R}^2$ where $\mathcal{R}^2$ is a two-dimensional Riemann surface with a non-vanishing 2-form on it

$$F_{mn} \sim f \epsilon_{mn} \ , \tag{2.5}$$

where f has the dimension of a mass squared and $m, n = 4, 5$. We can write the Einstein-Hilbert action as

$$S = \int d^6x \sqrt{-g_6} \left(\mathbf{R}_6 - F_{mn} F^{mn} \right) , \tag{2.6}$$

and reduce it to four dimensions by taking $\mathcal{R}^2$ to be, for example, a two-dimensional sphere of radius R

$$ds^2 = g_{\mu\nu} dx^\mu dx^\nu + R^2(x) g_{mn}(y) dy^m dy^n \ , \tag{2.7}$$

where g_{mn} is the metric on a two-sphere of unit radius. Reducing the previous action to 4D we find that $R^2(x)$ multiplies the Ricci tensor $\mathbf{R}_4$

$$S \sim \int d^4x \sqrt{-g_4} \left(R^2(x) \mathbf{R}_4 + 2 - R^2(x) \int_{S^2} F_{mn} F^{mn} dy^2 \right) , \tag{2.8}$$

We now turn N units of fluxes on the internal sphere S^2,

$$\int_{S^2} F_{mn} dy^m \wedge dy^n = N \tag{2.9}$$

and perform a Weyl rescaling to untangle the graviton kinetic term from the field $R(x)$. This can be achieved by setting $g_{\mu\nu} = \frac{1}{R^2} g_{\star \mu\nu}$ to obtain

$$S \sim \int d^4x \sqrt{-g_{\star 4}} \left(\mathbf{R}_{\star 4} - 6 g_\star^{\mu\nu} \partial_\mu R \partial_\nu R + \frac{2}{R^4} - \frac{N^2}{R^6} \right) \ . \tag{2.10}$$

In this case there is a potential for the radius of the compact space that is given by

$$V(R) \sim \frac{N^2}{R^6} - \frac{1}{R^4} \tag{2.11}$$

and it admits a minimum for $R \sim N$. The modulus R is therefore stabilized. In the previous example, the minimum of the potential is the result of two different sources:

one comes from the flux term and scales as N^2/R^6 and the other one comes from the curvature $\mathcal{R}_2$ which being positive makes a negative contribution, $-1/R^4$, to the potential.

Both the internal geometry and the background field strengths contribute to the vacuum energy of the system. In general, we shall see that they are only the leading contributions in a systematic expansion of the quantum vacuum energy, to be supplemented by both perturbative and nonperturbative contributions. All these effects can be summarized in a 4D effective potential, defined as the total vacuum energy, considered as a function of the moduli fields. This effective potential is defined in precise analogy to the effective potentials of conventional quantum field theory and can be used in a very similar way, namely, to determine the possible vacua of the theory, as the local minima of the effective potential.

Before we conclude this section, we shall describe the approach that we shall use to compute the effective potential in superstring theory compactifications. At energies low compared to the string tension, denoted as α' (the fundamental string scale), superstring theory is well described by 10D supergravity, a supersymmetric extension of general relativity, coupled to Yang-Mills theory. The dimensional reduction of classical 10D supergravity (supplemented by branes and fluxes) to 4D yields a tree approximation to the effective potential as a function of the moduli fields. In most of the cases that we shall study later, this classical potential will be supplemented with quantum corrections which are computed in the string coupling g_s or string tension α' expansions, or with known non-pertubative results.

In addition, the new results presented in this thesis are about the computation, beside perturbative and non-pertubative corrections, of finite temperature corrections to the 4D effective potential.

The rest of this chapter is organized as follows. In Section 2.2 we present the main results of type IIB flux compactification emphasizing the resulting four dimensional effective description and in Section 2.3, we recall the general form of the effective potential at finite temperature and discuss in detail the issue of thermal equilibrium in an expanding Universe and the cosmological moduli problem.

2.2 Type IIB flux vacua

We now start to add some quantitative material to the previous discussion. This is not going to be a fully-fledged review of flux compactification and we remind the reader of some excellent reviews on the subject [13, 14].

The most studied case of flux compactification involves type IIB vacua. They are better understood, compared to the type IIA ones, because there is a class of solutions in which the internal space is conformally Calabi-Yau and the back-reaction of the fluxes on the internal geometry is entirely encoded into warp factors[3] [13]. More specifically, we will be interested in type IIB Calabi-Yau orientifold compactifications with background fluxes, which preserve $\mathcal{N} = 1$ supersymmetry in 4D. The bosonic part of the IIB 10D supergravity action in the Einstein frame is given by ($M = 0, \ldots, 9$)

$$\begin{aligned} S_{IIB} &= \frac{1}{k_{10}^2}\int d^{10}x(-G_E)^{1/2}\left\{R - \frac{\partial_M S\partial^M \bar{S}}{2(\mathrm{Re}\ S)^2} - \frac{G_3\cdot\bar{G}_3}{12\mathrm{Re}S} - \frac{\tilde{F}_5^2}{4\cdot 5!}\right\} \\ &\quad + \frac{1}{8ik_{10}^2}\int \frac{C_4\wedge G_3\wedge\bar{G}_3}{\mathrm{Re}S} + S_{\mathrm{local}} \end{aligned} \tag{2.12}$$

The theory has Neveu-Scharwz (NS) field strengths H_3 with potential B_2 and Ramond-Ramond (RR) strengths $F_{1,3,5}$ with corresponding potential $C_{0,2,4}$. We have defined the combined RR-NS three-flux

$$G_3 = F_3 + iSH_3\ , \tag{2.13}$$

where S is the axio-dilaton defined as

$$S = iC_0 + e^{-\phi} \tag{2.14}$$

and

$$\tilde{F}_5 = F_5 - \frac{1}{2}C_2\wedge H_3 + \frac{1}{2}B_2\wedge F_3\ . \tag{2.15}$$

The 5-form $\tilde{F}_5$ is self-dual and one must impose the constraint[4] $\tilde{F}_5 = \star\tilde{F}_5$ by hand when solving the equations of motion. Finally, S_{local} in (2.12) allows for the possibility that we include the action of any localized sources in our background; in string theory possible sources are D-branes and O-planes.

We are interested in the vacua of the action (2.12) that lead to maximally supersymmetric four-dimensional spacetimes. These have Poincaré, SO(1,4) and SO(2,3) invariance and are called respectively Minkowski, anti-de Sitter space (AdS) or de Sitter (dS) spacetimes. The most general ten-dimensional metric consistent with

[3] As opposed to considering internal spaces manifolds with $SU(3)\times SU(3)$ structure.

[4] We will use the standard convention for the Hodge operator $\star$: for a k-form η in a n-dimensional spacetime, $(\star\eta)_{i_1,i_2,\ldots,i_{n-k}} = \frac{1}{k!}\sqrt{|\mathrm{det}g|}\epsilon_{j_1,\ldots,j_k,i_1\ldots,i_{n-k}}\eta^{j_1,\ldots,j_k}$ where ϵ is the Levi-Civita tensor.

four-dimensional maximal symmetry is

$$ds^2 = e^{2A(y)} g_{\mu\nu} dx^\mu dx^\nu + e^{-2A(y)} \tilde{g}_{mn} dy^m dy^n \tag{2.16}$$

with $\mu, \nu = 0, \ldots, 3$ and $m, n = 4, \ldots 9$ and we have allowed for the possibility of a warp factor $A(y)$. In order not to spoil the Lorentz invariance of the theory after compactification, we are allowed to turn on only those fluxes which have either no components or four components along space-time. Therefore the flux G_3 can only be internal, *i.e.*,

$$G_3 \equiv \frac{1}{3!} G_{MNP}\ dx^M \wedge dx^N \wedge dx^P = \frac{1}{3!} G_{mnp}\ dy^m \wedge dy^n \wedge dy^p \tag{2.17}$$

whereas F_5 is allowed to have also non-compact components: Poincarè invariance and the Bianchi identity allow in fact a five-form flux of the form

$$\tilde{F}_5 = (1 + \star_{10})\, \partial_m \alpha(y) \left\{ dy^m \wedge dx^0 \wedge dx^1 \wedge dx^2 \wedge dx^3 \right\} \ . \tag{2.18}$$

Einstein's equation, trace reversed, is

$$R_{MN} = {\kappa_{10}}^2 \left(T_{MN} - \frac{1}{8} g_{MN} T \right) , \tag{2.19}$$

where $T_{MN} = T^{\text{sugra}}_{MN} + T^{\text{loc}}_{MN}$ is the total stress tensor of the supergravity fields and the localized objects. The noncompact components take the form

$$R_{\mu\nu} = -g_{\mu\nu} \left(\frac{G_{mnp} \bar{G}^{mnp}}{48\, \text{Im}\, \tau} + \frac{e^{-8A}}{4} \partial_m \alpha \partial^m \alpha \right) + {\kappa_{10}}^2 \left(T^{\text{loc}}_{\mu\nu} - \frac{1}{8} g_{\mu\nu} T^{\text{loc}} \right) . \tag{2.20}$$

From the metric ansatz (2.16), one computes the Ricci components

$$R_{\mu\nu} = -\eta_{\mu\nu} e^{4A} \tilde{\nabla}^2 A = -\frac{1}{4} \eta_{\mu\nu} \left(\tilde{\nabla}^2 e^{4A} - e^{-4A} \partial_m e^{4A} \partial^{\tilde{m}} e^{4A} \right) . \tag{2.21}$$

(A tilde denotes use of the metric $\tilde{g}_{mn}$.) Using this and tracing (2.20) gives

$$\tilde{\nabla}^2 e^{4A} = e^{2A} \frac{G_{mnp} \bar{G}^{mnp}}{12\, \text{Im}\, \tau} + e^{-6A} \left[\partial_m \alpha \partial^m \alpha + \partial_m e^{4A} \partial^m e^{4A} \right] + \frac{{\kappa_{10}}^2}{2} e^{2A} (T^m_m - T^\mu_\mu)^{\text{loc}} \ . \tag{2.22}$$

These equations serve as stringent constraints on flux/brane configurations that can lead to warped solutions on *compact* manifolds. To see this, note that the integrals of their left sides over a compact manifold $\mathcal{M}_6$ vanish, whereas the flux and warp terms

on the right-hand side are positive definite. Thus, in the absence of localized sources there is a no-go theorem [26]: the fluxes must vanish and the warp factor must be constant. For a warped solution the stress terms on the RHS must be negative, which can only be true under certain circumstances.

For example, consider a p-brane wrapped on a $(p-3)$-cycle Σ of the manifold $\mathcal{M}_6$. One has [24]

$$(T_m^m - T_\mu^\mu)^{\rm loc} = (7-p)T_p\delta(\Sigma) \ . \tag{2.23}$$

Eq. (2.23) tells us that for $p < 7$, in order to have the required negative stress on the RHS of the constraint (2.22), the compactification must involve *negative* tension objects. String theory does have such objects, and so evades the no-go theorem. O3 planes are a simple example.

We have been discussing constraints from the integrated Einstein equation. The Bianchi identity/equations of motion for the 5-form flux is [24]

$$d\tilde{F}_{(5)} = H_{(3)} \wedge F_{(3)} + 2{\kappa_{10}}^2 T_3 \rho_3^{\rm loc} \tag{2.24}$$

where $\rho_3^{\rm loc}$ is the D3 charge density form from localized sources; this includes the contributions of the D7-branes or O3 planes, and also of mobile D3-branes that may be present. The integrated Bianchi identity

$$\frac{1}{2{\kappa_{10}}^2 T_3}\int_{\mathcal{M}_6} H_{(3)} \wedge F_{(3)} \ + \ Q_3^{\rm loc} = 0 \tag{2.25}$$

states that the total D3 charge from supergravity backgrounds and localized sources vanishes.

With general negative tension sources, the constraints from the integrated field equations appear to be rather weak. However, in the special case that

$$\frac{1}{4}(T_m^m - T_\mu^\mu)^{\rm loc} \geq T_3\rho_3^{\rm loc} \tag{2.26}$$

for all localized sources, the global constraints determine the form of the solution completely. In fact, the inequality (2.26) holds for all of the localized sources considered in this thesis. For D3-branes and O3 planes, whose integrated ρ_3 is respectively $+1$ and $-\frac{1}{4}$, the stress tensor is

$$T_0^0 = T_1^1 = T_2^2 = T_3^3 = -T_3\rho_3 \ , \quad T_m^m = 0 \ , \tag{2.27}$$

and so the inequality is actually saturated. Anti-D3-branes satisfy the inequality but

do not saturate it. D5-branes wrapped on collapsed cycles also satisfy the inequality, as their tension comes entirely from their induced D3 charge. D7-branes saturates the inequality too [24]. There are objects that do violate the inequality (2.26). O5-planes make a negative contribution to the LHS and zero contribution to the RHS. Anti-O3 planes make a negative contribution to the LHS and a positive contribution to the RHS.

In terms of the potential α the Bianchi identity (2.24) becomes

$$\tilde{\nabla}^2\alpha = ie^{2A}\frac{G_{mnp}(*_6\bar{G}^{mnp})}{12\,\mathrm{Im}\,\tau} + 2e^{-6A}\partial_m\alpha\partial^m e^{4A} + 2{\kappa_{10}}^2 e^{2A}T_3\rho_3^{\mathrm{loc}}\ , \tag{2.28}$$

where $*_6$ is the dual in the transverse directions. Subtracting this from the Einstein equation constraint (2.22) gives

$$\tilde{\nabla}^2(e^{4A}-\alpha) = \frac{e^{2A}}{6\,\mathrm{Im}\,\tau}\left|iG_{(3)}-*_6G_{(3)}\right|^2 + e^{-6A}|\partial(e^{4A}-\alpha)|^2 + 2{\kappa_{10}}^2e^{2A}\left[\frac{1}{4}(T_m^m-T_\mu^\mu)^{\mathrm{loc}}-T_3\rho_3^{\mathrm{loc}}\right]. \tag{2.29}$$

The LHS integrates to zero, while under the assumption (2.26) the RHS is nonnegative. Thus, if the inequality (2.26) holds, then

- The 3-form field strength is imaginary self-dual,

$$*_6G_{(3)} = iG_{(3)}\ . \tag{2.30}$$

- The warp-factor and 4-form potential are related,

$$e^{4A} = \alpha\ . \tag{2.31}$$

- The inequality (2.26) is actually saturated.

In summary, assuming that the localized sources satisfy (2.26), the necessary and sufficient conditions for a solution are closed 3-form fluxes $F_{(3)}$ and $H_{(3)}$ such that $G_{(3)}$ is imaginary self-dual, and vanishing total D3 charge.

The simplest examples of such solutions are perturbative IIB orientifolds. At leading order, the metric on the internal space is conformally *Calabi-Yau*, (CY) namely is given by $e^{-2A}g_{\mathrm{CY}}$. For this reason, these flux vacua are often described as Calabi-Yau compactifications with fluxes.

2.2.1 4D effective description

The effective description in 4D is given by a $\mathcal{N}=1$ supergravity characterised by a Kähler potential K, a superpotential W and a gauge kinetic function f_{ab}, where the indices a, b run over the various vector multiplets. In particular, the scalar potential of this theory has the standard form:

$$V = e^{K/M_P^2}\left(K^{i\bar{j}} D_i W D_{\bar{j}} \bar{W} - 3\frac{|W|^2}{M_P^2}\right), \tag{2.32}$$

where i, j run over all moduli of the compactification. Generically, the latter consist of the axio-dilaton (2.14), $h_{1,1}$ Kähler (T-moduli) and $h_{2,1}$ complex structure moduli (U-moduli). The tree level Kähler potential has the following form:

$$\frac{K_{tree}}{M_P^2} = -\ln\left(S+\bar{S}\right) - 2\ln\mathcal{V} - \ln\left(-i\int_{CY}\Omega\wedge\bar{\Omega}\right), \tag{2.33}$$

where $\mathcal{V}$ is the Einstein frame CY volume, in units of the string length $l_s = 2\pi\sqrt{\alpha'}$, and Ω is the CY holomorphic (3,0)-form. Note that the the T-moduli enter K_{tree} only through $\mathcal{V}$ and the U-moduli only through Ω. For later purposes, it will be useful to recall a couple of relations regarding the Kähler moduli. Expanding the Kähler form $J = \sum_{i=1}^{h_{1,1}} t^i D_i$ in a basis $\{D_i\}$ of $H^{1,1}(CY,\mathbb{Z})$ and considering orientifold projections such that[5] $h^-_{1,1} = 0 \Rightarrow h^+_{1,1} = h_{1,1}$, we obtain:

$$\mathcal{V} = \frac{1}{6}\int_{CY} J\wedge J\wedge J = \frac{1}{6}k_{ijk}t^i t^j t^k\,, \tag{2.34}$$

where k_{ijk} are related to the triple intersection numbers of the CY and the t^i are 2-cycle volumes. The volumes of the Poincarè dual 4-cycles are given by:

$$\tau_i = \frac{\partial\mathcal{V}}{\partial t^i} = \frac{1}{2}\int_{CY} D_i\wedge J\wedge J = \frac{1}{2}k_{ijk}t^j t^k\,. \tag{2.35}$$

Finally, the scalar components of the chiral superfields, corresponding to the Kähler moduli, that enter the 4D effective action are $T_i = \tau_i + ib_i$, where the axions b_i are the components of the RR 4-form C_4 along the 4-cycle Poincarè dual to D_i. Obviously,

[5]The cohomology groups $H_{p,q}$ split into two eigenspaces under the orientifold projection, $H_{p,q} = H^+_{p,q}\oplus H^-_{p,q}$. Considering orientifold projections such that $h^-_{1,1}=0$ projects out all the two-form moduli arising from the 10-dimensional reduction of $\mathcal{N}=1$ supergravity to the 4-dimensional $\mathcal{N}=2$ supergravity.

from (2.34) and (2.35) one can express $\mathcal{V}$ in (2.33) as a function of $\tau_i = \frac{1}{2}(T_i + \overline{T}_i)$.

Now, turning on background fluxes $G_3 = F_3 + iSH_3$, generates an effective superpotential of the form [22][6]:

$$W_{tree} \sim \int_{CY} G_3 \wedge \Omega. \tag{2.36}$$

As a result, one can stabilise the axio-dilaton S and the U-moduli. However, the Kähler moduli T_i do not enter W_{tree} and therefore remain massless at leading semi-classical level.

One can obtain an effective description for these fields by integrating out S and U.[7] Then the superpotential is constant, $W = \langle W_{tree} \rangle \equiv W_0$, and the Kähler potential reads $K = K_{cs} - \ln(2/g_s) + K_0$ with

$$K_0 = -2 \ln \mathcal{V} \qquad \text{and} \qquad e^{-K_{cs}} = \left\langle -i \int_{CY} \Omega \wedge \bar{\Omega} \right\rangle . \tag{2.37}$$

Before concluding this subsection, let us make a couple of remarks. First, note that the background flux G_3 may or may not break the remaining 4D $\mathcal{N} = 1$ supersymmetry, depending on whether or not $D_\alpha W = \partial_\alpha W + W \partial_\alpha K$ vanishes at the minimum of the resulting scalar potential. Second, the Kähler potential K_0 satisfies the no-scale property $K_0^{i\bar{j}} \partial_i K_0 \partial_{\bar{j}} K_0 = 3$, which implies that the scalar potential for the Kähler moduli vanishes in accord with the statement above that the fluxes do not stabilise those moduli.

2.2.2 Leading order corrections

As we recalled in the previous subsection, at leading classical order the scalar potential for the T-moduli vanishes. So, unlike the situation for the S and U-moduli, in order to stabilise T_i one has to consider the leading order corrections to the tree level action. The first such corrections to be studied were non-perturbative contributions to W. Recall that there is a non-renormalisation theorem forbidding W to be corrected perturbatively. On the other hand, the Kähler potential K does receive perturbative corrections both in α' and in g_s. Therefore, non-perturbative effects are subleading in K and we shall neglect them in the following. Let us now review briefly all these kinds of corrections.

[6] At this point, we neglect the effect of warping, generated by non-zero background fluxes, since we will be considering CY compactifications with large internal volume.

[7] See [27–29] for more details on the consistent supersymmetric implementation of this procedure.

Non-perturbative corrections

Non-perturbative corrections to the superpotential can be due to Euclidean D3 brane (ED3) instantons wrapping 4-cycles in the extra dimensions, or to gaugino condensation in the supersymmetric gauge theories located on D7 branes that also wrap internal 4-cycles. The superpotential that both kinds of effects generate is of the form:[8]

$$W = \frac{M_P^3}{\sqrt{4\pi}}\left(W_0 + \sum_i A_i e^{-a_i T_i}\right), \tag{2.38}$$

where the coefficients A_i correspond to threshold effects and, in principle, can depend on U and D3 position moduli, but not on T_i. The constants a_i are given by $a_i = 2\pi$ for ED3 branes, and by $a_i = 2\pi/N$ for gaugino condensation in an $SU(N)$ gauge theory[9]. Note that one can neglect multi-instanton effects in (2.38), as long as τ_i are stabilised such that $a_i\tau_i \gg 1$. From (2.32), the above superpotential leads to the following T_i-dependent contribution to the scalar potential (up to a numerical prefactor and powers of g_s and M_P, that we will be more precise about below):

$$\begin{aligned}\delta V_{(np)} &= e^{K_0} K_0^{j\bar{\imath}}\Big[a_j A_j\, a_i \bar{A}_i e^{-\left(a_j T_j + a_i \overline{T}_i\right)} \\ &\quad - \left(a_j A_j e^{-a_j T_j}\overline{W}\partial_{\bar{\imath}} K_0 + a_i \bar{A}_i e^{-a_i \overline{T}_i} W \partial_j K_0\right)\Big].\end{aligned} \tag{2.39}$$

α' corrections

The Kähler potential receives corrections at each order in the α' expansion. In the effective supergravity description these correspond to higher derivative terms. The leading α' contribution comes from the R^4 term and it leads to the following Kähler potential [31]:

$$\frac{K}{M_P^2} = -2\ln\left(\mathcal{V} + \frac{\xi}{2g_s^{3/2}}\right) \simeq -2\ln\mathcal{V} - \frac{\xi}{g_s^{3/2}\mathcal{V}}. \tag{2.40}$$

[8] The prefactor in (2.38) is due to careful dimensional reduction, as can be seen the Appendices of [30]. However, the authors of [30] define the Einstein metric via $g_{\mu\nu,s} = e^{(\phi-\langle\phi\rangle)/2} g_{\mu\nu,E}$, so that it coincides with the string frame metric in the physical vacuum. On the contrary, we opt for the more traditional definition $g_{\mu\nu,s} = e^{\phi/2} g_{\mu\nu,E}$, which implies no factor of g_s in the prefactor of W.

[9] The 4D gauge coupling of the $SU(N)$ Yang-Mills theory on the i-th wrapped brane satisfies

$$\frac{8\pi^2}{g_{YM^2}} = 2\pi\frac{\mathcal{M}_4}{g_s} = 2\pi\tau_i$$

.

Here ξ is given by $\xi = -\frac{\chi\zeta(3)}{2(2\pi)^3}$, where $\chi = 2\,(h_{1,1} - h_{2,1})$ is the CY Euler number, and the Riemann zeta function is $\zeta(3) \simeq 1.2$. Denoting for convenience $\hat{\xi} \equiv \xi/g_s^{3/2}$, eq. (2.40) implies to leading order the following contribution to V (again, up to a prefactor containing powers of g_s and M_P):

$$\delta V_{(\alpha')} = 3e^{K_0}\hat{\xi}\frac{\left(\hat{\xi}^2 + 7\hat{\xi}\mathcal{V} + \mathcal{V}^2\right)}{\left(\mathcal{V} - \hat{\xi}\right)\left(2\mathcal{V} + \hat{\xi}\right)^2}W_0^2 \simeq \frac{3\xi W_0^2}{4g_s^{3/2}\mathcal{V}^3}, \tag{2.41}$$

where $\mathcal{V} \gg \hat{\xi} > 1$ in order for perturbation theory to be valid.

g_s corrections

The Kähler potential receives also string loop corrections. At present, there is no explicit derivation of these corrections from string scattering amplitudes for a generic CY compactification. Nevertheless, it has been possible to conjecture their form indirectly [16, 32, 33]:

$$\delta K_{(g_s)} = \delta K_{(g_s)}^{KK} + \delta K_{(g_s)}^{W}\,, \tag{2.42}$$

where

$$\delta K_{(g_s)}^{KK} \sim \sum_{i=1}^{h_{1,1}} \frac{g_s \mathcal{C}_i^{KK}(U,\bar{U})\left(a_{il}t^l\right)}{\mathcal{V}}, \tag{2.43}$$

and

$$\delta K_{(g_s)}^{W} \sim \sum_i \frac{\mathcal{C}_i^{W}(U,\bar{U})}{(a_{il}t^l)\,\mathcal{V}}. \tag{2.44}$$

In (2.42), $\delta K_{(g_s)}^{KK}$ comes from the exchange of closed strings, carrying Kaluza-Klein momentum, between D7 and D3-branes. The expression (2.43) is valid for vanishing open string scalars and is based on the assumption that all the $h_{1,1}$ 4-cycles of the CY are wrapped by D7-branes. The other term $\delta K_{(g_s)}^{W}$ in (2.43) is due, from the closed string perspective, to the exchange of winding strings between intersecting stacks of D7-branes.

In addition, in (2.43) the linear combination $\left(a_{il}t^l\right)$ of the volumes of the basis 2-cycles is transverse to the 4-cycle wrapped by the i-th D7-brane, whereas in (2.44) it gives the 2-cycle where two D7-branes intersect. The functions $\mathcal{C}_i^{KK}(U,\bar{U})$ and $\mathcal{C}_i^{W}(U,\bar{U})$ are, in principle, unknown. However, for our purposes they can be viewed as $\mathcal{O}(1)$ constants[10] since the complex structure moduli are already stabilised at the

[10] In the $T^6/\left(\mathbb{Z}_2 \times \mathbb{Z}_2\right)$ orientifold case, where these constants can be computed explicitly [34], they turn out to be, in our conventions, of $\mathcal{O}(1)$ for natural values of the complex structure moduli:

classical level by background fluxes.

Comparing (2.43) with (2.40), we notice that $\delta K^{KK}_{(g_s)}$ is generically leading with respect to $\delta K_{(\alpha')}$ due to the presence of the linear combination $\left(a_{il}t^l\right)$ in the numerator of (2.43) and the fact that each 4-cycle volume $\tau_i = \frac{1}{2}k_{ijk}t^j t^k$ has to be fixed larger than the string scale in order to trust the effective field theory. However, in ref. [33] it was discovered that for an arbitrary CY background, the leading contribution of (2.43) to the scalar potential is vanishing, so leading to an *extended no-scale structure*. This result renders $\delta V_{(g_s)}$ generically subleading with respect to $\delta V_{(\alpha')}$ and the final formula can be expressed as(neglecting a prefactors with powers of g_s and M_P):

$$\delta V^{1-loop}_{(g_s)} = \left[\left(g_s \mathcal{C}^{KK}_i\right)^2 a_{ik}a_{ij}K^0_{k\bar{j}} - 2\delta K^W_{(g_s)}\right]\frac{W_0^2}{\mathcal{V}^2}. \tag{2.45}$$

Notice that for branes wrapped only around the basis 4-cycles the combination appearing in the first term degenerates to $a_{ik}a_{ij}K^0_{k\bar{j}} = K^0_{i\bar{i}}$. The fact that $\delta V_{(g_s)}$ is generically subleading with respect to $\delta V_{(\alpha')}$ can be easily seen by recalling the generic expression of the tree-level Kähler metric for an arbitrary CY: $K^0_{i\bar{j}} = t_i t_{\bar{j}}/(2\mathcal{V}^2) - (k_{i\bar{j}k}t^k)^{-1}/\mathcal{V} \sim 1/(\mathcal{V}t)$. Therefore the ratio between $\delta V_{(\alpha')}$ given by (2.41) (with $\xi \sim \mathcal{O}(1)$ for known CY three-folds) and the expression (2.45) for $\delta V_{(g_s)}$, scales as $\delta V_{(\alpha')}/\delta V_{(g_s)} \sim g_s^{-3/2}t \gg 1$ due to the fact that the size of each two-cycle has to be fixed at a value larger than 1 (in string units) in order to trust the effective field theory and, in addition, the string coupling has to be smaller than unity in order to be in the perturbative regime.

Effective potential at zero temperature

Combining (2.39), (2.41) and (2.45), we obtain the final form of the Kähler moduli effective scalar potential at *zero temperature*, that contains all the leading order corrections to the vanishing tree-level part (with all prefactors included):

$$\begin{aligned} V_{T=0} &= V_{tree} + \delta V_{(np)} + \delta V_{(\alpha')} + \delta V^{1-loop}_{(g_s)} = \\ &= \frac{g_s e^{K_{cs}} M_P^4}{8\pi\mathcal{V}^2}\left\{K_0^{j\bar{i}}a_j A_j\, a_i\bar{A}_i e^{-\left(a_j T_j + a_i\overline{T}_i\right)} + 4W_0\sum_i a_i A_i \tau_i \cos(a_i b_i) e^{-a_i\tau_i}\right. \\ &\quad \left. + \left[\frac{3\xi}{g_s^{3/2}} + \sum_i\left(g_s^2\left(\mathcal{C}^{KK}_i\right)^2\left(\frac{1}{2}\frac{t_i^2}{\mathcal{V}} - A^{ii}\right) - 8\frac{\mathcal{C}^W_i}{(a_{il}t^l)}\right)\right]\frac{{W_0}^2}{4\mathcal{V}}\right\}, \end{aligned} \tag{2.46}$$

$\mathrm{Re}(U) \sim \mathrm{Im}(U) \sim \mathcal{O}(1)$. Note that [34] uses conventions different from ours.

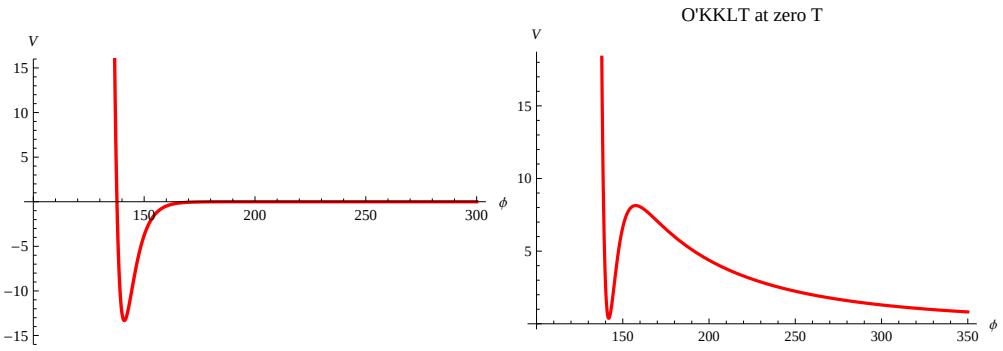

Figure 2.1: The plot shows the effective potential V at zero temperature versus the volume modulus ϕ for a typical type IIB flux compactification. On the left, the minimum is AdS. On the right, the same effective potential after the inclusion of an uplifing sector. The minimum is now metastable and describes a dS spacetime.

where $A_{ij} \equiv \frac{\partial \tau_i}{\partial t_j} = k_{ijk} t^k$.

The previous potential has at least one minimum that describes an AdS spacetime that may or may not break supersymmetry. See Figure 2.1.

Uplifiting sector

Uplifiting of the AdS minimum to the present nearly Minkowski vacuum occurs by adding to the potential a term of the form $\epsilon/\mathcal{V}^n$, where ϵ is a parameter that can be tuned to the cosmological constant and $n = 3$ for a generic compactifications and $n = 2$ for the highly warped throat geometry.

The resulting potential after uplifiting is shown in figure Figure 2.1. In the original KKLT model [35], the uplifting was obtained by adding a positive potential generated by the tension of anti-D3 branes which goes like

$$\delta V \sim \frac{T_3}{\mathcal{V}^3}. \tag{2.47}$$

Unfortunately, adding by hand anti-D3 branes breaks explicitly supersymmetry and it is problematic to describe this setup in supergravity. An improvement that does not require anti-D3 branes was proposed in [36]. There, the uplifting is achieved by having nonzero D-terms from world-volume fluxes on D7 branes that wrap a three-cycle in the CY 3-fold. However, because of the relationship between D- and F- terms in supergravity, this scenario turned out to be difficult to realize [37, 38]; although, there have been some progresses, see for example [39, 40]. The above difficulties can be circumvented by coupling the KKLT sector to a sector like the Intrilligator-

Seiberg-Shi (ISS) model [41] or, more generally, to a field theory sector that exhibits dynamical supersymmetry breaking to a metastable state (for brevity, MDSB) [42][11]. In this way, one has a natural uplifting that is also completely under control in the effective 4d $N = 1$ supergravity description.[12]

In the next section we will discuss temperature corrections to the previous uplifted 4D effective potential.

2.3 Thermal corrections and moduli stabilization

In the previous section we have seen that string compactifications with stabilised moduli typically admit a slightly de Sitter metastable vacuum that breaks supersymmetry along with a supersymmetric minimum at infinity. The two minima are separated by a potential barrier V_b, whose order of magnitude is very well approximated by the value of the potential at the AdS vacuum before uplifting.

The modulus related to the overall volume of the Calabi-Yau couples to any possible source of energy, due to the Weyl rescaling of the metric needed to obtain a 4D supergravity effective action in the Einstein frame. Thus, in the presence of any source of energy, greater than the height of the potential barrier, the system will be driven to a dangerous decompactification limit. For example, during inflation the energy of the inflaton φ could give an additional uplifting term of the form $\Delta V(\varphi, \mathcal{V}) = V(\varphi)/\mathcal{V}^n$ for $n > 0$, that could cause a run-away to infinity [55]. Another source of danger of decompactification is the following. After inflation, the inflaton decays to radiation and, as a result, a high-temperature thermal plasma is formed. This gives rise to temperature-dependent corrections to the moduli potential, which could again destabilise the moduli and drive them to infinity, if the finite-temperature potential has a run-away behaviour. The decompactification temperature, at which the finite-temperature contribution starts dominating over the $T = 0$ potential, is very well approximated by $T_{max} \sim V_b^{1/4}$ since $V_T \sim T^4$. Clearly, T_{max} sets also an upper bound on the reheating temperature after inflation. The discussion of this paragraph is schematically illustrated on Figure 2.2. On the other hand, if, instead of having a run-away behaviour, the finite-temperature potential develops new minima, then there could be various phase transitions, which might have played an important role in the early Universe and could have observable signatures today. The presence

[11] Since the work of [41], many more examples were found in the literature [43–53], thus showing that the phenomenon of MDSB is quite generic in supersymmetric field theories.

[12] An earlier proposal for F-term uplifting was considered in [54].

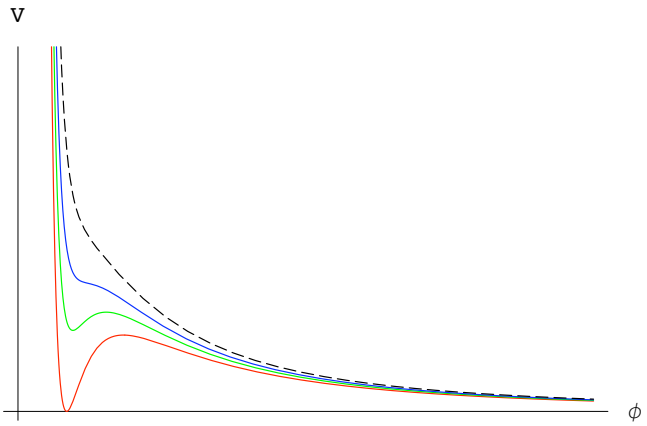

Figure 2.2: The effective potential V versus the volume modulus ϕ for a typical potential of KKLT or LARGE Volume compactifications. The different curves show the effect of various sources of energy that, if higher than the barrier of the potential, can lead to a decompactification of the internal space.

of minima at high T could also have implications regarding the question of how natural it is for the Universe to be in a metastable state at $T = 0$. More precisely, recent studies of various toy models [56–60] have shown that, despite the presence of a supersymmetric global minimum, it is thermodynamically preferable for a system starting in a high T minimum to end up at low temperatures in a (long-lived) local metastable minimum with broken supersymmetry. Similar arguments, if applicable for more realistic systems, could be of great conceptual value given the present accelerated expansion of the Universe.

Therefore, for cosmological reasons it is of great importance to understand the full structure of the finite temperature effective potential. We investigate this problem in great detail for the O'KKLT model [61] in chapter 3 and for the of LARGE Volume Scenario of [62] in chapter 4.

2.3.1 Effective potentials at finite temperature

At nonzero temperature, the effective potential receives a temperature-dependent contribution. In this Section, we review the general form of the finite temperature effective potential and discuss in detail the establishment of thermal equilibrium in an expanding Universe. In particular, we elaborate on the relevant interactions at the microscopic level.

The general structure of the effective scalar potential is the following one:

$$V_{TOT} = V_0 + V_T, \tag{2.48}$$

where V_0 is the $T = 0$ potential and V_T the thermal correction. As discussed in Section 2.2.2, V_0 has the general form:

$$V_0 = \delta V_{(np)} + \delta V_{(\alpha')} + \delta V_{(g_s)}, \tag{2.49}$$

where the tree level part is null due to the no-scale structure (recall that we are studying the scalar potential for the Kähler moduli), $\delta V_{(np)}$ arises due to non-perturbative effects, $\delta V_{(\alpha')}$ are α' corrections and the contribution $\delta V_{(g_s)}$ comes from string loops.

On the other hand, the finite temperature corrections V_T have the generic loop expansion:

$$V_T = V_T^{1-loop} + V_T^{2-loops} + \dots . \tag{2.50}$$

The first term V_T^{1-loop} is a 1-loop thermal correction describing an ideal gas of non-interacting particles. It has been derived for a renormalisable field theory in flat space in [63], using the zero-temperature functional integral method of [64], and reads:

$$V_T^{1-loop} = \pm \frac{T^4}{2\pi^2} \int_0^\infty dx\, x^2 \ln\left(1 \mp e^{-\sqrt{x^2 + m(\varphi)^2/T^2}}\right), \tag{2.51}$$

where the upper (lower) signs are for bosons (fermions) and $m(\phi)$ is the background field dependent mass parameter. At temperatures much higher than the mass of the particles in the thermal bath, $T \gg m(\varphi)$, the 1-loop finite temperature correction (2.51) has the following expansion:

$$V_T^{1-loop} = -\frac{\pi^2 T^4}{90}\alpha + \frac{T^2 m(\varphi)^2}{24} + \mathcal{O}\left(T m(\varphi)^3\right), \tag{2.52}$$

where for bosons $\alpha = 1$ and for fermions $\alpha = 7/8$. The generalisation of (2.52) to supergravity, coupled to an arbitrary number of chiral superfields, takes the form [65]:

$$V_T^{(1-loop)}(\hat{\chi}) = -\frac{\pi^2 T^4}{90}\left(g_B + \frac{7}{8} g_F\right) + \frac{T^2}{24}\left[\mathrm{Tr} M_s^2(\hat{\chi}) + \mathrm{Tr} M_f^2(\hat{\chi})\right] + \mathcal{O}(T), \tag{2.53}$$

where g_B and g_F are, respectively, the numbers of bosonic and fermionic degrees of freedom. Here $\{\chi^A\}$ denotes collectively all fields in the theory (the Kähler moduli in our case) and the quantities $\mathrm{Tr} M_s^2$ and $\mathrm{Tr} M_f^2$ are traces over the mass matrices of

all scalar and fermion fields respectively in the classical background $\{\hat{\chi}^A\}$. [13] They are given by [66]:

$$\mathrm{Tr}M_s^2 = 2\,\langle K^{C\bar{D}}\,\frac{\partial^2 V_0}{\partial\chi^C\partial\bar{\chi}^{\bar{D}}}\,\rangle, \tag{2.54a}$$

$$\mathrm{Tr}M_f^2 = \langle e^G\left[K^{A\bar{B}}K^{C\bar{D}}(\nabla_A G_C + G_A G_C)(\nabla_{\bar{B}} G_{\bar{D}} + G_{\bar{B}} G_{\bar{D}}) - 2\right]\rangle, \tag{2.54b}$$

where V_0 is as in (2.32) and $G = K + \ln|W|^2$. We should also stress that the high temperature expansion (2.53) is only valid in the regime, in which all masses are much smaller than the energy scale set by the temperature.

If the particles in the thermal bath interact among themselves, we need to go beyond the ideal gas approximation. The effect of the interactions is taken into account by evaluating higher thermal loops. The high temperature expansion of the 2-loop contribution looks like:

$$V_T^{2-loops} = \alpha_2 T^4\left(\sum_i f_i(g_i)\right) + \beta_2 T^2\left(TrM_b^2 + TrM_f^2\right)\left(\sum_i f_i(g_i)\right) + \ldots\,, \tag{2.55}$$

where α_2 and β_2 are known constants, i runs over all the interactions through which different species reach thermal equilibrium, and the functions f_i are determined by the couplings g_i and the number of bosonic and fermionic degrees of freedom. For example, for gauge interactions $f(g) = const \times g^2$, whereas for the scalar $\lambda\phi^4$ theory one has that $f(\lambda) = const \times \lambda$.

Now, since we are interested in the moduli-dependence of the finite temperature corrections to the scalar potential, we can drop the first term on the RHS of (2.53) and focus only on the T^2 term, which indeed inherits moduli-dependence from the bosonic and fermionic mass matrices. However, notice that in string theory the various couplings are generically functions of the moduli. Thus, also the first term on the RHS of (2.55) depends on the moduli and, even though it is a 2-loop effect, it could compete with the second term on the RHS of (2.53), because it scales as T^4 whereas the latter one scales only as T^2. This issue has to be addressed on a case by case basis, by studying carefully what particles form the thermal bath.

2.3.2 Thermal equilibrium

The Universe has for much of its history been very nearly in thermal equilibrium. Needless to say the departures from equilibrium have been very important: without

[13] In (2.53), $\mathrm{Tr}M_f^2$ is computed summing over Weyl fermions.

them the past history of the Universe would be irrelevant as the present state would be merely that of a system at 2.75 K. On general grounds, in an expanding Universe, a particle species is in equilibrium with the thermal bath if its interaction rate, Γ, with the particles in that bath is larger than the expansion rate of the Universe. The latter is given by $H \sim g_*^{1/2} T^2/M_P$, during the radiation dominated epoch, with g_* being the total number of degrees of freedom. Thermal equilibrium can be established and maintained by $2 \leftrightarrow 2$ interactions, like scattering or annihilation and the inverse pair production processes, and also by $1 \leftrightarrow 2$ processes, like decays and inverse decays (single particle productions). Let us now consider each of these two cases in detail.

$2 \leftrightarrow 2$ interactions

In this case the thermally averaged interaction rate can be inferred on dimensional grounds by noticing that:

$$\langle \Gamma \rangle \sim \frac{1}{\langle t_c \rangle}, \tag{2.56}$$

where $\langle t_c \rangle$ is the mean time between two collisions (interactions). Moreover

$$t_c \sim \frac{1}{n\sigma v}, \tag{2.57}$$

where n is the number density of the species, σ is the effective cross section and v is the relative velocity between the particles. Thus $\langle \Gamma \rangle \sim n\langle \sigma v \rangle$. For relativistic particles, one has that $\langle v \rangle \sim c$ ($\equiv 1$ in our units) and also $n \sim T^3$. Therefore

$$\langle \Gamma \rangle \sim \langle \sigma \rangle T^3 \,. \tag{2.58}$$

The cross-section σ has dimension of $(length)^2$ and for $2 \leftrightarrow 2$ processes its thermal average scales with the temperature as:

1. For renormalisable interactions:

$$\langle \sigma \rangle \sim \alpha^2 \frac{T^2}{\left(T^2 + M^2\right)^2}, \tag{2.59}$$

   where $\alpha = g^2/(4\pi)$ (g is the gauge coupling) and M is the mass of the particle mediating the interactions under consideration.

   a) For long-range interactions $M = 0$ and (2.59) reduces to:

$$\langle \sigma \rangle \sim \alpha^2 T^{-2} \quad \Rightarrow \quad \langle \Gamma \rangle \sim \alpha^2 T. \tag{2.60}$$

This is also the form that (2.59) takes for short-range interactions at energies $E \gg M$.

b) For short-range interactions at scales lower than the mass of the mediator, the coupling constant becomes dimensionful and (2.59) looks like:

$$\langle\sigma\rangle \sim \alpha^2 \frac{T^2}{M^4} \quad \Rightarrow \quad \langle\Gamma\rangle \sim \alpha^2 \frac{T^5}{M^4}. \tag{2.61}$$

2. For processes including gravity:

a) Processes with two gravitational vertices:

$$\langle\sigma\rangle \sim d \frac{T^2}{M_P^4} \quad \Rightarrow \quad \langle\Gamma\rangle \sim d \frac{T^5}{M_P^4}, \tag{2.62}$$

where d is a dimensionless moduli-dependent constant.

b) Processes with one renormalisable and one gravitational vertex:

$$\langle\sigma\rangle \sim \sqrt{d} \frac{g^2}{M_P^2} \quad \Rightarrow \quad \langle\Gamma\rangle \sim \sqrt{d} \frac{g^2 T^3}{M_P^2}, \tag{2.63}$$

where d is the same moduli-dependent constant as before.

Let us now compare these interaction rates with the expansion rate of the Universe, $H \sim g_*^{1/2} T^2 / M_P$, in order to determine at what temperatures various particle species reach or drop out of thermal equilibrium, depending on the degree of efficiency of the relevant interactions.

1.a) Renormalisable interactions with massless mediators:

$$\langle\Gamma\rangle > H \quad \Leftrightarrow \quad \alpha^2 T > g_*^{1/2} T^2 M_P^{-1} \quad \Rightarrow \quad T < \alpha^2 g_*^{-1/2} M_P. \tag{2.64}$$

QCD processes, like the ones shown in Figure 2.3, are the main examples of this kind of interactions. The same behaviour of σ is expected also for the other MSSM gauge groups for energies above the EW symmetry breaking scale. Therefore, MSSM particles form a thermal bath via strong interactions for temperatures $T < \alpha_s^2 g_*^{-1/2} M_P \sim 10^{15}$ GeV [67].

1.b) Renormalisable interactions with massive mediators:

$$\langle\Gamma\rangle > H \quad \Leftrightarrow \quad \alpha^2 \frac{T^5}{M^4} > g_*^{1/2} \frac{T^2}{M_P} \quad \Rightarrow \quad \left(\frac{g_*^{1/2} M^4}{\alpha^2 M_P} \right)^{1/3} < T < M. \tag{2.65}$$

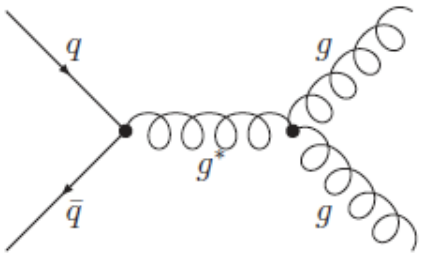

Figure 2.3: QCD scattering process $q\bar{q} \to gg$ through which quarks and gluons reach thermal equilibrium.

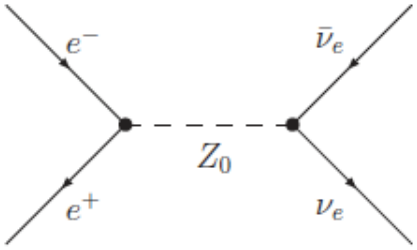

Figure 2.4: Weak interaction between electrons and neutrinos through which they reach thermal equilibrium.

Examples of interactions with effective dimensionful couplings are weak interactions below M_{EW}. In this case, the theory is well described by the Fermi Lagrangian. An interaction between electrons and neutrinos, like the one shown in Figure 2.4, gives rise to a cross-section of the form of (2.61):

$$\langle \sigma_w \rangle \sim \frac{\alpha_w^2}{M_Z^4} \langle p^2 \rangle \sim \frac{\alpha_w^2}{M_Z^4} T^2, \tag{2.66}$$

where α_w is the weak fine structure constant and $p \sim T$. Thus, neutrinos are coupled to the thermal bath if and only if

$$T > \left(\frac{g_*^{1/2} M_Z^4}{\alpha_w^2 M_P} \right)^{1/3} \sim 1 \ \text{MeV}. \tag{2.67}$$

2. Gravitational interactions:

a) $$\langle \Gamma \rangle > H \quad \Leftrightarrow \quad d \frac{T^5}{M_P^4} > g_*^{1/2} \frac{T^2}{M_P} \quad \Rightarrow \quad T > g_*^{1/6} \frac{M_P}{d^{1/3}}. \tag{2.68}$$

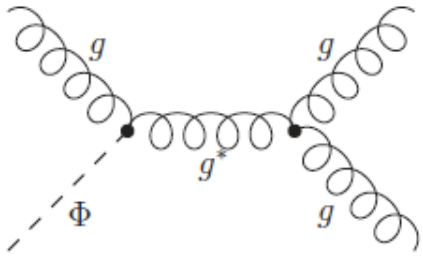

Figure 2.5: Scattering process $\Phi g \to gg$ through which the modulus Φ and gluons can reach thermal equilibrium.

$$\text{b)} \qquad \langle\Gamma\rangle > H \quad \Leftrightarrow \quad \sqrt{d}\frac{g^2T^3}{M_P^2} > g_*^{1/2}\frac{T^2}{M_P} \quad \Rightarrow \quad T > \frac{g_*^{1/2}M_P}{g^2\sqrt{d}}. \tag{2.69}$$

As before, case (a) refers to $2 \leftrightarrow 2$ processes with two gravitational vertices, whereas in case (b) one vertex is gravitational and the other one is a renormalisable interaction. A typical Kähler modulus of string compactifications generically couples to the gauge bosons of the field theory, that lives on the stack of branes wrapping the cycle whose volume is given by that modulus. Scattering processes, annihilation and pair production reactions, that arise due to that coupling, all have cross-sections of the form (2.62) and (2.63). In general, for all the Kähler moduli in type IIB compactifications $d \sim \mathcal{O}(1)$ and so $\langle\Gamma\rangle$ is never greater than H for temperatures below the Planck scale, for both cases (a) and (b). Therefore, those moduli will never thermalise through $2 \leftrightarrow 2$ processes. However, we shall see in Section 4.4 that the situation is different for the LARGE volume scenarios, since in that case $d \sim \mathcal{V}^2 \gg 1$. A typical $2 \leftrightarrow 2$ process of type (b), with a modulus Φ and a non-abelian gauge boson g going to two g's, is shown in Figure 2.5.

$1 \leftrightarrow 2$ interactions

In order to work out the temperature dependence of the interaction rate for decay and inverse decay processes, recall that the rest frame decay rate $\Gamma_D^{(R)}$ does not depend on the temperature. For renormalisable interactions with massless mediators or mediated by particles with mass M at temperatures $T > M$, it takes the form:

$$\Gamma_D^{(R)} \sim \alpha m, \tag{2.70}$$

where m is the mass of the decaying particle and $\alpha \sim g^2$, with g being either a gauge or a Yukawa coupling. On the other hand, for gravitational interactions or for renormalisable interactions mediated by particles with mass M at temperatures $T < M$, we have ($M \equiv M_P$ in the case of gravity):

$$\Gamma_D^{(R)} \sim D\frac{m^3}{M^2}, \tag{2.71}$$

with D a dimensionless constant (note that in the case of gravity $D = \sqrt{d}$, where d is the same moduli-dependent constant as in Subsection 2.3.2).

Now, the decay rate that has to be compared with H is not $\Gamma_D^{(R)}$, but its thermal average $\langle\Gamma_D\rangle$. In order to evaluate this quantity, we need to switch to the 'laboratory frame' where:

$$\Gamma_D = \Gamma_D^{(R)}\sqrt{1-v^2} = \Gamma_D^{(R)}\frac{m}{E}\,, \tag{2.72}$$

and then take the thermal average:

$$\langle\Gamma_D\rangle = \Gamma_D^{(R)}\frac{m}{\langle E\rangle}\,. \tag{2.73}$$

In the relativistic regime, $T \gtrsim m$, the Lorentz factor $\gamma = \langle E\rangle/m \sim T/m$, whereas in the non-relativistic regime, $T \lesssim m$, $\gamma = \langle E\rangle/m \sim 1$.

Notice that, by definition, in a thermal bath the decay rate of the direct process is equal to the decay rate of the inverse process. However, for $T < m$ the energy of the final states of the decay process is of order T, which means that the final states do not have enough energy to re-create the decaying particle. So the rate for the inverse decay, Γ_{ID}, is Boltzmann-suppressed: $\Gamma_{ID} \sim e^{-m/T}$. Hence, the conclusion is that, for $T < m$, one can never have $\Gamma_D = \Gamma_{ID}$ and thermal equilibrium will not be attained. Let us now summarize the various decay and inverse decay rates:

1. Renormalisable interactions with massless mediators or mediated by particles with mass M at $T > M$:

$$\langle\Gamma_D\rangle \simeq \begin{cases} g^2\frac{m^2}{T}, & \text{for } T \gtrsim m \\ g^2 m, & \text{for } T \lesssim m\,, \end{cases} \tag{2.74}$$

$$\langle\Gamma_{ID}\rangle \simeq \begin{cases} g^2\frac{m^2}{T}, & \text{for } T \gtrsim m \\ g^2 m\left(\frac{m}{T}\right)^{3/2} e^{-m/T}, & \text{for } T \lesssim m\,. \end{cases} \tag{2.75}$$

Therefore, particles will reach thermal equilibrium via decay and inverse decay

processes if and only if

$$\langle\Gamma\rangle > H \quad \Leftrightarrow \quad g^2\frac{m^2}{T} > g_*^{1/2}\frac{T^2}{M_P} \quad \Rightarrow \quad m < T < \left(\frac{g^2 m^2 M_P}{g_*^{1/2}}\right)^{1/3} . \tag{2.76}$$

2. Gravity or renormalisable interactions mediated by particles with mass M at $T < M$:

$$\langle\Gamma_D\rangle \simeq \begin{cases} D\frac{m^4}{M^2 T}, & \text{for } T \gtrsim m \\ D\frac{m^3}{M^2}, & \text{for } T \lesssim m \ , \end{cases} \tag{2.77}$$

$$\langle\Gamma_{ID}\rangle \simeq \begin{cases} D\frac{m^4}{M^2 T}, & \text{for } T \gtrsim m \\ D\frac{m^3}{M^2}\left(\frac{m}{T}\right)^{3/2} e^{-m/T}, & \text{for } T \lesssim m \end{cases} \tag{2.78}$$

with $M \equiv M_P$ in the case of gravity. Therefore, particles will reach thermal equilibrium via decay and inverse decay processes if and only if

$$\langle\Gamma\rangle > H \quad \Leftrightarrow \quad D\frac{m^4}{M^2 T} > g_*^{1/2}\frac{T^2}{M_P} \quad \Rightarrow \quad 1 < \frac{T}{m} < \left(D\frac{m M_P}{g_*^{1/2} M^2}\right)^{1/3} . \tag{2.79}$$

In the case of gravitational interactions, (2.79) becomes

$$1 < \frac{T}{m} < \left(D\frac{m}{g_*^{1/2} M_P}\right)^{1/3} . \tag{2.80}$$

In general, in string theory constructions, $D \sim \mathcal{O}(1)$ and $m \sim m_{3/2}$. So (2.80) can never be satisfied and hence moduli cannot reach thermal equilibrium via decay and inverse decay processes. However, we shall see in Section 4.4 that in LVS one has $D \sim \mathcal{V} \gg 1$ and so $1 \leftrightarrow 2$ processes could, in principle, play a role in maintaining thermal equilibrium between moduli and ordinary MSSM particles.

2.3.3 Cosmological moduli problem

In the previous section we saw that in general moduli have couplings to the observable sector that are suppressed by powers of the Planck scale and masses of the order of the gravitino mass[14] that is expected to be around 1 TeV in order to solve the hierarchy problem. The previous properties are quite generic and independent of the particular

[14] This is unavoidable in the conventional picture of gravity-mediated supersymmetry breaking, where moduli obtain masses comparable to the supersymmetry breaking scale $m_\phi \sim m_{3/2}$.

string theory compactification considered and particles with these properties and masses are problematic for cosmology [68].

Let us briefly review the source of the problem. The moduli fields are expected to be initially shifted from their zero-temperature minimum at some initial value ϕ_{in} either due to the effect of thermal fluctuation or quantum fluctuations during inflation. In a Friedmann-Robertson-Walker Universe, the evolution of a modulus field ϕ, canonically normalized, is determined by

$$\ddot{\phi} + (3H + \Gamma_\phi)\dot{\phi} + V'(\phi) = 0 \tag{2.81}$$

where the dots above ϕ denote derivatives with respect to time and the prime denotes the derivative with respect to ϕ. Furthermore, $H = \frac{\dot{a}}{a}$ is the Hubble parameter, a the scale factor, V the scalar potential and $\Gamma_\phi \sim m_\phi^3/M_P^2$ the ϕ decay rate. While $t < t_{in} \sim m_\phi^{-1}$ and $H > m_\phi$ the friction term $3H\dot{\phi}$ dominates the time evolution of ϕ, causing it to remain at $\phi \sim \phi_{in}$. The modulus begins to oscillate around its minimum at a temperature T_{osc} where the mass $m_\phi(T)$ is comparable to the overall Hubble parameter $H \sim T^2/M_P$. Coherent oscillations of the field after this time will come to dominate the energy density of the universe since the initial energy density $\rho_\phi(T_{in}) \sim m^2\phi_{in}^2$ decrease with temperature as $\rho_\phi \sim T^{-3}$, whereas radiation decreases faster $\rho_r \sim T^{-4}$. Therefore we can write:

$$\rho_\phi(T) = \rho_\phi(T_{in}) \left(\frac{T}{T_{in}}\right)^3 \sim m_\phi^2\phi_{in}^2 \left(\frac{T_0}{\sqrt{m_\phi M_P}}\right)^3 \tag{2.82}$$

where T_0 is the temperature today. If the field ϕ is stable, these oscillations will dominate the energy density of the universe and may overclose it. Imposing that $\rho_\phi(T_0) < \rho_{critical} = 3H_0^2M_P^2 \sim (10^{-3}\text{eV})^3$ puts a constraint on ϕ_{in}:

$$\phi_{in} < 10^{-10} \left(\frac{m_\phi}{100\text{GeV}}\right)^{-1/4} M_P$$

that is, for $\phi_{in} \sim M_P$, a stable scalar field of mass

$$m_\phi > 10^{-26}\text{eV} \tag{2.83}$$

will overclose the Universe.

However, in general ϕ decays. If it decays late, as often happens since the field couples with gravitational strength, it can dilute or alter the light elements abundance

thus destroying the good predictions of the standard Big-Bang nucleosynthesis (BBN). This can be quantified as follows. The scalar field ϕ decays at a temperature T_D for which $H(T_D) \sim \Gamma_\phi$. Using $\Gamma_\phi \sim m_\phi^3/M_P^2$ and the FRW equation for H we find

$$\Gamma_\phi^2 \sim \left(\frac{m_\phi^3}{M_P^2}\right)^2 \sim \frac{\rho_\phi(T_D)}{M_P^2} = \frac{\rho_\phi(T_{in})}{M_P^2}\left(\frac{T_D}{T_{in}}\right)^3 \tag{2.84}$$

Using this and $\rho_\phi(T_{in}) \sim m_\phi^2\phi_{in}^2$, $T_{in}^2 \sim m_\phi M_P$ we find the decay temperature

$$T_D \sim \frac{m_\phi^{11/6}}{M_P^{1/6}\phi_{in}^{2/3}} \ . \tag{2.85}$$

At a temperature T_D the energy density $\rho_\phi(T_D)$ gets converted into radiation of temperature

$$T_{RH} \sim (\rho_\phi(T_D))^{1/4} \sim (M_P\Gamma_\phi)^{1/2} \sim \left(\frac{m_\phi^3}{M_P}\right)^{1/2} \ . \tag{2.86}$$

The decay of ϕ causes an increase in entropy given by:

$$\Delta = \left(\frac{T_{RH}}{T_D}\right)^3 \sim \frac{\phi_{in}^2}{m_\phi M_P} \tag{2.87}$$

which for $\phi_{in} \sim M_P$ gives a very large entropy increase washing out any previously generated baryon asymmetry. However, another possibility is provided if the late-time decay of the moduli reheat the universe to temperatures greater than a few MeV. Such reheating will then allow BBN to proceed as usual. Requiring that $T_{RH} \gtrsim 10$ MeV puts a bound on m_ϕ of

$$m_\phi \gtrsim 10\text{TeV} \ . \tag{2.88}$$

Therefore, the standard cosmological moduli problem forbids gravity coupled scalars in the range $m_\phi \lesssim 10$ TeV.

There are two main solutions to this problem: dilution of the unwanted relics by a late period of low-energy inflation caused by thermal effects, namely, thermal inflation [69, 70] or by the entropy released by the non-thermal decay of a heavier modulus which is dominating the energy density of the Universe [71, 72]. We will discuss the cosmological moduli problem and its possible solutions in chapter 4 in the context of the LARGE volume compactifications.

3 Finite temperature corrections to the KKLT model

Summary. In this chapter, we study whether finite temperature corrections decompactify the internal space in *Kachru-Kallosh-Linde-Trivedi* (KKLT) compactifications with an uplifting sector given by a system that exhibits metastable dynamical supersymmetry breaking. More precisely, we calculate the one-loop temperature corrections to the effective potential of the volume modulus in the KKLT model coupled to the quantum corrected O'Raifeartaigh model. We prove that for the original KKLT model, namely with one exponent in the non-perturbative superpotential, the finite temperature potential is runaway when at zero temperature there is a dS minimum. On the other hand, for a non-perturbative superpotential of the race-track type with two exponents, we demonstrate that the temperature-dependent part of the effective potential can have local minima at finite field vevs. However, it turns out that these minima do not affect the structure of the full effective potential and so the volume modulus is stabilized at the local minimum of the zero temperature potential for the whole range of validity of the supergravity approximation.

Although we use a different approach, the results presented here are in agreement with those in [73] where the authors showed that the inclusion of thermal corrections do not decrease dramatically the region of initial conditions for which the field would end up at the zero temperature minimum.

3.1 Introduction

In the previous chapter we discussed the reasons why it is important to give a vacuum expectation value (VEV) to all moduli in string compactifications and that the resolution of this problem requires the inclusion of background fluxes. This leads, in type IIB, to the stabilization of all the complex structure moduli [24] whereas the remaining Kähler moduli are stabilized by taking into account non-perturbative effects [35] or a combination of perturbative and non-perturbative corrections [30, 62].

The first low-energy string theory model in the literature to achieve moduli stabilization was the KKLT proposal of [35] in which the inclusion of background fluxes and non-perturbative effects in the superpotential leads to a 4D effective supergravity theory with all moduli stabilized at an AdS vacuum. Unfortunately, the need to add by hand anti-D3 branes in order to lift the original AdS vacuum to dS makes it problematic to describe this setup in supergravity.

As discussed in the previous chapter, the above difficulties can be circumvented by coupling the KKLT sector to a field theory sector that exhibits MDSB. In this way, one has a natural uplifting that is also completely under control in the effective 4D $N = 1$ supergravity description. In fact, one can capture the essential features of F-term uplifting due to MDSB in the KKLT setup by taking the uplifting sector to be the O'Raifeartaigh model. The reason is that many theories with dynamical supersymmetry breaking can be approximated near the origin of field space by this model [74].[1] The O'Raifeartaigh-uplifted KKLT, termed O'KKLT, model was first proposed and studied in [61]. It was pointed out there that the original KKLT proposal, *i.e.*, with one exponent in the superpotential, leads to a tension between low scale supersymmetry breaking and the standard high scale cosmological inflation. This undesirable situation can be resolved by considering a racetrack-type superpotential with two exponentials [55, 61, 77].

We will study here thermal corrections to the effective potential of the O'KKLT model with both one or with two exponentials. We will make the assumptions, following [65], that the moduli sector is in thermal equilibrium with the MDSB sector for temperature ranges in-between $M_{GUT} < T < M_P$. Temperature corrections to a model with MDSB (more precisely, the ISS model) were considered in [57, 58]. The motivation there was to address the question how natural is it for the system to be in a local minimum with broken susy, given that it has global supersymmetric minima. It turned out that the metastable minimum is thermodynamically preferable. More precisely, [58] showed that if one starts from a local minimum of the effective potential at finite temperature and considers what happens as the temperature decreases, then one finds that the system rolls towards the metastable, and not towards a global, vacuum of the zero-temperature potential. This picture persists upon coupling the ISS model to supergravity [59]. Unfortunately though, including the volume modulus and considering the full KKLT-ISS model in thermal equilibrium at high temperatures, is rather complicated technically. The main reason is that the Kähler potential for volume modulus is not canonical, unlike the Kähler potential for the ISS fields. This

[1] More precisely, this is true for the theories that realize DSB via the mechanism of [75, 76].

leads to rather intractable expressions for the effective potential at nonzero temperature. Initial steps in analyzing the latter were discussed in [59] and a more detailed analysis can be found in [60] where the computations were done in the approximation in which the moduli act as background fields, thus not contributing to thermal loops. The authors of [78, 79] studied finite temperature corrections to the KKLT with D-term or anti-D3 uplifting in the same approximation in which the moduli are not in thermal equilibrium. All the approaches agree on the existence of a maximal temperature above which the zero temperature dS vacuum is destabilized. However, the analysis of the equation of motions for the moduli fields in the presence of thermal corrections [73] shows that the initial conditions for which the field would end up at the minimum do not change in a dramatic way upon the inclusion of thermal corrections.

We also obtain here similar results when considering the static O'KKLT model. The latter is tractable enough to enable us to study the phase structure of the finite temperature effective potential for the volume modulus in thermal loops. At the same time, as already mentioned above, it captures all the main features of the MDSB-uplifted KKLT scenario; see [61][2].

We shall restrict our considerations to the tree level and one-loop contributions to the O'KKLT effective potential at nonzero temperature. So we shall make use of the general finite temperature results of [65, 66] for chiral multiplets coupled to supergravity at one-loop. As is well-understood by now, the nonrenormalizability of this theory is not an issue since it is not supposed to be viewed as a fundamental theory, but rather as an effective low-energy description.[3]

The organization of this chapter is the following. In Section 3.2 we briefly review the O'KKLT model and the relevant properties of its zero-temperature potential. We also introduce useful notation and give a clear derivation of an order of magnitude relation between parameters, that is necessary for the existence of dS vacua when the non-perturbative superpotential contains a single exponent (as in the original KKLT proposal). In Sections 3.3 and 3.4 we compute the zero and finite temperature contribution, V_0 and V_T respectively, to the effective potential at one loop. In Subsection

[2] Clearly, for nonzero temperature this statement includes the assumption that the starting point at high T is the minimum of the MDSB-uplifted KKLT potential, which is near the origin of field space of the MDSB sector.

[3] For more details on one-loop computations in nonrenormalizable theories (supergravity coupled with various matter multiplets) see [80–86]. As was shown there for the zero-temperature case, there are many subtleties that one has to be careful about when considering arbitrary curved backgrounds. It is undoubtedly of great interest to achieve the same level of understanding for $T \neq 0$ as well, but this goes well beyond the scope of our thesis.

3.4.1 and Appendices 3.A and 3.B we show that V_T does not have any minima at finite field vevs for the one-exponential case. In Section 3.5 we study the case of a race-track type superpotential with two-exponentials. We find various sets of parameters for which V_T has minima at finite vevs. However, it turns out that for these parameters the minima of the total effective potential are still determined by those of the zero-temperature part, as long as the temperature is much smaller than the Planck mass (which is necessary for the reliability of the supergravity approximation). Hence, there is a regime in which the zero-temperature dS minimum of the field ρ is not destabilized by thermal corrections in the supergravity approximation. In view of that, in Section 3.6 we reconsider the one-exponential case and find the conditions under which the minimum of V_{eff} is not destabilized by the runaway temperature contribution, again for temperatures smaller than the Planck mass.

3.2 The O'KKLT model

The KKLT model of [61] is given by the following Kähler potential and superpotential

$$K = -2\ln\mathcal{V}\,, \qquad W = W_0 + Ae^{-a\rho} \tag{3.1}$$

In the previous expression the volume depends on a single complex scalar field ρ as follows

$$\mathcal{V} = (\rho+\bar{\rho})^{3/2}\,. \tag{3.2}$$

The O'KKLT model of [61] is a combination of the original KKLT model and the O'Raifeartaigh model. The latter has three scalar fields. However, [61] considered the regime in which the two heavy ones are integrated out. One is then left with a single field S with a superpotential and Kähler potential given by

$$W_{O'} = -\mu^2 S\,, \qquad K_{O'} = S\bar{S} - \frac{(S\bar{S})^2}{\Lambda^2}\,. \tag{3.3}$$

The last term in $K_{O'}$ is due to the leading contribution in the one-loop correction in an expansion in $\frac{\lambda^2 S\bar{S}}{m^2} \ll 1$, where m and λ are the remaining couplings in the full O'Raifeartaigh superpotential: $m\phi_1\phi_2 + \lambda S\phi_1^2 - \mu^2 S$. The parameter Λ in $K_{O'}$ denotes a particular combination of couplings, namely $\Lambda^2 = \frac{16\pi^2 m^2}{c\lambda^4}$ with c being a numerical constant of order 1. As in [61], we will assume that $m, \mu, \Lambda \ll 1$ (we work in units $M_P = 1$). Also, the validity of the approximation (3.3) requires small S, such that $S\bar{S} \ll m^2/\lambda^2 \ll 1$.

In fact, as explained in [61], for cosmological reasons it is valuable to consider a modification of (3.1) with two exponentials:

$$W = W_0 + Ae^{-a\rho} + Be^{-b\rho}\,. \tag{3.4}$$

The reason is that this race-track type superpotential, unlike (3.1), allows one to reconcile light gravitino mass with standard models of inflation.

Let us see in more detail the source of the cosmological problem. The depth of the AdS vacuum in the KKLT scenario is given by $V_{\rm AdS} = -3e^K|W|^2 = -3m_{3/2}^2$. Here $V_{\rm AdS}$ is the depth of the AdS minimum prior to the uplifting and $m_{3/2}$ is the gravitino mass after the uplifting. Uplifting creates a barrier which separates the KKLT minimum form the 10D Minkowski Dine-Seiberg minimum. The height of the barrier is somewhat smaller than the depth of the original AdS minimum prior to the uplifiting:

$$V_{\rm b} \sim |V_{\rm AdS}| \sim 3m_{3/2}^2\ . \tag{3.5}$$

Inflation requires the existence of an additional contribution $V_{\rm infl}$ to the scalar potential, but all such contributions in the effective 4D theory have the following general structure: $V_{\rm infl} = \frac{V(\phi)}{(\rho+\bar\rho)^3}$, where ϕ is the inflation field. Such term destabilize the potential for $V_{\rm infl} \gg V_{\rm b} \sim m_{3/2}^2$. Since during inflation $V_{\rm infl} = H^2/3$, one finds that the following constraint on the Hubble constant during the last stage of inflation [55]

$$H \lesssim m_{3/2}\ . \tag{3.6}$$

If the mass of the gravitino is light, e.g. $m_{3/2} \leqslant 1$ TeV, one would need to consider non-standard low-scale inflationary models. Therefore, the constraint (3.6) is quite restrictive and undesirable. The racetrack potential allows to make the barrier many orders higher than $m_{3/2}^2$.

For convenience, from now on we will call O'KKLT model the combined system:

$$K = -3\ln(\rho+\bar\rho) + S\bar S - \frac{(S\bar S)^2}{\Lambda^2}\,, \qquad W = W_0 + f(\rho) - \mu^2 S\,, \tag{3.7}$$

where the function f is either

$$f(\rho) = Ae^{-a\rho} \qquad \text{or} \qquad f(\rho) = Ae^{-a\rho} + Be^{-b\rho}\,. \tag{3.8}$$

Recall that, when the non-perturbative superpotential is due to gaugino condensation, the parameters in the exponents are of the form $a = 2\pi/n$ and $b = 2\pi/m$ with integer

n and m. In the following, however, we will only consider the effective model determined by (3.7)-(3.8), without being concerned with the microscopic physics behind it.

3.3 Zero temperature potential

At zero temperature the KKLT model alone, (3.1), has a single AdS vacuum at finite value of ρ. The O'Raifeartaigh model uplifts this minimum to a positive cosmological constant vacuum. Similarly, the modified superpotential (3.4) leads to two AdS vacua at finite ρ and the presence of the O'Raifeartaigh field lifts one of them to dS[4]. Our goal will be to study the phase structure of the theory (3.7) at finite temperature aiming to answer the question whether the fields roll towards the dS vacuum upon cooling down. Let us first review some results about the zero temperature scalar potential, that we will need in later sections.

At zero temperature the scalar potential of the system (3.7) is given by the standard $N = 1$ supergravity expression given in eq. (2.32) that we rewrite here for convenience:

$$V_0 = e^K (K^{A\bar{B}} D_A W D_{\bar{B}} \overline{W} - 3|W|^2) \,. \tag{3.9}$$

One can show that its minima are obtained for vanishing imaginary parts of the scalars ρ and S [61]. Let us denote the real parts by $\mathrm{Re}\rho = \sigma$ and $\mathrm{Re}S = s$. As we only consider the moduli space region where S is small, we can expand (2.32) in powers of s:

$$V_0 = V_0^{(0)} + V_0^{(1)} s + V_0^{(2)} s^2 + \mathcal{O}(s^3) \,. \tag{3.10}$$

The value of s at the minimum is determined by $\partial V_0 / \partial s = 0$ and so, up to $\mathcal{O}(s^3)$, it is [61]:

$$s = -\frac{V_0^{(1)}}{2V_0^{(2)}} \approx \frac{\sqrt{3}}{6} \Lambda^2 \,. \tag{3.11}$$

It will be useful for the future to record here the general expressions for the first

[4] Of course, the Dine-Seiberg minimum at infinity is always there too.

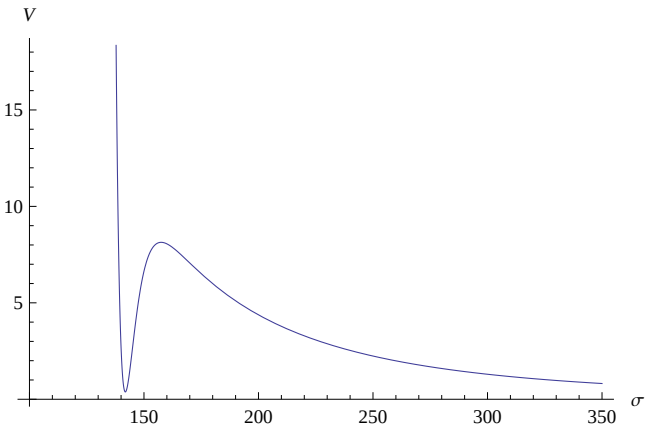

Figure 3.1: O'KKLT potential (multiplied by 10^{30}) for the one exponential case without MDSB sector. The parameter values: $A = 1$, $a = 0.20$, $W_0 = -10^{-11}$, $\mu^4 = 28 \times 10^{-23}$ and $\Lambda = 10^{-5}$.

three coefficients of the expansion with K and W as in (3.7) and $\rho = \bar{\rho} = \sigma$:

$$V_0^{(0)} = \frac{\mu^4}{8\sigma^3} - \frac{(3W_0 + 3f - \sigma f')f'}{6\sigma^2} \tag{3.12a}$$

$$V_0^{(1)} = -\frac{\mu^2 (W_0 + f - 2\sigma f')}{4\sigma^3} \tag{3.12b}$$

$$V_0^{(2)} = \frac{1}{8\sigma^3}\left[\left(\frac{4\mu^4}{\Lambda^2} + 3\mu^4 + W_0^2\right) + 2W_0(f - 2\sigma f') + f^2 - 4\sigma f f' + \frac{4}{3}\sigma^2 (f')^2\right] \tag{3.12c}$$

where we have denoted $f' \equiv \partial f/\partial\sigma$. Note that the constant term in the numerator of $V_0^{(2)}$, namely $\frac{4\mu^4}{\Lambda^2} + 3\mu^4 + W_0^2$, is really just $\frac{4\mu^4}{\Lambda^2} + W_0^2$ since $\Lambda \ll 1$.

Let us now take a more careful look at the cases of a superpotential with one and with two exponentials in turn. This will also enable us to introduce some useful notation.

3.3.1 One exponential

In this case, we have (3.7) with

$$f(\sigma) = Ae^{-a\sigma}\,. \tag{3.13}$$

In Figure 3.1 we plotted the resulting effective potential. A good approximation for the position of the dS vacuum is the position of the supersymmetric AdS minimum.

The latter is determined by the solution of $D_\rho W_{KKLT} = 0$, which implies [35]:

$$W_0 = -Ae^{-a\sigma}\left(1 + \frac{2}{3}a\sigma\right). \tag{3.14}$$

It is easy to see that the requirement that the zeroth order, $V_0^{(0)}$, in the expansion (3.10) be small and positive at the dS minimum leads to:

$$W_0^2 \approx \mu^4\,, \tag{3.15}$$

meaning that $|W_0|$ and μ^2 are of the same order of magnitude. In order to show the latter expression recall that at zeroth order the vacuum energy density is:

$$V_0^{(0)} = V_{KKLT} + \frac{\mu^4}{(\rho+\bar{\rho})^3}\,. \tag{3.16}$$

Since at the AdS minimum $V_{KKLT} = -3|W_{KKLT}|^2$ and also $\rho = \bar{\rho} = \sigma$, then the condition $V_0^{(0)}|_{min} \approx 0$ implies that

$$3(W_0 + Ae^{-a\sigma})^2 \approx \mu^4\,. \tag{3.17}$$

Substituting in the latter equation $Ae^{-a\sigma}$ from (3.14), we find:

$$3W_0^2\left(\frac{\frac{2}{3}a\sigma}{1+\frac{2}{3}a\sigma}\right)^2 \approx \mu^4\,. \tag{3.18}$$

Obviously, the number $\frac{2}{3}a\sigma/(1+\frac{2}{3}a\sigma)$ is less than 1 for any finite $a\sigma$. In addition, it is always of order 1 as we only consider $a\sigma > 1$ in order to have a reliable one-instanton contribution to the non-perturbative superpotential. Hence, one concludes that W_0^2 and μ^4 have to be of the same order of magnitude in order for a dS vacuum with small cosmological constant to exist.

Now, it is clear that using $f' = -af$ one can get rid of all derivatives in (3.12). Then it is easy to notice that the parameter a becomes just an overall rescaling upon introducing the new variable $x = a\sigma$. For example:

$$V_0^{(0)} = \frac{a^3}{2x^3}\left[\frac{\mu^4}{4} + W_0 f x + f^2\left(\frac{x^2}{3} + x\right)\right] \tag{3.19}$$

and hence

$$\frac{\partial V_0^{(0)}}{\partial \sigma} = -\frac{a^4}{x^4}\left[Q_3(x)\, f^2 + W_0 Q_2(x) f + \frac{3\mu^4}{8}\right] , \tag{3.20}$$

where

$$Q_2(x) = x + \frac{1}{2}x^2 , \qquad Q_3(x) = x + \frac{7}{6}x^2 + \frac{1}{3}x^3 . \tag{3.21}$$

Clearly, varying a does not change the vacuum structure of the model; it only shifts the positions of the extrema along the σ-axis. We will always choose a such that the minima occur for $\sigma \sim \mathcal{O}(100)$, so that the supergravity approximation is good. It is also clear that the value of the parameter A does not affect the vacuum structure either: one can reduce it to an overall rescaling of the scalar potential by redefining $W_0 \to AW_0$ and $\mu^2 \to A\mu^2$. So for convenience we will set $A = 1$ from now on. Thus, in this case one is left with the following essential parameters: W_0, μ and Λ[5]. Notice that (3.20) has zeros only for $W_0 < 0$, as all other terms in the bracket are positive definite (recall that $x \geq 0$).

Finally, notice that the O'Raifeartaigh model uplifts the AdS minimum with the depth $|V_{\rm AdS}| \sim m_{3/2}^2$ by $\frac{a^3}{2x^3}\frac{\mu^4}{4}$, so that

$$\frac{a^3}{2x^3}\frac{\mu^4}{4} + V_{\rm AdS} \sim 10^{-120} \approx 0 \ . \tag{3.22}$$

This implies that

$$m_{3/2} \sim \frac{\mu^2}{2\sigma^{3/2}} \sim \frac{|W_0|}{M_P^2 \mathcal{V}} \ . \tag{3.23}$$

where $\mathcal{V}$ is the overall volume of the extra dimensions. In KKLT models, one tunes the values of the fluxes to yield a small value for the superpotential $W_0 \ll 1$ and thus the scale of SUSY breaking. In the next chapter, we will consider another class of models, the LARGE volume models in which quite naturally one finds $\mathcal{V} \sim 10^{14}$ and thus W_0 can take the natural value $W_0 \simeq 1$.

3.3.2 Two exponentials

Now the function f in (3.7) is given by

$$f(\sigma) = Ae^{-a\sigma} + Be^{-b\sigma} . \tag{3.24}$$

Realizing that again the parameter A can be reduced to an overall rescaling of the scalar potential by redefining $W_0 \to AW_0$, $\mu^2 \to A\mu^2$ and $B \to AB$, we set $A = 1$ in

[5] Although Λ does not occur in $V_0^{(0)}$, it is present in the total potential, see (3.12).

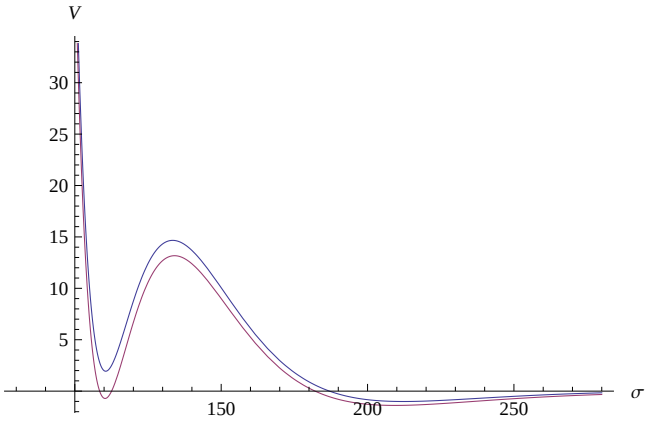

Figure 3.2: The racetrack potential (multiplied by 10^{15}) before and after the uplifting. The parameter values: $A = 1$, $B = -1.026$, $a = \frac{\pi}{100}$, $b = \frac{\pi}{99}$, $W_0 = -2.4 \times 10^{-4}$, $\mu = 13 \times 10^{-3}$ and $\Lambda = 10^{-2}$.

this case too. Introducing $x = a\sigma$ as before and denoting $p \equiv b/a$, we can write $V_0^{(0)}$ of (3.12) as:

$$V_0^{(0)} = \frac{a^3}{2x^3}\left[e^{-2x}\left(\frac{x^2}{3}+x\right)+B^2e^{-2p\,x}\left(\frac{p^2x^2}{3}+p\,x\right)+Be^{-(p+1)\,x}\left(\frac{2px^2}{3}+(p+1)\,x\right)\right.$$
$$\left.+\,W_0\,e^{-x}\left(1+Be^{-(p-1)x}p\right)x+\frac{\mu^4}{4}\right]. \tag{3.25}$$

Clearly, the essential parameters now are W_0, B, p, μ and Λ.

This potential has either one (AdS) or two extrema at finite x. Without uplifting, the latter are either both AdS or one Minkowski and one AdS [55, 77]. Upon adding the uplifting sector, the first of them (i.e., the one that occurs at smaller value of x) becomes dS, see Figure 3.2.

As before, one can again argue that the position of this extremum is very close to the position of the original supersymmetric vacuum and therefore the gravitino mass is given by

$$m_{3/2} \sim \frac{a^3}{2x^3}\frac{\mu^4}{4}\ . \tag{3.26}$$

However, differently from the one exponential case studied above, now the potential barrier separating the two minima is not uniquely linked to the gravitino mass but also to other parameters in the superpotential such as B. This gives the freedom to have a small gravitino mass while keeping the potential barrier high. Also, one again finds that the field S is stabilized at $S = \bar{S} = \frac{\sqrt{3}}{6}\Lambda^2$ [61].

3.4 One-loop effective potential at finite T

In the following we will be interested in the one-loop finite temperature effective potential for the O'KKLT model. We will compute the effective potential in the classical background:

$$\langle \rho \rangle = \langle \bar{\rho} \rangle = \sigma \,, \qquad \langle S \rangle = \langle \bar{S} \rangle = s \,. \tag{3.27}$$

As one can notice, we are using the same notation for the above vevs as for the real and imaginary parts of the fields ρ and S. This is convenient since the classical potential is always understood to be evaluated in a classical background which in our case is (3.27). This abuse of notation should not cause any confusion; it will always be clear from the context what we mean.

In the rest of this section we will concentrate on the temperature-dependent part, V_T, of the effective potential. The reason is that at high temperature it is expected that V_T dominates the behaviour of V_{eff}.

As announced in the Introduction we will work in the approximation that the moduli are in thermal equilibrium and postpone a detailed analysis about the issue of moduli thermalization when we consider the more phenomenological appealing LARGE Volume compactifications in the next chapter. For the time being, we recall that, as discussed in section 2.3.2, quite generically the moduli fields are in thermal equilibrium with matter until the temperature drops to $T = M_P$. From then on, the moduli decouple from the thermal bath. However, as argued in [65], because gravitational interactions keep all species in equilibrium for $T \gtrsim M_P$, there is no difference in temperature between moduli and matter fields from $T = M_P$ until there is a substantial reheating of ordinary matter which in general takes place at $T = M_{GUT}$. For example, in the case of strong interactions, matter fields reach thermal equilibrium for temperatures of the order of 10^{15} GeV. Thus for $M_{GUT} < T < M_P$, moduli fields and ordinary matter, although decoupled, are at the same temperature.

We now proceed to the study of the temperature-dependent potential describing the self-interactions of the moduli fields. As before, we will confine our considerations to the region of field space, in which s is small. So, similarly to (3.10), we can expand the temperature-dependent part of the effective potential as:

$$V_T = V_T^{(0)} + V_T^{(1)} s + V_T^{(2)} s^2 + \mathcal{O}(s^3). \tag{3.28}$$

Applying formulae (2.53) and (2.54) for K and W given by (3.7), one finds:

$$\begin{aligned} V_T^{(0)} &= \frac{T^2}{24}\frac{1}{\sigma^3}\left[\frac{\mu^4}{\Lambda^2}+\frac{1}{2}W_0^2+W_0\left(f-\frac{13}{3}\sigma f'+2\sigma^2 f''\right)\right. \\ &+ \left.\frac{f^2}{2}-\frac{13}{3}\sigma f f'+\sigma^2\left(\frac{25}{9}(f')^2+2ff''\right)-\frac{8}{3}\sigma^3 f' f''+\frac{2}{3}\sigma^4(f'')^2\right] \qquad (3.29a) \\ V_T^{(1)} &= -\frac{T^2}{12}\frac{\mu^2}{\sigma^3}\left[\frac{1}{\Lambda^2}(W_0+f)-\frac{11}{3}\sigma f'+\sigma^2 f''\right] \qquad (3.29b) \\ V_T^{(2)} &= \frac{T^2}{24}\frac{1}{\sigma^3}\left[22\frac{\mu^4}{\Lambda^4}+\frac{W_0^2}{\Lambda^2}+W_0\left(\frac{2}{\Lambda^2}f-\frac{22}{3}\sigma f'+2\sigma^2 f''\right)\right. \\ &+ \left.\frac{1}{\Lambda^2}f^2-\frac{22}{3}\sigma f f'+\sigma^2\left(\frac{34}{9}(f')^2+2ff''\right)-\frac{8}{3}\sigma^3 f' f''+\frac{2}{3}\sigma^4(f'')^2\right] \qquad (3.29c) \end{aligned}$$

Here, in expressions like $3+1/\Lambda^2$ we have kept only the last term since $\Lambda^2 \ll 1$. Also, it is understood that $f' \equiv \langle\, \partial f/\, \partial\rho\rangle$ and $f'' \equiv \langle\, \partial^2 f/\, \partial\rho^2\rangle$ [6]. Note that, similarly to Section 3.3, the value of s at the minimum is

$$s_{min} = -\left.\frac{V_T^{(1)}}{2V_T^{(2)}}\right|_{\sigma=\sigma_{min}}\,, \qquad (3.30)$$

up to $\mathcal{O}(s^3)$ in V_T.

Let us now take a more careful look at the temperature-dependent effective potential V_T for each of the two cases in (3.8). We will concentrate on the leading contribution $V_T^{(0)}$. At the end we will check that (3.30) gives $|s_{min}| \ll 1$, as in the zero-temperature case, and so the zeroth order of the s-expansion in (3.28) is indeed a good approximation for V_T.

3.4.1 One exponential

We consider first

$$f(\rho) = Ae^{-a\rho} \quad \text{, i.e.} \qquad W = W_0 + Ae^{-a\rho} - \mu^2 S\,. \qquad (3.31)$$

Similarly to the $T=0$ case, one can use $f' = -af$ and $f'' = a^2 f$ to get rid of all derivatives. Then, after introducing the variable $x = a\sigma$, one has:

$$V_T^{(0)} = \frac{T^2}{24}\frac{a^3}{x^3}\left[P_4(x)f^2 + W_0 P_2(x) f + C_0\right], \qquad (3.32)$$

[6] Obviously $\langle\, \partial f/\, \partial\rho\rangle = \langle\, \partial\bar{f}/\, \partial\bar{\rho}\rangle$.

where

$$\begin{aligned} P_4(x) &= \frac{2x^4}{3} + \frac{8x^3}{3} + \frac{43x^2}{9} + \frac{13x}{3} + \frac{1}{2}\,, \\ P_2(x) &= 2x^2 + \frac{13x}{3} + 1\,, \end{aligned} \tag{3.33a}$$

and

$$C_0 \equiv \frac{\mu^4}{\Lambda^2} + \frac{W_0^2}{2}\,. \tag{3.34}$$

So the extrema are determined by:

$$\frac{\partial V_T^{(0)}}{\partial \sigma} = -\frac{T^2}{24}\,\frac{a^4}{x^4}\big(C + P_5(x)e^{-2x} + W_0 P_3(x)e^{-x}\big) = 0\,, \tag{3.35}$$

where $C \equiv 3C_0$ and

$$\begin{aligned} P_5(x) &= \frac{3}{2} + \frac{29}{3}x + \frac{121}{9}x^2 + \frac{86}{9}x^3 + \frac{14}{3}x^4 + \frac{4}{3}x^5\,, \\ P_3(x) &= 3 + \frac{29}{3}x + \frac{19}{3}x^2 + 2x^3\,. \end{aligned} \tag{3.36}$$

As in the zero temperature case, the constant a is just an overall rescaling which does not affect the presence or absence of minima. Also, the constant A can again be reduced to an overall rescaling by redefining $W_0 \to AW_0$ and $\mu^2 \to A\mu^2$. So again we can set $A = 1$ without loss of generality. Of course, this is not a surprise; as we are describing the same system at $T = 0$ and $T \neq 0$, we should have the same parameters in both cases.

Looking at (3.35), one immediately sees that an obvious minimum of $V_T^{(0)}$ is obtained for $x \to \infty$. However, we are interested in solutions at finite field vevs. In other words, we would like to solve

$$C + P_5(x)e^{-2x} + W_0 P_3(x)e^{-x} = 0\,, \tag{3.37}$$

or equivalently:

$$e^{2x} = -C^{-1}(P_5(x) + W_0 P_3(x)e^{x}) \equiv H(x)\,. \tag{3.38}$$

Unfortunately, this equation cannot be solved analytically. Clearly though, its solutions (and, in fact, the presence or absence of such) depend(s) on the values of the parameters C and W_0. In Appendix 3.B we use the method described in Appendix 3.A in order to show that (3.38) *does not* have any solutions for parameters such that the zero-temperature potential has a dS minimum at finite x (equivalently, at finite

σ). This is not trivial as removing the restriction for the existence of a dS minimum at $T = 0$, for instance by taking $\mu = 0$ and so completely turning off the uplifting, one finds that $V_T^{(0)}$ *can* have a minimum at finite σ. See Figure 3.3 for an explicit example.

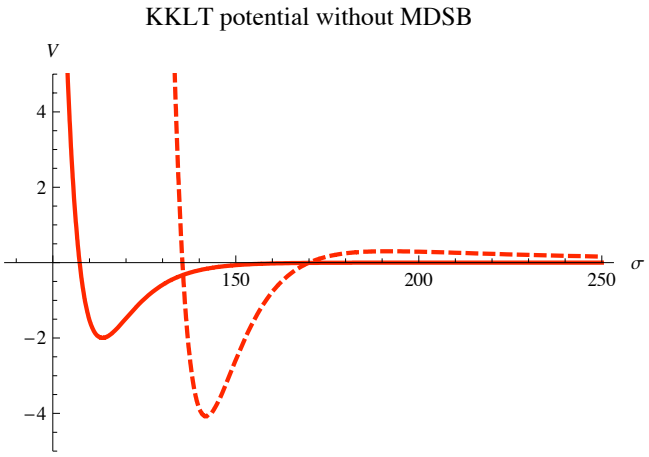

Figure 3.3: KKLT potential prior to uplifting (multiplied by 10^{15}) for the parameter values $W_0 = -10^{-4}$ and $a = 0.1$. One can see that, unlike the case with MDSB sector, both the zero temperature potential (red continuous line) and the finite temperature part (red dashed line) have a minimum for finite vev of σ. (For convenience, the graph of the temperature-dependent part is actually a plot of $V_T/(\frac{T^2}{24})$ vs σ.

3.4.2 Two exponentials

Now we turn to the second case in (3.8). Namely, we consider

$$f(\rho) = Ae^{-a\rho} + Be^{-b\rho}\,. \tag{3.39}$$

In terms of $x = a\sigma$ and $p = b/a$ one has from (3.29):

$$\begin{aligned} V_T^{(0)} \;=\; & \frac{T^2}{24}\frac{a^3}{x^3}\Big[e^{-2x}P_4(x) + B^2e^{-2p\,x}P_4(p\,x) + Be^{-(p+1)x}\,Q_4(x) \\ & + W_0\left(e^{-x}P_2(x) + e^{-p\,x}P_2(p\,x)\right) + C_0\Big]\,, \end{aligned} \tag{3.40}$$

where the polynomials P_2, P_4 were defined in (3.33) and

$$Q_4(x) = P_2(x) + P_2(p\,x) - 1 + \frac{2p\,x^2}{3}\left(2p\,x^2 + 4(1+p)x + 25\right)\,. \tag{3.41}$$

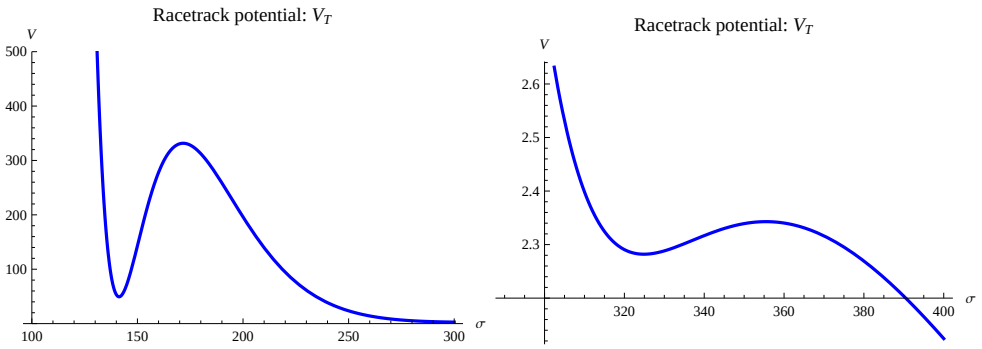

Figure 3.4: Temperature-dependent part of the effective potential (multiplied by 10^{15}) in the case of a race-track type superpotential for parameter values: $a = \pi/100$, $B = -1.028$, $p = \frac{100}{99}$, $W_0 = -2.4 \times 10^{-4}$, $\mu = 0.66 \times 10^{-3}$, $\Lambda = 10^{-3}$. One can see that there are two local minima at finite σ; note also that the second one (right) is significantly shallower than the first (left). As in Figure 3.3, for convenience we have actually plotted $V_T/(\frac{T^2}{24})$ vs σ.

Unlike in the previous subsection, $V_T^{(0)}$ of (3.40) *can* have finite σ minima for parameters, for which V_0 has a dS vacuum. This is examplified in Figure 3.4 for a particular choice of parameters. Thus, in the next section we will concentrate on investigating the phase structure of the system for the case of two exponentials in the non-perturbative superpotential.

3.5 Phase structure at finite T

In this section we study the finite temperature phase structure of the O'KKLT model with two exponentials in the superpotential. Let us first summarize the necessary ingredients of the setup and the questions we would like to address.

As we reviewed in Subsection 3.3.2, the zero temperature potential generically has two minima with finite field vevs. The same is true also for $V_T^{(0)}$ (see Figure 3.4). One naturally expects that at high temperature the system is in a local minimum of the temperature-dependent part of the effective potential. We assume that this starting point is the lower-x minimum of $V_T^{(0)}$ [7]. Then, as the temperature decreases, a point will be reached at which a second order phase transition will occur and the system will start rolling towards one of the zero temperature minima. The critical

[7] This is preferable than the other finite-x minimum, as the latter one is much shallower. Of course, if one were to start from the global minimum, which is at infinity, then clearly there would be nothing to discuss − the system would remain there at any temperature and so one would have the undesirable situation of decompactified internal space at $T = 0$.

temperature T_c for this to happen, as well as the relevant field space position x_c, can be found by solving the following set of equations:

$$V'_{eff}(T_c, x_c) = 0 \qquad \text{and} \qquad V''_{eff}(T_c, x_c) = 0\,, \tag{3.42}$$

where $'$ denotes d/dx. We would like to know whether as a result of this phase transition the system will start rolling towards the zero-temperature dS vacuum or in the opposite direction, *i.e.*, towards the $T=0$ supersymmetric vacuum [8]. Clearly, this would be determined by the sign of $V'''_{eff}(T_c, x_c)$.

Note that for systems with $x \to -x$ symmetry, as is the case for the ISS model for example (see [58]), the origin of field space is a local minimum of V_{eff}. If one takes this as the starting point at high T, then the first equation in (3.42) is identically satisfied. So, from the second equation, one is left with the familiar

$$V''_T = -m^2 \tag{3.43}$$

as the condition that determines T_c of a second order phase transition. Recall that m^2 here is the classical mass, clearly originating from V_0, of the scalar field with nonzero background vev. In our case however, none of the equations in (3.42) is trivial and so we have to solve simultaneously both of them.

To facilitate our considerations, let us change variables to the real components of the fields: $\rho = \mathrm{Re}\rho + i\mathrm{Im}\rho$, $\bar{\rho} = \mathrm{Re}\rho - i\mathrm{Im}\rho$. As in the background (3.27) one has $\langle \mathrm{Re}\rho \rangle = \sigma$ and $\langle \mathrm{Im}\rho \rangle = 0$, clearly the field $\mathrm{Re}\rho$ is the one that drives the phase transition we are after. So (3.42) acquires the form:

$$\frac{\partial V_T}{\partial x} = -\frac{\partial V_0}{\partial x}\,, \qquad \frac{\partial^2 V_T}{\partial x^2} = -m^2_{\mathrm{Re}\rho}, \tag{3.44}$$

where in the second equation we have used that $\partial_x^2 V_0(x) = m^2_{\mathrm{Re}\rho}(x)$. One can compute the first and second derivatives of V_0 and V_T using (3.25) and (3.40), respectively. Before turning to that however, let us first show that the variables $\mathrm{Re}\rho$ and $\mathrm{Im}\rho$ diagonalize the classical mass matrix.

[8] As we will see below, the finite T minimum, that is our starting point, is always between the dS and the susy $T=0$ vacua.

3.5.1 Mass matrix

From (2.32) one can easily find the tree-level mass-squared matrix in the background (3.27)[9]. It is of the form:

$$M = \begin{pmatrix} m^2_{\rho\rho} & m^2_{\rho\bar\rho} \\ m^2_{\bar\rho\rho} & m^2_{\bar\rho\bar\rho} \end{pmatrix}, \tag{3.45}$$

where $m^2_{\rho\bar\rho} \equiv \langle \partial_\rho \partial_{\bar\rho} V_0 \rangle = \partial_\rho \partial_{\bar\rho} V_0|_{\rho=\bar\rho=\sigma,\, S=\bar S=0}$ etc. with all matrix elements being nonzero and $m^2_{\rho\rho} = m^2_{\bar\rho\bar\rho}$, $m^2_{\rho\bar\rho} = m^2_{\bar\rho\rho}$. It is clear then, that the real components of ρ have diagonal mass matrix with masses[10]:

$$m^2_{\mathrm{Re}\rho} = 2\left(m^2_{\rho\bar\rho} + m^2_{\rho\rho}\right), \qquad m^2_{\mathrm{Im}\rho} = 2\left(m^2_{\rho\bar\rho} - m^2_{\rho\rho}\right). \tag{3.46}$$

In terms of a generic function $f(\rho)$ in (3.7), these expressions are:

$$\begin{aligned} m^2_{\mathrm{Re}\rho} &= \frac{1}{6\sigma^5}\Big[9\mu^4 + 3W_0\left(-6\sigma f' + 4\sigma^2 f'' - \sigma^3 f^{(3)}\right) \\ &\quad -18\sigma f f' + 2\sigma^2\left(7(f')^2 + 6 f f''\right) - \sigma^3\left(13 f' f'' + 3 f f^{(3)}\right) + 2\sigma^4\left((f'')^2 + f' f^{(3)}\right)\Big] \end{aligned} \tag{3.47a}$$

$$m^2_{\mathrm{Im}\rho} = \frac{1}{6\sigma^5}\left[3W_0\,\sigma^3 f^{(3)} - 3\sigma^3\left(f' f'' - f f^{(3)}\right) + 2\sigma^4\left((f'')^2 - f' f^{(3)}\right)\right]. \tag{3.47b}$$

Specializing (3.47) to the case of two exponents and introducing $x = a\sigma$ and $p = b/a$ as before, we can also write:

$$\begin{aligned} m^2_{\mathrm{Re}\rho} &= \frac{a^5}{3x^5}\Big[e^{-2x} R_4(x) + B^2 e^{-2p\,x} R_4(p\,x) + B e^{-(p+1)x} S_4(x) \\ &+ W_0\left(e^{-x} R_3(x) + B e^{-p\,x} R_3(p\,x)\right) + \frac{9\mu^4}{2}\Big], \end{aligned} \tag{3.48}$$

where

$$\begin{aligned} R_4(x) &= 2x^4 + 8x^3 + 13x^2 + 9x\,, \qquad R_3(x) = \frac{3x^3}{2} + 6x^2 + 9x\,, \\ S_4(x) &= R_3(x) + R_3(p\,x) + p x^2\left[14 + (p+1)x\left((p+1)x + \frac{13}{2}\right)\right], \end{aligned} \tag{3.49}$$

[9] As before, we only consider the zeroth order in the s-expansion.

[10] Obviously, the matrix M is diagonalized by the change of variables $\rho_+ = \frac{\rho+\bar\rho}{\sqrt{2}}$ and $\rho_- = \frac{\rho-\bar\rho}{\sqrt{2}}$ with the corresponding eigenvalues being $m^2_{\rho_\pm} = m^2_{\rho\rho} \pm m^2_{\rho\bar\rho}$. On the other hand, $\rho_+ = \sqrt{2}\,\mathrm{Re}\rho$ and so $m^2_{\mathrm{Re}\rho} = 2m^2_{\rho_+}$; similarly $m^2_{\mathrm{Im}\rho} = -2m^2_{\rho_-}$.

and

$$m^2_{\mathrm{Im}\rho} = -\frac{a^5}{2x^5}\left[Be^{-(p+1)x}(p-1)^2x^2\left((p+1)x+\frac{2}{3}p\,x^2\right)+W_0(e^{-x}+Be^{-p\,x}p^3)x^3\right]. \tag{3.50}$$

Recall that $W_0 < 0$ and so, despite the overall minus in the above formula, $m^2_{\mathrm{Im}\rho}$ is not negative definite.

3.5.2 Critical temperature

Let us now turn to solving (3.44) in order to find T_c. As we already mentioned, one can compute the relevant derivatives of V_0 and V_T from (3.25) and (3.40). However, the resulting equations are of the same type as (3.38), only significantly more complicated. Thus, one cannot hope to analyze them analytically. So we will study them numerically for various values of the parameters.

We should note first, that clearly there are many parameter values for which the system does not exhibit the behaviour we described in the beginning of this section. Namely, it could happen that even though V_0 has a dS vacuum, the only minimum that V_T has is the Minkowski one at $\langle\rho\rangle = \infty$; or it could be that, instead of two minima at finite $\langle\rho\rangle$, V_T has only one. This is similar to the situation at zero-temperature: There are many values of the parameters for which V_0 does not have a dS minimum. The important point, however, is that there are also many values for which a dS vacuum does exist at $T = 0$ [61]; they are exactly the parameter values of interest in the search for moduli stabilized dS vacua. Similarly, here we concentrate on the regime for which V_T does have at least one finite-vevs minimum *when* V_0 has a dS vacuum. The corresponding choices of parameters are exactly those for which the internal space of a dS compactification has the chance of not being destabilized by thermal effects. And that possibility is precisely what we want to explore.

Several sets of parameters, for which the system is in the desired regime, are given in Table 3.1. This table suggests that the O'KKLT model exhibits the behaviour, that we want to study, only at discrete points in parameter space. However, this is not completely true: for some of the sets one can vary somewhat one (or more) parameter(s) without exiting the regime of interest. [11] Nevertheless, it is an interesting observation that a more significant change of one parameter (with the exception of Λ)

[11] For example, in the first row μ can be anything between 8×10^{-4} and 1×10^{-3}; in the third row Λ can also be 10^{-3}; another variation of the third row is for instance $B = -1.031$, $W_0 = -1.8\times10^{-4}$, $\mu = 10^{-3}$, $\Lambda = 10^{-2}$ or 10^{-3}; in the fifth row W_0 can be anything between -3.532×10^{-4} and -3.535×10^{-4}; in the seventh row Λ can be anything between 10^{-3} and 10^{-2} etc..

B	W_0	μ	Λ	$x_{dS}^{(0)}$	$x_{AdS}^{(0)}$	$x_{min}^{(T)}$	x_c	T_c
-1.040	-7.6×10^{-5}	8×10^{-4}	10^{-2}	4.88	7.84	5.62	5.54	0.27
-1.036	-1.1×10^{-4}	2×10^{-3}	10^{-2}	4.50	7.40	5.25	5.10	0.27
-1.032	-1.64×10^{-4}	10^{-3}	10^{-2}	4.11	6.92	4.83	4.73	0.30
-1.028	-2.4×10^{-4}	0.66×10^{-3}	10^{-3}	3.73	6.44	4.44	4.31	0.30
-1.024	-3.533×10^{-4}	0.66×10^{-3}	10^{-3}	3.34	6.00	4.04	3.91	0.33
-1.020	-5.21×10^{-4}	0.95×10^{-3}	10^{-3}	2.96	5.52	3.64	3.47	0.34
-1.016	-7.67×10^{-4}	1.4×10^{-3}	10^{-2}	2.55	5.02	3.20	3.08	0.38

Table 3.1: Each row of this table represents a set of parameters for which both V_0 and V_T have minima at finite field vevs *and* the lower-x minimum of V_0 is dS. In each set $p = 100/99$ as in the examples of [61]. The positions of the minima are denoted by $x_{dS}^{(0)}$ and $x_{AdS}^{(0)}$ for V_0 and by $x_{min}^{(T)}$ for the lower-x minimum of V_T. Recall also that $x = a\sigma$ and so, taking $a = \frac{\pi}{100}$ for instance, the various minima occur for $\sigma \sim \mathcal{O}(100)$.

seems to require such a change in at least one other parameter. This pattern is there, regardless of the (runaway or not) behaviour of V_T, as long as one looks for parameter values giving dS vacua of the zero temperature potential studied in [61]. Hence, the O'KKLT model may be an example of how arguments of the kind of [87–89] might fail. Namely, in those arguments one usually varies a single constant of nature (the cosmological constant, for instance) while keeping all other coupling constants fixed. And one concludes that such variations lead to drastic changes in the resulting physics. However, it might be that in order to get to a new background, that is quite similar to the original vacuum, one has to change in a discrete way (as opposed to varying continuously) more than one constant of nature at the same time. It is conceivable then, that the above-mentioned anthropic/environmental arguments for the value of the cosmological constant could break down under such more general variations. [12] This is certainly worth investigating in more depth and within more realistic models. As one can see from Table 3.1, the V_T minimum of interest is always between the zero temperature dS and AdS vacua. So it might seem that a meaningful question to ask is whether the system rolls towards the metastable or the supersymmetric $T = 0$ vacua as it cools down. However, the critical temperature for the relevant second order phase transition turns out to be always of order 0.1 (see Table 3.1; an example is illustrated in Figure 3.5[13]). Since we work in units in which $M_P = 1$,

[12] See however [90] for arguments in favor of Weinberg's argument in the case when only the cosmological constant and the Higgs mass are varied.

[13] The graph of V_{eff} (the green continuous line) on this figure still does not include the term $\sim T^4$

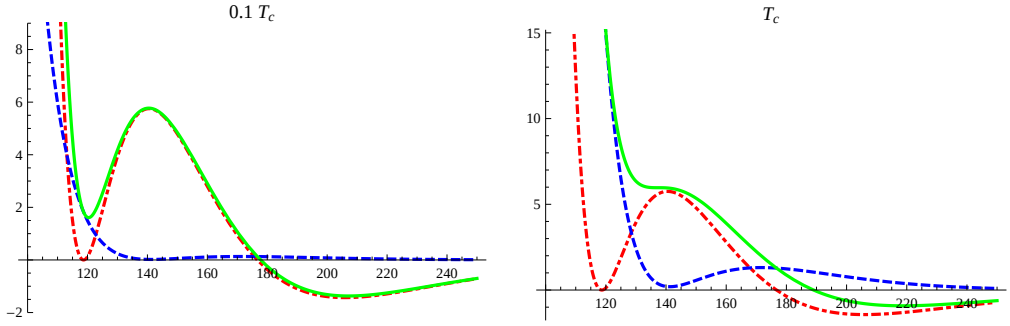

Figure 3.5: Effective potential V_{eff} (green continuous line), multiplied by 10^{15}, as a function of σ for the race-track type model compared to $V_0(\sigma)$ (red dot-dashed line) and $V_T(\sigma)$ (blue dashed line) for $T = 0.1 \times T_c$ (left) and for $T = T_c$ (right). The values of the parameters are the following: $a = \pi/100$, $B = -1.028$, $p = \frac{100}{99}$, $W_0 = -2.4 \times 10^{-4}$, $\mu = 0.6 \times 10^{-3}$, $\Lambda = 10^{-3}$; the resulting critical temperature is $T_c = 0.3$.

this means that $T_c \sim \mathcal{O}(0.1\, M_P)$. For such a high temperature the supergravity approximation is not reliable anymore and so we cannot make any statement about the occurrence or not of a phase transition.[14] Nevertheless, turning this around, we can conclude that for the whole range of validity of the supergravity approximation (i.e., for $T \ll M_P$)[15] the extrema of the effective potential of the system are determined by the zero-temperature part and not by V_T.[16]

Hence at the level of supergravity, the $T = 0$ de Sitter minimum is not destabilized by thermal effects. This is quite unexpected, not only because it turned out that V_T can have minima at finite field vevs (as opposed to having runaway behaviour discussed in [73,78]), but also because the potential barrier in V_{eff}, that separates those minima from the $T = 0$ ones, is many orders of magnitude smaller than the Planck scale (more precisely, it is $\sim 10^{-15}$; see Figure 3.5 which is a typical representative for all rows of Table 3.1) and so intuitively one might have expected thermal fluctuations

in (2.53); as the latter is x-independent, it only leads to an irrelevant for us overall shift of the V_{eff} plot down the vertical axis, which just makes it rather inconvenient to illustrate the main features of the remaining graphs on the same figure.

[14] We should note that the Planck scale is the only cut-off of concern as long as one is studying the field theory defined by (3.7) on its own, which is the viewpoint we take here. However, if one wants to view it necessarily as the low-energy effective description of the O'Raifeartaigh model that is obtained by integrating out the two heavy fields, which was the original motivation to think about it, then there is another lower cut-off. Namely, this is the scale at which the single field approximation to the full O'Raifeartaigh model stops being valid.

[15] Clearly then, this is even more so for the whole range of validity of the single field low-energy approximation to the full O'Raifeartaigh model.

[16] Note that, because of the constant term $\sim T^4$ that we are omitting, this does not mean that the magnitude of V_{eff} itself is determined by V_0.

to get the system over it at a temperature $\ll M_P$.

The above behaviour could have implications for the early Universe, if one views the O'KKLT model as a simple toy model for the latter. Namely, at the end of the inflationary stage the universe is very cold and so it would be in a local minimum of V_0.[17] Let us assume that this is the lower-x dS vacuum. Now, the exit from inflation comes with the decay of the inflaton into various other particles and the subsequent reheating of the universe to some temperature T_R. If $T_R \ll M_P$, as one expects in many phenomenological models, then after reheating the system will still be in the metastable minimum; in other words, the dS vacuum will not be destabilized by the thermal corrections.

Having in mind this new perspective, one may wonder whether the dS vacuum remains a local minimum of V_{eff} even when the temperature-dependent part of the potential does not have other minima except the runaway one at infinity (of course, as long as $T \ll M_P$). Indeed, our interest in finite-σ minima of V_T was stemming from the expectation that their presence would be the obstacle for decompactification of the internal space (whose volume σ is proportional to). However, as we saw above, in the range of validity of our considerations this obstacle turned out to be different. So it is a legitimate question to ask whether the minima of V_0 determine the minima of V_{eff} even for parameter values for which V_T has runaway behaviour. One can easily check that this is indeed the case for sets of parameters that are close to those in Table 3.1, but such that V_0 still has a dS vacuum while V_T does not have any finite-x minima.

Before concluding this section, let us note that one can easily verify from (3.48) and (3.50) that $m^2_{\mathrm{Re}\rho}$ and $m^2_{\mathrm{Im}\rho}$ are quite small for all sets of parameters in Table 3.1. That is, there is an appreciable interval for the temperature T, given by $m_{\mathrm{Re}\rho},\ m_{\mathrm{Im}\rho} \ll T \ll M_P$, in which the high-temperature expansion (2.53) is well-justified. Clearly, if the minima of the effective potential are determined by V_0 (instead of by V_T) in this interval, they will remain determined by V_0 at lower temperatures as well. Finally, one can also check from (3.30) that, similarly to the zero-temperature case, the potential $V_T(x, s)$ stabilizes the variable s at a value $|s| \ll 1$ and so the leading term in the small-s expansion is indeed a good approximation for the full expression.

[17] Note that the volume modulus σ *should not* be confused with the inflaton field.

3.6 One exponential revisited

As we saw in the previous section, in the case of two exponents the stabilization of the zero temperature dS vacuum at finite temperatures is not due to the presence of a local minimum of V_T at finite field vevs. Rather, it comes from the fact that the minima of V_{eff} are determined by the $T = 0$ contribution, and not by the temperature-dependent one, even at high T, as long as $T \ll M_P$. Given that, it is worth to re-examine the one-exponential case in order to see whether there is a range of parameter values for which the same thing happens in this case too.

Since the T-dependent contribution to the effective potential has runaway behaviour (see Section 3.4.1), the dS minimum of V_0 is completely washed out in the total potential only when the magnitude of V_T is much larger than the magnitude of V_0 at the position of this minimum x_{dS}. Recall that in the O'KKLT model with one exponential in the superpotential, the potential barrier separating the metastable dS minimum from the 10D Minkowski vacuum at infinity is "coupled" to the value of the gravitino mass at the AdS minimum: in particular it is given by $V_{\rm b} \sim m_{3/2}^2 M_P^2$. If we examine the equation (3.32) that gives the leading finite temperature correction, it is easy to see that around $x_{\rm dS}$ the leading contribution is

$$V_T^{(0)} = \frac{T^2}{24}\frac{a^3}{x_{\rm dS}^3}\frac{\mu^4}{\Lambda^2} \sim \frac{T^2}{24\Lambda^2} m_{3/2}^2 M_P^2 \tag{3.51}$$

Requiring that $V_T^{(0)} \lesssim V_b$, we obtain that the maximal temperature is

$$T_{\rm max} \lesssim \Lambda \ . \tag{3.52}$$

At this point it may useful to recall that Λ is a particular combination of parameters in the O'Rafeartaigh sector, namely $\Lambda \sim \frac{4\pi m}{\lambda^2}$, where the parameters m and λ appear in the superpotential $W_{O'} = m\varphi_1\varphi_2 + \lambda S\varphi_1^2 - \mu^2 S$ and we integrate out the heavy fields ϕ_1 and ϕ_2.

Thus, when $T < \Lambda$ the zero temperature minimum persists in V_{eff}, whereas for $T > \Lambda$ the effective potential has the runaway behaviour of V_T; see Figure 3.6 for an example.[18] Clearly, for $\Lambda \sim \mathcal{O}(10^{-2})$ the finite-x minimum of V_0 is not washed out by V_T in the whole range of validity of supergravity. For any smaller Λ, though, this is not the case; the critical temperature above which V_{eff} has a runaway behaviour is well within the range $T \ll M_P$ and so one can reliably conclude that there is a

[18] Recall that these inequalities are only order-of-magnitude estimates; the transition does not have to happen precisely at $T = \Lambda$, only at T that is of $\mathcal{O}(\Lambda)$.

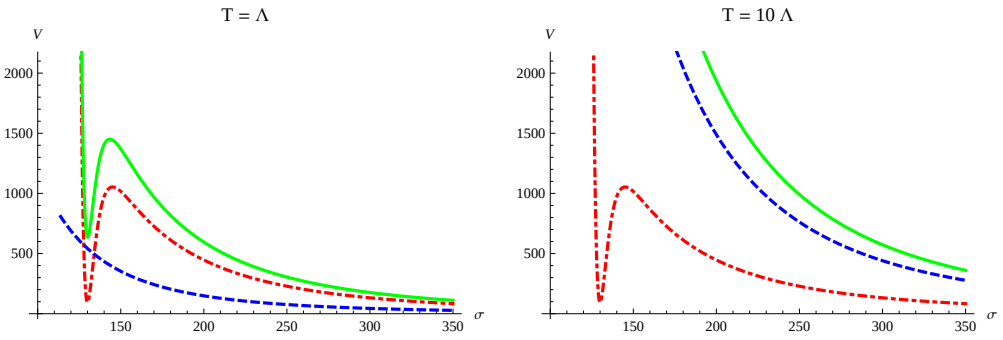

Figure 3.6: Effective potential (multiplied by 10^{30}) for the one exponential case (green continuous line) compared to V_0 (red dot-dashed line) and V_T (blue dashed line) for $T \approx \Lambda$ (left) and $T \approx 10\Lambda$ (right). The values of the parameters are the following: $a = 0.2$, $W_0 = -10^{-10}$, $\mu = 1.3 \times 10^{-5}$, $\Lambda = 10^{-5}$.

phase transition towards the minimum at infinity.

The previous result should be compared to the maximal temperature computed in [78]. There, it was assumed that the moduli are not in thermal equilibrium and thus temperature corrections come from the thermal bath of radiation whose energy density scales with temperature as T^4. In that case one obtains

$$T_{\max} \lesssim \sqrt{m_{3/2} M_P} \ . \tag{3.53}$$

We learn already at this point that if the potential at high temperatures is runaway, the maximal temperature above which the zero temperature metastable minimum is washed away depends on the particular 4D effective Kähler potential and superpotential and on whether or not the moduli are in thermal equilibrium. Both conditions depend on the particular string compactification scenario considered and on the particular D-brane setup used to build the MSSM. We will study these issues in detail in the context of the more "realistic" LARGE Volume compactifications in chapter 4.

3.7 Conclusions

In this chapter, we studied the one-loop temperature corrections to the effective potential of the O'KKLT model in the hypothesis [65] that the moduli and the MDSB sectors are in thermal equilibrium at high temperatures.

It turns out that, when the non-perturbative superpotential contains only one exponent, the temperature dependent part V_T has runaway behaviour. For a superpotential with two exponentials, on the other hand, V_T *can* have minima at finite field

vevs. Surprisingly however, the minima of V_{eff} still turned out to be determined by the minima of the zero-temperature contribution, in the range of validity of supergravity. So, although our initial motivation was to see how the system evolves as T decreases, assuming that it started at a finite-vevs minimum of V_T, we ended up with a quite different interpretation of our results. Namely, that there is a regime in which reheating does not destabilize the zero-temperature de Sitter minimum of the volume modulus in the O'KKLT model (in the supergravity approximation). These results agree with the dynamical analysis at finite temperature performed in [73].

Note that the existence of this regime is in stark contrast with the situation in [58] (and the coupling of that model to supergravity [59]), where the relevant critical temperature was found to be $T_c \ll M_P$. The main differences between their model and the one we studied here are that in our case the superpotential contains exponentials, in addition to polynomials in the fields, and the Kähler potential is non-canonical. It would be interesting to understand which of these two features is more essential, and to what degree, in order to obtain the kind of result that we did.

In the next chapter, we will determine whether our conclusions about the finite temperature behaviour of the O'KKLT model persist in more realistic cases, like the LARGE volume compactifications of [30, 62].

Appendix 3.A Counting solutions of $e^x = F(x)$

In the main text, we will encounter on plenty of occasions equations of the type

$$e^{cx} = F(x)\,, \tag{3.54}$$

where x is a real variable, c is a constant and $F(x)$ is an expression containing (ratios) of polynomials and possibly other exponentials. In general, the analytic solution of this equation is not known.[19] Nevertheless, one can find an upper bound on the number of its solutions, as we explain below.

For simplicity, let us take $c = 1$ in the rest of this appendix; the generalization for arbitrary c will be obvious. Since e^x is a monotonically increasing function, if F were monotonically decreasing (and continuous, which will always be the case) then clearly there could be only one or zero solutions depending on whether the value of F is greater or smaller than the value of the exponential in the beginning of the interval of interest. The difficult case to analyze is when F is also monotonically increasing;

[19] In the very simple case $F = x^m$ it is. However, we will have to deal with significantly more complicated functions F.

we will turn to it in a moment. Generically, in the cases of interest for us F will not be monotonic. However, one can split the interval, that one wants to solve (3.54) in, into subintervals in which it is monotonic by considering the equation[20]

$$F'(x) = 0\,, \tag{3.55}$$

where $'$ denotes d/dx. Let us denote by $y_1, ..., y_m$ the solutions of (3.55), where for convenience we have assumed the ordering $y_j < y_{j+1}$ for every $j = 1, ..., m$. In each interval (y_j, y_{j+1}) the function F is monotonic: monotonically increasing if $F' > 0$ for $x \in (y_j, y_{j+1})$ and monotonically decreasing if $F' < 0$ for $x \in (y_j, y_{j+1})$.[21] As already mentioned above, the intervals in which F is decreasing are trivial to analyze. So let us from now on consider an interval (y_k, y_{j+1}) such that in it $F' > 0$.

To recapitulate, we are considering now the equation

$$e^x = F(x) \tag{3.56}$$

in an interval (y_k, y_{k+1}) such that

$$\forall x \in (y_k, y_{k+1}) : \qquad F'(x) > 0\,. \tag{3.57}$$

In other words, in the interval of interest the function F does not have any extrema or inflection points (nor any divergences except possibly at the end points y_k and y_{k+1}) and is monotonically increasing. Let us denote the solutions of (3.56) by $x_1, ..., x_n$.[22] Again we assume the ordering $x_i < x_{i+1}$ $\forall i = 1, ..., n$. We should also mention that we are considering only continuous functions, i.e. both F and F' are continuous.

Now, let us take two successive solutions, say x_1 and x_2. If at x_1 the derivative of one side of (3.56) is greater than the derivative of the other, say

$$F'(x_1) > e^{x_1}\,, \tag{3.58}$$

then clearly at x_2 the opposite inequality, or at least equality, has to be satisfied, i.e. $F'(x_2) < e^{x_2}$ or $F'(x_2) = e^{x_2}$. (Think of the tangents to the curves that represent the

[20] Here we are assuming that $F(x)$ does not diverge anywhere inside the interval of interest. Otherwise an additional division into subintervals is necessary which, although complicating the considerations, does not lead to anything new conceptually.

[21] In fact, in mathematics the term 'monotonic' refers to functions for which $F' \geq 0$ or $F' \leq 0$. The case when $F' > 0$ or $F' < 0$ is called 'strictly monotonic'. Since in our context it is clear what we mean, we will drop the adjective 'strictly' so as not to burden the language unnecessarily.

[22] Unless stated otherwise, from now on we mean solutions in the interval (y_k, y_{k+1}).

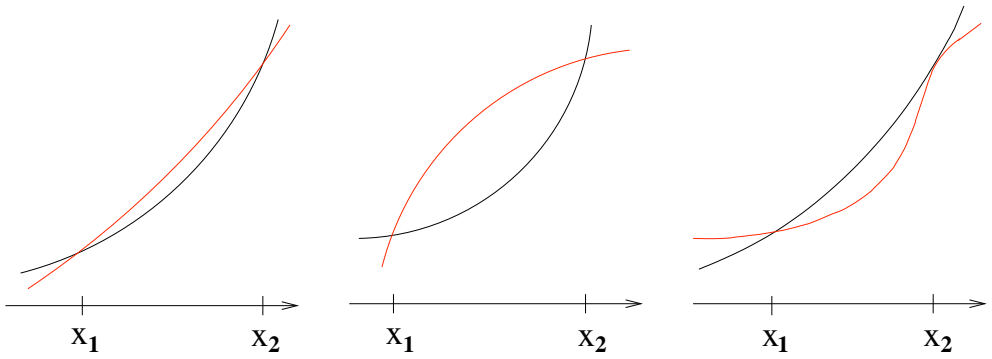

Figure 3.7: Schematic depiction of the possible ways of intersection of two monotonically increasing functions, $f_1(x)$ and $f_2(x)$, at two successive solutions of $f_1(x) = f_2(x)$ for the case when $f_1'(x) = f_2'(x)$ has a single solution in the interval (x_1, x_2).

graphs of the functions at the two intersection points; see Figure 3.7.) Let us first consider the case when

$$F'(x_2) < e^{x_2}\,. \tag{3.59}$$

Since F' is a continuous function, equations (3.58) and (3.59) imply that there has to exist a point $t \in (x_1, x_2)$ such that $F'(t) = e^t$. In other words, between two successive solutions of (3.56) there is at least one solution of

$$e^x = F'(x)\,. \tag{3.60}$$

Although slightly less obvious, the same conclusion can be reached also for the case when $F'(x_2) = e^{x_2}$. Indeed, if $F'(x) > e^x$ at x_1 and at every point between x_1 and x_2, then it is not possible that at x_2 the two functions are equal. (Think of two points moving on a straight line, the vertical axes, with different velocities. If they start from the same place at a moment of time x_1 and one is always slower than the other up until the moment x_2, then it is not possible that they meet at the moment x_2.) It has to be true that at least in some part of the interval (x_1, x_2) the opposite inequality $F'(x) < e^x$ is satisfied in order for x_2 to be a solution. Therefore, again there has to be a point in between x_1 and x_2, in which the derivatives of the two functions are equal.

So we conclude that between each two successive solutions of (3.56) there has to be at least one solution of (3.60). Let us denote the number of solutions of the latter equation by p. Then the above considerations are summarized by the following

statement about the number of solutions, n, of (3.56):

$$n \leq p + 1\,. \tag{3.61}$$

One reason that the RHS of (3.61) is just an upper bound and not the exact number of solutions of (3.56) is the possibility, that we already considered above, for a solution x_l of (3.56) to also be a solution of (3.60).[23] Another is that the function F could 'wobble' as in Figure 3.8[24] and so there could be more than one solution of (3.60) between two successive solutions of (3.56).

It is clear now what is the algorithm for counting (or rather putting an upper bound on) the number of solutions of $e^x = F(x)$. Namely, first find the solutions $\{y_j\}_{j=1}^m$ of $F'(x) = 0$ and then in each interval (y_j, y_{j+1}), where y_0 and y_{m+1} are resp. the beginning and the end of the interval in which we are solving $e^x = F(x)$, count the solutions of $e^x = F'(x)$. If F' is still a complicated function, it may not be immediately obvious that it is a significant improvement to consider the latter equation rather than the original one. However, clearly one can develop a recursion, i.e. as a next step view $e^x = F'(x)$ as the starting point for the above considerations and so find the solutions of $F''(x) = 0$. Then in each interval between two successive ones look for the number of solutions of $e^x = F''(x)$ etc. until one reaches a rather simple equation.[25] This procedure is exactly the tool that enables us in Appendix B to prove that there are no local minima of V_T for finite ρ in the original KKLT proposal (i.e., with a non-perturbative superpotential given by a *single* exponential) for the range of parameters for which the zero temperature potential has a dS minimum.

Appendix 3.B No finite-ρ minima of V_T for one-exponential case

In this Appendix we show that the equation

$$e^{2x} = -C^{-1}\left(P_5(x) + W_0 P_3(x) e^x\right) \equiv H(x) \tag{3.62}$$

does not have any solution whenever $|W_0|$ and μ^2 are of the same order of magnitude, which is the condition (3.15) for the presence of dS vacua with a small cosmological

[23] Clearly, if two successive solutions of (3.56) solve (3.60) too, then the inequality in (3.61) only gets stronger.

[24] Recall that in general its second (and higher) derivative(s) is (are) also nontrivial function(s) of x.

[25] Of course, here we assume that all relevant derivatives of F are continuous.

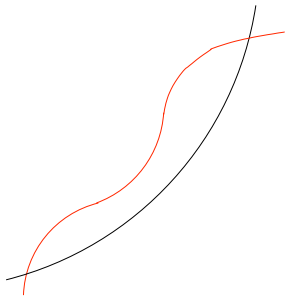

Figure 3.8: Schematic depiction of two monotonically increasing functions $f_1(x)$ and $f_2(x)$, which exemplifies how the equation $f_1'(x) = f_2'(x)$ can have more than one solution between two successive solutions of $f_1(x) = f_2(x)$.

constant at zero temperature.

Following the logic of Appendix A, we consider as a first step the equation $H'(x) = 0$, where $'$ denotes differentiation w.r.t. x. The strategy is to split the half axes $[0, \infty)$ into intervals in which the function H is monotonic (the intervals between successive solutions of $H' = 0$ plus, of course, the interval to the left of the smallest solution and the interval to the right of the largest one) and find bounds on the number of solutions of (3.62) in each such interval.

Let us write the equation $H' = 0$ in the form:

$$e^x = -\frac{1}{W_0}\frac{29 + \frac{242}{3}x + 86x^2 + 56x^3 + 20x^4}{38 + 67x + 37x^2 + 6x^3} \equiv -\frac{1}{W_0}\frac{P_4}{\hat{P}_3} \equiv h(x)\,. \tag{3.63}$$

Clearly, we are again facing a transcendental equation of the type (3.54). Nevertheless, things have improved significantly since now we have on the RHS a function that we can fully analyze. As all coefficients of both polynomials P_4 and $\hat{P}_3$ are positive (and zero is obviously not a root of any of them), $h(x)$ does not diverge anywhere in the interval $[0, \infty)$ and is a monotonic function there. Hence (3.63) has a single solution when $h(x)|_{x=0} \geq e^x|_{x=0} = 1$.[26] So we find that $-0.76 \leq W_0 < 0$. Since for the uplifting of the local zero-temperature minimum to dS one needs $|W_0| \approx \mu^2 \ll 1$, clearly for the case of interest for us the equation $H'(x) = 0$ has one solution. Let us denote it by x_0. One can find x_0 numerically[27] and one can verify that $H'(x) < 0$ for

[26] For an arbitrary function $h(x)$ this would only be true if it were monotonically decreasing, unlike the case at hand. However, the rational function $P_4/\hat{P}_3$ approaches the behavior of its asymptote, $\frac{10}{3}x$, around $x \sim 10$ and so if it does not cross e^x for smaller x it never does. One easily sees, by plotting the two functions for $x \in [0, 10]$, that they can intersect only if $h(x)$ was the greater function at $x = 0$.

[27] As equation (3.63) depends on the value of W_0 so does x_0. For $|W_0| = 10^{-1}, 10^{-2}, ..., 10^{-6}$ it is $x_0 = 4.6,\ 7.5,\ 10.2,\ 12.7,\ 15.3$, and 17.7 respectively. However, the conclusions of our subsequent

$x < x_0$ and $H'(x) > 0$ for $x > x_0$.

Hence we have determined that there are two intervals in which the function $H(x)$ is monotonic: $[0, x_0)$ and $[x_0, \infty)$. In fact, we can discard the first of them immediately. The reason is that $H' < 0$ in it and that in its beginning $H(0) < 0$ for any W_0 in the range of interest (as mentioned above, this means $|W_0| \ll 1$). Therefore $H(x)$ remains negative throughout the whole interval and so cannot be equal to e^{2x} at any x there. So from now on we will only consider $x \in [x_0, \infty)$.[28]

According to Appendix A, we have to aim now at counting the number of solutions of $(e^{2x})' = H'(x)$ in this interval. However, this is still a rather complicated equation. So we go to the next level of iteration by considering it as the starting point and looking for the solutions of $H''(x) = 0$ in order to find the intervals in which H' is monotonic. For that purpose, let us write $H''(x) = 0$ in the following way:

$$e^x = -\frac{1}{W_0}\,\frac{\frac{242}{9} + \frac{172}{3}x + 56x^2 + \frac{80}{3}x^3}{35 + 47x + \frac{55}{3}x^2 + 2x^3} \equiv r(x)\,. \tag{3.64}$$

It is obvious that, similarly to $h(x)$, the function $r(x)$ does not diverge anywhere in the interval of interest and is monotonic in the whole of it. However, at the beginning of this interval $e^{x_0} > r(x_0)$ and hence (3.64) does not have any solution.[29] Then one easily verifies that $H''(x) > 0$ for any $x \in [x_0, \infty)$. Unfortunately though, the equation $(e^{2x})'' = H''(x)$ is still not simple enough for us to be able to count its solutions. So we have to go to the next level, i.e. look for zeros of the third derivative, $H^{(3)}(x)$.

However, at this point it is clear how the iteration procedure will converge. Each further derivative decreases the power of the polynomial in the numerator, until what started as $P_5(x)$ completely disappears. At the level of $H^{(6)}(x) = 0$ one finds the equation $2^6 e^{2x} = e^x Q_3(x)$, where $Q_3(x)$ is still a degree-three polynomial. Clearly then this becomes $2^6 e^x = Q_3$ and after 3 more differentiations one finds $e^x = const$, which can have at most one solution. Also, at each step of the procedure the corresponding derivative of $H(x)$ is easily seen to be positive-definite in the whole interval of interest. Therefore, from Appendix A it follows that for the moment we have restricted the number of solutions of (3.62) to be at most 1+6+3=10.

At first sight this may not seem very encouraging. However, recall that at the last step we arrived at an equation that can have at most one solution. More precisely, it

analysis are the same for any $|W_0| < 0.76$.

[28] Clearly, we could shift upwards the lower end of the interval of interest by taking it to be the point t at which $H(t) = 0$, since obviously $t > x_0$. However, for our subsequent considerations it will not matter whether we consider $[x_0, \infty)$ or $[t, \infty)$. So we do not bother determining t.

[29] Similar remark as in footnote 26 applies here.

is

$$2^6 e^x = \frac{12|W_0|}{C}. \tag{3.65}$$

Now, since

$$C = 3\,\frac{\mu^4}{\Lambda^2} + \frac{3}{2}W_0^2\,, \tag{3.66}$$

it is easy to see that (3.65) does not have a solution neither for the uplifted case (in which $|W_0| \approx \mu^2$ and so $C \gg W_0^2$) nor for the case with no uplifting (for example, take $\mu = 0$ and so $C \approx W_0^2$)[30]. This in turn means that the equation $(e^{2x})^{(8)} = H^{(8)}(x)$ can have at most one solution. And since $H^{(8)}$ is monotonic in the whole interval of interest, it is again very easy to verify that it too does not have any. Therefore $(e^{2x})^{(7)} = H^{(7)}(x)$ can have at most one solution etc.. Actually, we should mention that the equation$(e^{2x})^{(7)} = H^{(7)}(x)$ is the stage at which a difference appears between the cases with and without uplifting. Namely, for the case with no uplifting the two sides of this equation are of the same order of magnitude at the point x_0; for the lower derivative equations the side of the exponential is the smaller one and hence we cannot decrease the bound on the number of solutions of $e^{2x} = H(x)$ any further. On the other hand, for the uplifted case we find that there are no solutions at each step until $(e^{2x})' = H'(x)$ and finally $e^{2x} = H(x)$ itself.

[30]For instance, for $W_0 = -10^{-4}$ we have $x_0 = 12.7$ (see footnote 27) and so the LHS of (3.65) is $2^6 \times 3 \times 10^5$, whereas the RHS is 4×10^{-2} for the uplifted case with $\Lambda = 10^{-3}$ and 8×10^4 for no uplifting with $\mu = 0$. In fact, one can easily convince oneself that our considerations are independent of the particular value of W_0 (and the resulting value of x_0). Namely, one can check that although the ratio between the LHS and RHS of (3.65) varies for the six values of W_0 in footnote 27, its order of magnitude remains the same for all six values. (For example, for the uplifted case one always finds that LHS/RHS $\sim 10^8$.)

4 Finite temperature corrections to the LARGE Volume models

Summary. In this chapter we present a detailed study of the finite-temperature behaviour of the so-called LARGE Volume type IIB flux compactifications [30, 62, 91]. These scenarios are phenomenologically interesting because, as we shall see, the volume of the internal space being exponentially large allows to explain many hierarchies observed in nature and guarantees that the low-energy effective field theory is under good control.

The finite temperature analysis is motivated by the observation that in general the scalar field associated to the overall CY volume mode is affected by the cosmological moduli problem and that temperature effects such as thermal inflation and moduli decay can provide a solution to the problem. In particular, we study in detail the issue of moduli thermalization and show that certain moduli can be in thermal equilibrium at high temperatures. Despite that, their contribution to the finite-temperature effective potential is always negligible and the latter has a runaway behaviour. We compute the maximal temperature T_{max}, above which the internal space decompactifies, as well as the temperature T_*, that is reached after the decay of the heaviest moduli. The natural constraint $T_* < T_{max}$ implies a lower bound on the allowed values of the internal volume $\mathcal{V}$. We find that this restriction rules out a significant range of values corresponding to smaller volumes of the order $\mathcal{V} \sim 10^4 l_s^6$, which lead to standard GUT theories. Instead, the bound favours values of the order $\mathcal{V} \sim 10^{15} l_s^6$, which lead to TeV scale SUSY desirable for solving the hierarchy problem.

Finally, we pose a two-fold challenge for the solution of the cosmological moduli problem [68] which these scenarios are affected by. First, we show that the heavy moduli decay before they can begin to dominate the energy density of the Universe. Hence they are not able to dilute any unwanted relics. Second, we argue that, in order to obtain thermal inflation in the closed string moduli sector, one needs to go beyond the present effective field theory (EFT) description.

4.1 Introduction

LARGE Volume scenarios [62] are excellent examples of IIB compactifications with stabilized moduli, which are very appealing both for particle physics phenomenology and for cosmology. According to the general analysis of [91], in these compactifications, α' and g_s corrections are combined with non-perturbative effects to generate a potential for the Kähler moduli which fixes the overall volume at exponentially large values, whereas the background fluxes induce a potential for the dilaton and the complex structure moduli. The exponentially large volume minimum of LVS is AdS with broken SUSY, even before any uplifting. In contrast, in KKLT constructions the AdS minimum is supersymmetric and the uplifting term is the source of SUSY breaking. Furthermore, the moduli stabilisation is performed without fine-tuning of the values of the internal fluxes, namely without fine-tuning W_0. As a consequence, one has a very reliable four-dimensional effective description, as well as a tool for the generation of phenomenologically desirable hierarchies. For example, for $\mathcal{V} \sim 10^{15} l_s^6$ the masses scales of LVS would look like

- Planck scale: $M_P = 2.4 \cdot 10^{18}$ GeV,
- Majorana scale for right handed neutrinos: $M_{\nu_R} \sim \frac{M_P}{\mathcal{V}^{1/3}} \sim 10^{14}$ GeV,
- String scale: $M_s \sim \frac{M_P}{\mathcal{V}} \sim 10^{10}$ GeV,
- QCD axionic scale: $f_a \sim M_s \sim 10^{10}$ GeV
- Kaluza-Klein scale: $M_{KK} \sim \frac{M_P}{\mathcal{V}^{2/3}} \sim 10^8$ GeV,
- Blow-up modes: $m_{\tau_s} \sim m_{3/2} \ln\left(M_P/m_{3/2}\right) \sim 10^6$ GeV,
- Gravitino mass: $m_{3/2} \sim \frac{M_P}{\mathcal{V}} \sim 10^4$ GeV
- Complex structure moduli: $m_U \sim m_{3/2} \sim 10^4$ GeV,
- Soft supersymmetry breaking terms: $M_{soft} \sim \frac{m_{3/2}}{\ln\left(M_P/m_{3/2}\right)} \sim 10^3$ GeV,
- Volume modulus: $m_{\tau_{big}} \sim \frac{M_P}{\mathcal{V}^{3/2}} \sim 1$ MeV,
- Large fibration moduli: $m_{\tau_{fib}} \sim \frac{M_P}{\mathcal{V}^{5/3}} \sim 10$ KeV.

However, if the volume is set such that $\mathcal{V} \sim 10^{15} l_s^6$, some shortcomings of these models are the following:

1. *No gauge coupling unification*, given that the string scale in this case is intermediate, and so ruins the standard picture of the running of all three non-gravitational coupling constants which merge around $M_{GUT} \sim 10^{16}$ GeV.

2. *Cosmological Moduli Problem* for the overall volume mode given that their decay would spoil the success of the Big-Bang nucleosynthesis.

We shall not address here the first problem since, in general, in all the five perturbative string theories, it is extremely difficult to derive an explicit string model which is able to reproduce the standard picture of gauge coupling unification.

In order to solve the second problem, namely the cosmological moduli problem, we need to have either a trapping mechanism to keep the fields in or close to their minima or alternatively a period of late entropy production that can dilute any unwanted relics. The latter can be achieved either with a period of late inflation such as thermal inflation [70] or with moduli decay. Both issues require studying the finite temperature behaviour of the moduli sector in LVS.

Contrary to the traditional thought that moduli cannot thermalize due to their Planck-suppressed couplings to ordinary matter and radiation, we show that in LVS some of the moduli *can* be in thermal equilibrium with MSSM particles for temperatures well below the Planck scale. The main reason is the presence of an additional large scale, namely the exponentially large CY volume, which enters the various couplings and thus affects the relevant interaction rates. The unexpected result, that some moduli can thermalize, in principle opens up the possibility that the finite temperature potential could develop new minima instead of just having a run-away behaviour as, for example, in [78,79]. However, we show that this is not the case since, for temperatures below the Kaluza-Klein scale, the T-dependent potential still has a run-away behaviour. Although it is impossible to find exactly the decompactification temperature T_{max}, as it is determined by a transcendental equation, we are able to extract a rather precise analytic estimate for it. As expected, we find that T_{max} is controlled by the potential barrier $V_b = m_{3/2}^3$ giving $T_{max} \sim m_{3/2}^{3/4} M_P^{1/4}$ between the metastable dS minimum and the one at infinity. Therefore, on general analysis, the maximal temperature in the LVS is lower than the maximal temperature in the KKLT case that was examined in the previous chapter where the potential barrier is of order of $m_{3/2}^2$.

We also pose a challenge for the solution of the cosmological moduli problem, that the overall breathing mode of LVS with $\mathcal{V} > 10^{10} l_s^6$ is afflicted by [92]. This is so, because we show that unwanted relics cannot be diluted by the entropy released

by the decay of the heaviest moduli of LVS, nor by a low-energy period of thermal inflation. More precisely, we show that the heaviest moduli of LVS decay before they can begin to dominate the energy density of the Universe and, also, that in order to study thermal inflation in the closed string moduli sector, it is necessary to go beyond our low energy EFT description.

The present chapter is organized as follows. In Section 4.2, we review the basic features of the type IIB LVS. In Section 4.3, we derive the masses and the couplings to visible sector particles of the moduli and modulini in LVS. Using these results, in Section 4.4 we investigate moduli thermalization and show that, generically, the moduli corresponding to the small cycles can be in thermal equilibrium with MSSM particles, due to their interaction with the gauge bosons. In Section 4.5, we study the finite temperature effective potential in LVS and show that it has a runaway behaviour that allows us to find the decompactification temperature T_{max}. Furthermore, we establish a lower bound on the CY volume, which follows from the constraint that the temperature of the Universe just after the small moduli decay should not exceed T_{max}. In Section 4.6 we discuss some open issues, among which the question why thermal inflation does not occur within our approximations. Finally, after we give a summary of our results in Section 4.7. (Appendix 4.A contains technical details on the computation of the moduli couplings.)

4.2 Large Volume Scenarios

The distinguishing feature of the type IIB Large Volume Scenarios (LVS) of [62] is that, in addition to the non-perturbative effects considered in [35], α' corrections are also taken into account, which lead to moduli stabilisation at an exponentially large volume of the internal manifold. In [62], the Calabi-Yau 3-fold was assumed to have a characteristic topology with one exponentially large cycle and several small del Pezzo 4-cycles. Including string loop corrections, as in [91], extends these scenarios to a larger class of Calabi-Yau manifolds which can also have fibration structure.

In [91] the topological conditions that an arbitrary CY has to satisfy in order for the general potential (2.46) to have a non-supersymmetric AdS minimum at *exponentially large* volume were derived. These conditions can be summarised as follows:

1. $h_{2,1} > h_{1,1} > 1 \Leftrightarrow \xi \sim (h_{2,1} - h_{1,1}) > 0$, where $h_{2,1}$, $h_{1,1}$ and ξ are defined in eq. (2.40) and below,

2. The CY 3-fold has to have at least one Kähler modulus τ_s corresponding to

a blow-up mode resolving a point-like singularity (the volume of a del Pezzo 4-cycle). τ_s must get non-perturbative corrections, $W = W_0 + A_s e^{-a_s\tau_s}$, then the overall volume can be fixed such that $\mathcal{V} \simeq \sqrt{\tau_s} e^{a_s\tau_s}$.

Both conditions give rise to two different LVS. On the one hand, we have a CY with a typical Swiss-cheese topological structure where there is just one LARGE cycle controlling the size of the overall volume and all the other 4-cycles are blow-up modes. The string loop corrections turn out to be negligible in this case. On the other hand, we have a fibred CY manifolds with the presence of modes which do not resolve point-like singularities or correspond to the overall volume modulus. In this case g_s corrections play a crucial role to lift the fibration moduli that are left unfixed by $\delta V_{(np)} + \delta V_{(\alpha')}$ (more precisely, the string loop corrections for these modes are always dominant compared to non-perturbative effects). We will describe these two cases in more detail in the next subsections.

4.2.1 Swiss-cheese Calabi-Yaus

The original example of LVS of [62], and the one we will study in most detail, is the degree 18 hypersurface in $\mathbb{C}P^4_{[1,1,1,6,9]}$ whose volume is given by

$$\mathcal{V} = \frac{1}{9\sqrt{2}} \left(\tau_b^{3/2} - \tau_s^{3/2} \right), \tag{4.1}$$

where τ_b and τ_s are the two Kähler moduli and the subscripts b and s stand for *big* and *small* respectively. The general expression (2.46) for the scalar potential, in this case takes the form[1]

$$V = \frac{g_s e^{K_{cs}} M_P^4}{8\pi} \left(\lambda \sqrt{\tau_s} \frac{e^{-2a_s\tau_s}}{\mathcal{V}} - \mu \frac{\tau_s e^{-a_s\tau_s}}{\mathcal{V}^2} + \frac{\nu}{\mathcal{V}^3} \right), \tag{4.2}$$

with

$$\lambda = 24\sqrt{2} a_s^2 A_s^2, \quad \mu = 4 a_s A_s W_0, \quad \nu = \frac{3\xi W_0^2}{4 g_s^{3/2}}, \tag{4.3}$$

Also, in (4.2) the minimisation with respect to the axion b_s has already been performed. For natural values of the tree-level superpotential $W_0 \sim \mathcal{O}(1)$, the scalar potential (4.2) admits a non-supersymmetric AdS minimum at exponentially large volume due to the interplay of α' and non-perturbative effects. This minimum is

[1] The string loop corrections can be safely neglected since they are subdominant relative to the other corrections due to inverse powers of $\mathcal{V}$ and factors of g_s.

located at

$$\mathcal{V} \sim W_0\, e^{a_s \tau_s} \gg \tau_s \sim \hat{\xi}^{2/3} \gg 1\,. \tag{4.4}$$

There are several ways to up-lift this minimum to Minkowski or dS: adding $\overline{D3}$ branes [35], considering D-terms from magnetised D7 branes [36] or F-terms from a hidden sector [93] etc.

An immediate generalisation of the $\mathbb{C}P^4_{[1,1,1,6,9]}$ model is given by the so-called 'Swiss-cheese' Calabi-Yaus, whose volume looks like

$$\mathcal{V} = \alpha \left(\tau_b^{3/2} - \sum_{i=1}^{N_{small}} \lambda_i \tau_i^{3/2} \right), \quad \alpha > 0, \quad \lambda_i > 0 \quad \forall i = 1, ..., N_{small}. \tag{4.5}$$

Examples having this form with $h_{1,1} = 3$ are the the degree 15 hypersurface embedded in $\mathbb{C}P^4_{[1,3,3,3,5]}$ and the degree 30 hypersurface in $\mathbb{C}P^4_{[1,1,3,10,15]}$ [94]. More generally, in [95] it was showed how to build Swiss-cheese CY 3-folds with $h_{1,1} = n + 2$, $0 \leq n \leq 8$. In this case, assuming that all the small cycles get non-perturbative effects, the 4-cycle τ_b, controlling the overall size of the CY, is stabilised exponentially large, $\mathcal{V} \simeq \alpha \tau_b^{3/2} \sim W_0 e^{a_i \tau_i}$, while the various 4-cycles, τ_i, controlling the size of the 'holes' of the Swiss-cheese, get fixed at small values $\tau_i \sim \mathcal{O}(10)$, $\forall i = 1, ..., N_{small}$.[2]

4.2.2 Fibred Calabi-Yaus

The first examples of LVS with a topological structure more complicated than the Swiss-cheese one, were discovered in [91]. The authors focused on a K3 fibred CY with $h_{2,1} > h_{1,1} = 3$, obtained by adding a blow-up mode to the geometry $\mathbb{C}P^4_{[1,1,2,2,6]}$. The volume reads:

$$\mathcal{V} = \alpha \left(\sqrt{\tau_1} \tau_2 - \gamma \tau_s^{3/2} \right) = t_1 \tau_1 - \alpha \gamma \tau_s^{3/2}, \tag{4.6}$$

where the constants α and γ are positive, and t_1 is the volume of the $\mathbb{C}P^1$ base of the K3 fibration. Working in the parameter regime $\tau_2 > \tau_1 \gg \tau_s$, where the volume of the CY is large, while the blow-up cycle τ_s remains comparatively small[3], the general expression (2.46) for the potential at zero temperature becomes (having

[2] However, in ref. [96] it was discovered that the Swiss-cheese structure of the volume is not enough to guarantee that all the rigid 'small' cycles τ_i can indeed be stabilised small. In fact, a further condition is that each rigid 'small' cycle τ_i must be del Pezzo. In [96], there are 3 examples of Swiss-cheese CY 3-folds with $h_{1,1} = 4$ where just one 4-cycle has the topology $\mathbb{C}P^2$.

[3] In this limit $t_1 \sim \tau_2/\sqrt{\tau_1} > \sqrt{\tau_1}$, corresponding to interesting geometries having the two dimensions of the base, spanned by the cycle t_1, larger than the other four of the K3 fibre, spanned by τ_1.

already minimised V with respect to the axion $b_s = \mathrm{Im}\, T_s$):

$$V = \frac{g_s e^{K_{cs}} M_P^4}{8\pi}\left[\beta\sqrt{\tau_s}\frac{e^{-2a_s\tau_s}}{\mathcal{V}} - \mu\frac{\tau_s e^{-a_s\tau_s}}{\mathcal{V}^2} + \frac{\nu}{\mathcal{V}^3} + \left(\frac{A}{\tau_1^2} - \frac{B}{\mathcal{V}\sqrt{\tau_1}} + \frac{C\tau_1}{\mathcal{V}^2}\right)\frac{W_0^2}{\mathcal{V}^2}\right], \tag{4.7}$$

with λ, μ and ν as given in (4.3) and

$$\beta = \frac{\lambda}{9\sqrt{2}\alpha\gamma}\,, \qquad A = (g_s C_1^{KK})^2\,, \qquad B = 4\alpha C_{12}^{W}\,, \qquad C = 2(\alpha g_s C_2^{KK})^2. \tag{4.8}$$

It is evident that the leading $\delta V_{(\alpha')} + \delta V_{(np)}$ part of the potential depends only on two Kähler moduli, $\mathcal{V}$ and τ_s, instead of all three. In fact, it turns out to be of exactly the same form as (4.2) above. Hence, viewing $\mathcal{V}$, τ_s and τ_1 as the three independent moduli (instead of τ_1, τ_2 and τ_s), it is clear that, without taking into account the subleading g_s corrections, τ_1 is a flat direction of the scalar potential. Also, it is evident that at this order, $\mathcal{V}$ and τ_s are stabilised as in the $\mathbb{C}P^4_{[1,1,1,6,9]}$ model of subsection 4.2.1:

$$\langle\tau_s\rangle = \left(\frac{\hat{\xi}}{2\,\alpha\gamma}\right)^{2/3} \qquad \text{and} \qquad \langle\mathcal{V}\rangle = \left(\frac{3\,\alpha\gamma}{4a_sA_s}\right) W_0\,\sqrt{\langle\tau_s\rangle}\; e^{a_s\langle\tau_s\rangle}\;. \tag{4.9}$$

Obviously, loop corrections shift insignificantly the VEVs of these two moduli. However, g_s corrections are crucial to generate a potential for τ_1 that admits a minimum at

$$\frac{1}{\tau_1^{3/2}} = \left(\frac{B}{8A\mathcal{V}}\right)\left[1 + (\mathrm{sign}\, B)\sqrt{1 + \frac{32AC}{B^2}}\right]. \tag{4.10}$$

Some concrete numerical choices for the various underlying parameters, without any fine-tuning, are listed in Table 4.1. The 'LV' case gives very large volumes,

	g_s	ξ	W_0	a_s	A_s	α	γ	C_1^{KK}	C_2^{KK}	C_{12}^{W}
LV	0.1	0.4	1	π	1	0.5	0.39	0.1	0.1	5
SV	0.3	0.9	100	$\pi/5$	1	0.13	3.65	0.15	0.08	1

	$\langle\tau_s\rangle$	$\langle\tau_1\rangle$	$\langle\mathcal{V}\rangle$
LV	10.5	10^6	$3\cdot 10^{13}$
SV	4.3	9	1710

Table 4.1: Some model parameters and the resulting minima for the 4-cycles.

$\mathcal{V} \simeq 10^{13}$ and the modulus τ_1 is stabilised at hierarchically large values, $\tau_2 > \tau_1 \gg \tau_s$.

The string scale and the gravitino mass turn out to be

$$M_s = \frac{M_P}{\sqrt{4\pi\mathcal{V}}} \sim 10^{11}\text{GeV}, \;\; m_{3/2} = e^{K/2M_P^2}\frac{W}{M_P^2} = \frac{g_s^{1/2}e^{K_{cs}/2}W_0 M_P}{\sqrt{8\pi}\mathcal{V}} \sim 10\text{TeV}. \tag{4.11}$$

This gives a solution of the hierarchy problem but the huge value of the volume destroys the standard picture of gauge coupling unification. The 'SV' case instead has $\mathcal{V} \sim 10^3$ much smaller (and so with $M_s \sim M_{GUT}$ and a very high gravitino mass). This set of parameter values is not chosen just in relation to GUT theories but also in order to provide observable density fluctuations for the inflationary model of [97]. In that model, the inflaton is the modulus τ_1, whose potential is loop-generated, and the main feature of the model is that it produces detectable gravity waves. More general examples of this kind of LVS have been discovered in [95] whose volumes look like

$$\mathcal{V} = Vol\,(X_{n-r}) - \sum_{i=1}^{r}\lambda_i\tau_i^{3/2}, \quad \lambda_i > 0 \;\; \forall i = 1, ..., r, \tag{4.12}$$

where X_{n-r} is the resulting elliptical fibration over a dP_{n-r} base. It is natural to expect that the scalar potential for these examples has an AdS minimum at exponentially large volume, together with $(h_{1,1} - N_{small} - 1) = n - r$ flat directions that will be lifted by g_s corrections.

We should note that string loop corrections can play an important role for compactifications on Swiss-cheese CY manifolds as well. Namely, they can be crucial, even in this case, to achieve full moduli stabilisation when the topological condition, that all rigid 4-cycles be del Pezzo, is not satisfied or when one imposes the phenomenological condition that the 4-cycles supporting chiral matter do not get non-perturbative effects [94].[4]

4.3 Moduli masses and couplings

The Universe has for much of its history been very nearly in thermal equilibrium. However, the departures from equilibrium have been very important - without them the past history of the Universe would be irrelevant. In order to compute the temperature at which a thermal bath is established or some particles drop out of thermal equilibrium we need to know the masses and the couplings of the particles in the thermal bath. To determine the latter, one needs to use canonically normalised fields.

[4] Also D-terms could play a significant role as pointed out still in [94].

In this section, we study the canonical normalisation of the Kähler moduli kinetic terms and use the results to compute the masses of those moduli and their couplings to visible sector particles.

4.3.1 Single-hole Swiss-cheese

We start by focusing on the simplest Calabi-Yau realisation of LVS, the 'single-hole Swiss-cheese' case described in subsection 4.2.1 (i.e., the degree 18 hypersurface embedded in $\mathbb{C}P^4_{[1,1,1,6,9]}$). First of all, we shall review the canonical normalisation derived in [92]. In order to obtain the Lagrangian in the vicinity of the zero temperature vacuum, one expands the moduli fields around the $T = 0$ minimum:

$$\begin{aligned} \tau_b &= \langle \tau_b \rangle + \delta\tau_b \,, \\ \tau_s &= \langle \tau_s \rangle + \delta\tau_s \,. \end{aligned}$$

where $\langle \tau_b \rangle$ and $\langle \tau_s \rangle$ denote the VEV of τ_b and τ_s. One then finds:

$$\mathcal{L} = K_{i\bar{j}} \partial_\mu (\delta\tau_i) \partial^\mu (\delta\tau_j) - \langle V_0 \rangle - \frac{1}{2} V_{i\bar{j}} \delta\tau_i \delta\tau_j + \mathcal{O}(\delta\tau^3) \,, \tag{4.13}$$

where $i = b, s$ and $\langle V_0 \rangle$ denotes the value of the zero temperature potential at the minimum. To find the canonically normalized fields Φ and χ, let us write $\delta\tau_b$ and $\delta\tau_s$ as:

$$\delta\tau_i = \frac{1}{\sqrt{2}} \left[(\vec{v}_\Phi)_i \Phi + (\vec{v}_\chi)_i \chi \right] . \tag{4.14}$$

The conditions for the Lagrangian (4.13) to take the canonical form:

$$\mathcal{L} = -\frac{1}{2} \partial_\mu \Phi \partial^\mu \Phi - \frac{1}{2} \partial_\mu \chi \partial^\mu \chi - \langle V_0 \rangle - \frac{1}{2} m_\Phi^2 \Phi^2 - \frac{1}{2} m_\chi^2 \chi^2 \tag{4.15}$$

are the following:

$$K_{i\bar{j}} (\vec{v}_\alpha)_i (\vec{v}_\beta)_j = \delta_{\alpha\beta} \quad \text{and} \quad \frac{1}{2} V_{i\bar{j}} (\vec{v}_\alpha)_i (\vec{v}_\beta)_j = m_\alpha^2 \delta_{\alpha\beta} \,. \tag{4.16}$$

These relations are satisfied when $\vec{v}_\Phi$, $\vec{v}_\chi$ (properly normalised according to the first of (4.16)) and m_Φ^2, m_χ^2 are, respectively, the eigenvectors and the eigenvalues of the mass-squared matrix $\left(M^2\right)_{ij} \equiv \frac{1}{2} \left(K^{-1}\right)_{i\bar{k}} V_{\bar{k}j}$.

Substituting the results of [92] for $\vec{v}_\Phi$ and $\vec{v}_\chi$ in (4.14), we can write the original

Kähler moduli $\delta\tau_i$ as (for $a_s\tau_s \gg 1$):

$$\delta\tau_b = \left(\sqrt{6}\langle\tau_b\rangle^{1/4}\langle\tau_s\rangle^{3/4}\right)\frac{\Phi}{\sqrt{2}} + \left(\sqrt{\frac{4}{3}}\langle\tau_b\rangle\right)\frac{\chi}{\sqrt{2}} \sim \mathcal{O}\left(\mathcal{V}^{1/6}\right)\Phi + \mathcal{O}\left(\mathcal{V}^{2/3}\right)\chi \quad (4.17a)$$

$$\delta\tau_s = \left(\frac{2\sqrt{6}}{3}\langle\tau_b\rangle^{3/4}\langle\tau_s\rangle^{1/4}\right)\frac{\Phi}{\sqrt{2}} + \left(\frac{\sqrt{3}}{a_s}\right)\frac{\chi}{\sqrt{2}} \sim \mathcal{O}\left(\mathcal{V}^{1/2}\right)\Phi + \mathcal{O}(1)\,\chi\,. \quad (4.17b)$$

As expected, these relations show that there is a mixing of the original fields. Nevertheless, $\delta\tau_b$ is mostly χ and $\delta\tau_s$ is mostly Φ in the LARGE volume approximation, $\mathcal{V} \gg 1$. On the other hand, the mass-squared are [92]:

$$m_\Phi^2 \simeq \mathrm{Tr}\left(M^2\right) \simeq \left(\frac{g_s e^{K_{cs}}}{8\pi}\right)\frac{24\sqrt{2}\nu a_s^2\langle\tau_s\rangle^{1/2}}{\mathcal{V}^2}M_P^2 \sim \left(\frac{\ln\mathcal{V}}{\mathcal{V}}\right)^2 M_P^2 \quad (4.18a)$$

$$m_\chi^2 \simeq \frac{\det\left(M^2\right)}{\mathrm{Tr}\left(M^2\right)} \simeq \left(\frac{g_s e^{K_{cs}}}{8\pi}\right)\frac{27\nu}{4a_s\langle\tau_s\rangle\mathcal{V}^3}M_P^2 \sim \frac{M_P^2}{\mathcal{V}^3\ln\mathcal{V}}. \quad (4.18b)$$

We can see that there is a large hierarchy of masses among the two particles, with Φ being heavier than the gravitino mass (recall that $m_{3/2} \sim M_P/\mathcal{V}$) and χ lighter by a factor of $\sqrt{\mathcal{V}}$.

Using the above results and assuming that the MSSM is built via magnetised D7 branes wrapped around the small cycle, we can compute the couplings of the Kähler moduli fields of the $\mathbb{C}P^4_{[1,1,1,6,9]}$ model to visible gauge and matter fields. This is achieved by expanding the kinetic and mass terms of the MSSM particles around the moduli VEVs. The details are provided in Appendix 4.A, where we focus on $T > M_{EW}$ since we are interested in thermal corrections at high temperatures. This, in particular, means that all fermions and gauge bosons are massless and the mixing of the Higgsinos with the EW gauginos, that gives neutralinos and charginos, is not present. We summarise the results for the moduli couplings in Tables 4.2 and 4.3.

	Gauge bosons ($F_{\mu\nu}F^{\mu\nu}$)	Gauginos ($\bar{\lambda}\lambda$)	Matter fermions ($\bar{\psi}\psi$)	Higgsinos ($\tilde{H}\tilde{H}$)
χ	$\frac{1}{M_p\ln\mathcal{V}}$	$\frac{1}{\mathcal{V}\ln\mathcal{V}}$	No coupling	$\frac{1}{\mathcal{V}\ln\mathcal{V}}$
Φ	$\frac{\sqrt{\mathcal{V}}}{M_p}$	$\frac{1}{\mathcal{V}^{3/2}\ln\mathcal{V}}$	No coupling	$\frac{1}{\sqrt{\mathcal{V}}\ln\mathcal{V}}$

Table 4.2: $\mathbb{C}P^4_{[1,1,1,6,9]}$ case: moduli couplings to spin 1 and 1/2 MSSM particles for $T > M_{EW}$.

	Higgs ($\bar{H}H$)	Higgs-Fermions ($H\bar{\psi}\psi$)	SUSY scalars ($\bar{\varphi}\varphi$)	χ^2	Φ^2
χ	$\frac{M_P}{\mathcal{V}^2(\ln\mathcal{V})^2}$	$\frac{1}{M_P\mathcal{V}^{1/3}}$	$\frac{M_P}{\mathcal{V}^2(\ln\mathcal{V})^2}$	$\frac{M_P}{\mathcal{V}^3}$	$\frac{M_P}{\mathcal{V}^2}$
Φ	$\frac{M_P}{\mathcal{V}^{5/2}(\ln\mathcal{V})^2}$	$\frac{1}{M_P\mathcal{V}^{5/6}}$	$\frac{M_P}{\mathcal{V}^{5/2}(\ln\mathcal{V})^2}$	$\frac{M_P}{\mathcal{V}^{5/2}}$	$\frac{M_P}{\mathcal{V}^{3/2}}$

Table 4.3: $\mathbb{C}P^4_{[1,1,1,6,9]}$ case: moduli couplings to spin 0 MSSM particles and cubic self-couplings for $T > M_{EW}$.

4.3.2 Multiple-hole Swiss-cheese

Let us now consider the more general Swiss-cheese CY three-folds with more than one small modulus and with volume given by (4.5). In this case we find:

$$\begin{aligned}\mathcal{L}_{kin} &= \frac{3}{4\langle\tau_b\rangle^2}\partial_\mu(\delta\tau_b)\partial^\mu(\delta\tau_b) + \frac{3}{8}\sum_i \frac{\lambda_i\epsilon_i}{\langle\tau_b\rangle\langle\tau_i\rangle}\partial_\mu(\delta\tau_i)\partial^\mu(\delta\tau_i) \\ &\quad -\frac{9}{4}\sum_i \frac{\lambda_i\epsilon_i}{\langle\tau_b\rangle^2}\partial_\mu(\delta\tau_b)\partial^\mu(\delta\tau_i) + \frac{9}{4}\sum_{i<j}\frac{\lambda_i\lambda_j\epsilon_i\epsilon_j}{\langle\tau_b\rangle^2}\partial_\mu(\delta\tau_i)\partial^\mu(\delta\tau_j)\ , \quad (4.19)\end{aligned}$$

where $\epsilon_i \equiv \sqrt{\frac{\tau_i}{\tau_b}} \ll 1$ and also we have kept only the leading (in the limit $\tau_b \gg \tau_i\ \forall i$) contribution in each term. Notice that the mixed terms are subleading compared to the diagonal ones. So, to start with, one can keep only the first line in (4.19). Then at leading order the canonically normalized fields χ and Φ_i, $i = 1, ..., N_{small}$, are defined via:

$$\delta\tau_b = \sqrt{\frac{2}{3}}\langle\tau_b\rangle\chi \sim \mathcal{O}\left(\mathcal{V}^{2/3}\right)\chi\,, \qquad \delta\tau_i = \frac{2}{\sqrt{3\lambda_i}}\langle\tau_b\rangle^{3/4}\langle\tau_i\rangle^{1/4}\Phi_i \sim \mathcal{O}\left(\mathcal{V}^{1/2}\right)\Phi_i\,. \quad (4.20)$$

As was to be expected, this scaling with the volume agrees with the behaviour of $\delta\tau_b$ and $\delta\tau_s$ in (4.17). Now, let us work out the volume scaling of the subdominant mixing terms since it is important for the computation of the various moduli couplings. Proceeding order by order in a large-$\mathcal{V}$ expansion, we end up with:

$$\delta\tau_b \sim \mathcal{O}\left(\mathcal{V}^{2/3}\right)\chi + \sum_i \mathcal{O}\left(\mathcal{V}^{1/6}\right)\Phi_i\,, \quad (4.21a)$$

$$\delta\tau_i \sim \mathcal{O}\left(\mathcal{V}^{1/2}\right)\Phi_i + \mathcal{O}(1)\,\chi + \sum_{j\neq i}\mathcal{O}\left(\mathcal{V}^{-1/2}\right)\Phi_j\,. \quad (4.21b)$$

This shows that the mixing between the small moduli is strongly suppressed by inverse powers of the overall volume, in accord with the subleading behaviour of the last term in (4.19). Furthermore, the fact that the leading order volume-scaling of (4.21) is the same as (4.17), implies that all small moduli behave in the same way as the only small modulus of the $\mathbb{C}P^4_{[1,1,1,6,9]}$ model. Hence, if all the small moduli are stabilised by non-perturbative effects, the moduli mass spectrum in the general case will look like (4.18), with (4.18a) valid for all the small moduli. In addition, if we assume that all the 4-cycles corresponding to small moduli are wrapped by MSSM D7 branes, the moduli couplings to matter fields are again given by Tables 4.2 and 4.3, where now Φ stands for any small modulus Φ_i.

However, in general the situation may be more complicated. In fact, in [94] it was pointed out that 4-cycles supporting MSSM chiral matter cannot always get non-perturbative effects.[5] A possible way to stabilise these 4-cycles is to use g_s corrections as proposed in [91]. In this case, the leading-order behaviour of (4.18a) should not change: $m^2_{\Phi_i} \sim \frac{M_P^2}{\mathcal{V}^2}$.[6] However, the moduli couplings to MSSM particles depend on the underlying brane set-up. So let us consider the following main cases:

1. All the small 4-cycles are wrapped by MSSM D7 branes except τ_{np} which is responsible for non-perturbative effects, being wrapped by an ED3 brane. It follows that the MSSM couplings of Φ_{np} are significantly suppressed compared to the MSSM couplings of the other small cycles (still given by Tables 4.2 and 4.3). This is due to the mixing term in (4.21b) being highly suppressed by inverse powers of $\mathcal{V}$.

2. All the small 4-cycles are wrapped by MSSM D7 branes except τ_{np} which is supporting a pure $SU(N)$ hidden sector that gives rise to gaugino condensation. This implies that the coupling of Φ_{np} to hidden sector gauge bosons will have the same volume-scaling as the coupling of the other small moduli with visible sector gauge bosons. However, the coupling of the MSSM 4-cycles with hidden sector gauge bosons will be highly suppressed.

3. All the small 4-cycles τ_i support MSSM D7 branes which are also wrapped around the 4-cycle responsible for non-perturbative effects τ_{np}, but they have

[5] This is because an ED3 wrapped on the same cycle will have, in general, chiral intersections with the MSSM branes. Thus the instanton prefactor would be dependent on the VEVs of MSSM fields which are set to zero for phenomenological reasons. In the case of gaugino condensation, this non-perturbative effect would be killed by the arising of chiral matter.

[6] It may be likely that $m^2_{\Phi_i}$ depends on subleading powers of $(\ln \mathcal{V})$ due to the fact that the loop corrections are subdominant with respect to the non-perturbative ones (see [91]), but the main $\mathcal{V}^{-2}$ dependence should persist.

chiral intersections only on the other small cycles. In this case, the coupling of Φ_{np} to MSSM particles would be the same as the other Φ_i. However, if τ_{np} supports an hidden sector that undergoes gaugino condensation, the coupling of the MSSM 4-cycles with the gauge bosons of this hidden sector would still be highly suppressed.

4.3.3 K3 Fibration

We turn now to the K3 fibration case described in Section 4.2.2. We shall consider first the 'LV' case, in which the modulus related to the K3 divisor is fixed at a very large value, and then the 'SV' case, in which the overall volume is of the order $\mathcal{V} \sim 10^3$ and the K3 fiber is small.

In order to compute the moduli mass spectroscopy and couplings, it suffices to canonically normalise the fields just in the vicinity of the vacuum. The non-canonical kinetic terms look like (with $\varepsilon \equiv \sqrt{\langle\tau_s\rangle/\langle\tau_1\rangle}$):

$$\begin{aligned}\mathcal{L}_{kin} &= \frac{1}{4\langle\tau_1\rangle^2}\partial_\mu(\delta\tau_1)\partial^\mu(\delta\tau_1) + \frac{1}{2\langle\tau_2\rangle^2}\partial_\mu(\delta\tau_2)\partial^\mu(\delta\tau_2) - \frac{3\gamma\varepsilon}{4\langle\tau_2\rangle\langle\tau_1\rangle}\partial_\mu(\delta\tau_1)\partial^\mu(\delta\tau_s) \\ &\quad - \frac{3\gamma\varepsilon}{2\langle\tau_2\rangle^2}\partial_\mu(\delta\tau_2)\partial^\mu(\delta\tau_s) + \frac{\gamma\varepsilon^3}{2\langle\tau_2\rangle^2}\partial_\mu(\delta\tau_1)\partial^\mu(\delta\tau_2) + \frac{3\gamma\varepsilon}{8\langle\tau_2\rangle\langle\tau_s\rangle}\partial_\mu(\delta\tau_s)\partial^\mu(\delta\tau_s).\end{aligned} \tag{4.22}$$

Large K3 fiber

In the 'LV' case where the K3 fiber is stabilised at large value, $\varepsilon \ll 1$. Therefore at leading order in a large volume expansion, where $\langle\tau_2\rangle > \langle\tau_1\rangle \gg \langle\tau_s\rangle$, all the cross-terms in (4.22) are subdominant to the diagonal ones, and so can be neglected:

$$\mathcal{L}_{kin} \simeq \frac{1}{4\langle\tau_1\rangle^2}\partial_\mu(\delta\tau_1)\partial^\mu(\delta\tau_1) + \frac{1}{2\langle\tau_2\rangle^2}\partial_\mu(\delta\tau_2)\partial^\mu(\delta\tau_2) + \frac{3\gamma\varepsilon}{8\langle\tau_2\rangle\langle\tau_s\rangle}\partial_\mu(\delta\tau_s)\partial^\mu(\delta\tau_s). \tag{4.23}$$

Therefore, at leading order the canonical normalisation close to the minimum becomes rather easy and reads:

$$\delta\tau_1 = \sqrt{2}\langle\tau_1\rangle\chi_1 \sim \mathcal{O}\left(\mathcal{V}^{2/3}\right)\chi_1, \tag{4.24a}$$

$$\delta\tau_2 = \langle\tau_2\rangle\chi_2 \sim \mathcal{O}\left(\mathcal{V}^{2/3}\right)\chi_2, \tag{4.24b}$$

$$\delta\tau_s = \sqrt{\frac{4\langle\tau_1\rangle^{1/2}\langle\tau_2\rangle\langle\tau_s\rangle^{1/2}}{3\gamma}}\Phi \sim \mathcal{O}\left(\mathcal{V}^{1/2}\right)\Phi. \tag{4.24c}$$

However, in order to derive all the moduli couplings, we need also to work out the leading order volume-scaling of the subdominant mixing terms in (4.24b) and (4.24c). This can be done order by order in a large-$\mathcal{V}$ expansion and, after some algebra, we obtain:

$$\delta\tau_1 = \alpha_1\langle\tau_1\rangle\chi_1 + \alpha_2\frac{\sqrt{\langle\tau_1\rangle}}{\langle\tau_2\rangle}\langle\tau_s\rangle^{3/2}\chi_2 + \alpha_3\frac{\langle\tau_1\rangle^{3/4}}{\sqrt{\langle\tau_2\rangle}}\langle\tau_s\rangle^{3/4}\Phi, \tag{4.25a}$$

$$\delta\tau_2 = \alpha_4\frac{\sqrt{\langle\tau_1\rangle}}{\langle\tau_2\rangle}\langle\tau_s\rangle^{3/2}\chi_1 + \alpha_5\langle\tau_2\rangle\chi_2 + \alpha_6\frac{\sqrt{\langle\tau_2\rangle}}{\langle\tau_1\rangle^{1/4}}\langle\tau_s\rangle^{3/4}\Phi, \tag{4.25b}$$

$$\delta\tau_s = \alpha_7\frac{\langle\tau_1\rangle}{\langle\tau_2\rangle}\langle\tau_s\rangle\chi_1 + \alpha_8\langle\tau_s\rangle\chi_2 + \alpha_9\langle\tau_1\rangle^{1/4}\sqrt{\langle\tau_2\rangle}\langle\tau_s\rangle^{1/4}\Phi, \tag{4.25c}$$

where the α_i, $i = 1, ..., 9$ are $\mathcal{O}(1)$ coefficients. The volume-scalings of (4.25) are the following:

$$\delta\tau_1 \sim \mathcal{O}\left(\mathcal{V}^{2/3}\right)\chi_1 + \mathcal{O}\left(\mathcal{V}^{-1/3}\right)\chi_2 + \mathcal{O}\left(\mathcal{V}^{1/6}\right)\Phi, \tag{4.26}$$

$$\delta\tau_2 \sim \mathcal{O}\left(\mathcal{V}^{-1/3}\right)\chi_1 + \mathcal{O}\left(\mathcal{V}^{2/3}\right)\chi_2 + \mathcal{O}\left(\mathcal{V}^{1/6}\right)\Phi, \tag{4.27}$$

$$\delta\tau_s \sim \mathcal{O}\left(1\right)\chi_1 + \mathcal{O}\left(1\right)\chi_2 + \mathcal{O}\left(\mathcal{V}^{1/2}\right)\Phi. \tag{4.28}$$

This shows that, if we identify each of τ_1 and τ_2 with the large modulus τ_b in the Swiss-cheese case, (4.26) and (4.27) have the same volume scaling as (4.17a), as one might have expected. Moreover, the similarity of (4.28) and (4.17b) shows that also the small moduli in the two cases behave in the same way. Therefore, we can conclude that (4.18a) is valid also for the K3 Fibration case under consideration:

$$m_\Phi \sim \left(\frac{\ln\mathcal{V}}{\mathcal{V}}\right)M_P. \tag{4.29}$$

On the other hand, we need to be more careful in the study of the mass spectrum of the large moduli τ_1 and τ_2. We can work out this 'fine structure', at leading order in a large-$\mathcal{V}$ expansion, first integrating out τ_s and then computing the eigenvalues of the matrix. The latter are obtained by multiplying the inverse Kähler metric by the Hessian of the potential both evaluated at the minimum. The leading order behaviour of the determinant of this matrix is:

$$\det\left(K^{-1}d^2V\right) \sim \frac{\tau_2^4\sqrt{\ln\mathcal{V}}}{\mathcal{V}^9}, \quad \text{with} \quad \mathcal{V} \sim \sqrt{\tau_1}\tau_2. \tag{4.30}$$

Because $m^2_{\chi_2} \gg m^2_{\chi_1}$, we have at leading order at large volume:

$$m^2_{\chi_2} \simeq \mathrm{Tr}\left(K^{-1}d^2V\right) \sim \frac{\sqrt{\ln \mathcal{V}}}{\mathcal{V}^3}M_P^2 \tag{4.31}$$

$$m^2_{\chi_1} \simeq \frac{\det\left(K^{-1}d^2V\right)}{\mathrm{Tr}\left(K^{-1}d^2V\right)} \sim \frac{\tau_2^4}{\mathcal{V}^6}M_P^2 \sim \frac{M_P^2}{\tau_1^3\tau_2^2}. \tag{4.32}$$

Identifying τ_1 with τ_2, (4.32) simplifies to $m^2_{\chi_1} \sim \mathcal{V}^{-10/3}$, confirming the qualitative expectation that the τ_1 direction is systematically lighter than $\mathcal{V}$ in the large-$\mathcal{V}$ limit.

Using the results of this Section and assuming that the MSSM branes are wrapped around the small cycle[7], it is easy to repeat the computations of Appendix 4.A for the K3 fibration. Due to the fact that the leading order $\mathcal{V}$-scaling of (4.25) matches that of the single-hole Swiss-cheese model, we again find the same couplings as those given in Tables 4.2 and 4.3, where now χ stands for any of χ_1 and χ_2.

Small K3 fiber

In the 'SV' case the K3 fiber is stabilised at small value, $\varepsilon \simeq 1$. Therefore at leading order in a large volume expansion, where $\langle\tau_2\rangle \gg \langle\tau_1\rangle > \langle\tau_s\rangle$, the first term in (4.22) is dominating the whole kinetic Lagrangian. Hence we conclude that, at leading order, the canonical normalisation of $\delta\tau_1$ close to the $T = 0$ minimum is again given by (4.24a). However, now its volume scaling reads:

$$\delta\tau_1 \sim \mathcal{O}(1)\,\chi_1 + (\text{subleading mixing terms}). \tag{4.33}$$

To proceed order by order in a large volume expansion, note that the third and the sixth term in (4.22) are suppressed by just one power of $\langle\tau_2\rangle$, whereas the second, fourth and fifth term are suppressed by two powers of the large modulus. Thus, we obtain the following leading order behaviour for the canonical normalisation of the two remaining moduli:

$$\delta\tau_2 \sim \mathcal{O}(\mathcal{V})\,\chi_1 + \mathcal{O}(\mathcal{V})\,\chi_2 + \mathcal{O}(\mathcal{V})\,\Phi, \tag{4.34}$$

$$\delta\tau_s \sim \mathcal{O}\left(\mathcal{V}^{1/2}\right)\chi_1 + \mathcal{O}\left(\mathcal{V}^{1/2}\right)\Phi + \text{subleading mixing terms}. \tag{4.35}$$

Notice that the canonically normalised field χ_1 corresponds to the K3 divisor τ_1, whereas Φ is a mixing of τ_1 and the blow-up mode τ_s. Finally χ_2 is a combination

[7] We also ignore the incompatibility between localising non-perturbative effects and the MSSM on the same 4-cycle.

of all the three states, and so plays the role of the 'large' field. The moduli mass spectrum will still be given by (4.29), (4.31) and (4.32). However now the volume scaling of (4.32) simplifies to $m_{\chi_1}^2 \sim \mathcal{V}^{-2}$, confirming the qualitative expectation that χ_1 is also a small field with a mass of the same order of magnitude of m_Φ.

The computation of the moduli couplings depends on the localisation of the MSSM within the compact CY. As we have seen in subsection 4.2.2, the scalar potential receives non-perturbative corrections in the blow-up mode τ_s. Therefore, in order for the non-perturbative contributions to be non-vanishing, the MSSM branes have to wrap either the small K3 fiber τ_1 or the 4-cycle given by the formal sum $\tau_s + \tau_1$ with chiral intersections on τ_1. In both cases, we cannot immediately read off the moduli couplings from the results of Appendix 4.A. This is due to the difference of the leading order volume scaling of the canonical normalisation between the 'SV' case for the K3 fibration and the Swiss-cheese scenario.[8]

However, as we shall see in the next section, in the Swiss-cheese case, the relevant interactions through which the small moduli can thermalise, are with the gauge bosons. As we shall see in section 4.4.3, these interactions will also be the ones that are crucial for moduli thermalisation in the K3 fibration case. Therefore, here we shall focus on them only. Following the calculations in subsection 4.A.1 of Appendix 4.A, we infer that if only τ_1 is wrapped by MSSM branes, then the coupling of χ_1 with MSSM gauge bosons is of the order $g \sim 1/M_P$ without any factor of the overall volume, while the coupling of Φ with gauge bosons will be more suppressed by inverse powers of $\mathcal{V}$. On the other hand, if both τ_1 and τ_s are wrapped by MSSM branes, then the couplings of both small moduli with the gauge bosons are similar to the ones in the Swiss-cheese case: $g \sim \sqrt{\mathcal{V}}/M_P$. Moreover, if gaugino condensation is taking place in the pure $SU(N)$ theory supported on τ_s, then both χ_1 and Φ couple to the hidden sector gauge bosons with strength $g \sim \sqrt{\mathcal{V}}/M_P$.

We end this subsection by commenting on K3 fibrations with more than one blow-up mode. In such a case, it is possible to localise the MSSM on one of the small blow-up modes and the situation is very similar to the one outlined for the multiple-hole Swiss-cheese. The only difference is the presence of the extra modulus related to the K3 fiber, which will couple to the MSSM gauge bosons with the same strength as the small modulus supporting the MSSM. This is because of the particular form of the canonical normalisation, which, for example in the case of two blow-up modes

[8] We stress also that presently there is no knowledge of the Kähler metric for chiral matter localised on deformable cycles.

τ_{s1} and τ_{s2}, looks like (4.33) and (4.34) together with:

$$\delta\tau_{s1} \sim \mathcal{O}\left(\mathcal{V}^{1/2}\right)\chi_1 + \mathcal{O}\left(\mathcal{V}^{1/2}\right)\Phi_1 + \text{subleading mixing terms}, \tag{4.36}$$

$$\delta\tau_{s2} \sim \mathcal{O}\left(\mathcal{V}^{1/2}\right)\chi_1 + \mathcal{O}\left(\mathcal{V}^{1/2}\right)\Phi_2 + \text{subleading mixing terms}. \tag{4.37}$$

4.3.4 Modulini

In this subsection we shall concentrate on the supersymmetric partners of the moduli, the modulini. More precisely, we will consider the fermionic components of the chiral superfields, whose scalar components are the Kähler moduli. The kinetic Lagrangian for these modulini reads:

$$\mathcal{L}_{kin} = \frac{i}{4}\frac{\partial^2 K}{\partial\tau_i\partial\tau_j}\delta\bar{\tilde{\tau}}_j\gamma^\mu\partial_\mu(\delta\tilde{\tau}_i)\,, \tag{4.38}$$

where the Kähler metric is the same as the one that appears in the kinetic terms of the Kähler moduli. Therefore, the canonical normalisation of the modulini takes exactly the same form as the canonical normalisation of the corresponding moduli. For example, in the single-hole Swiss-cheese case, we have:

$$\delta\tilde{\tau}_b = \left(\sqrt{6}\langle\tau_b\rangle^{1/4}\langle\tau_s\rangle^{3/4}\right)\frac{\tilde{\Phi}}{\sqrt{2}} + \left(\sqrt{\frac{4}{3}}\langle\tau_b\rangle\right)\frac{\tilde{\chi}}{\sqrt{2}} \sim \mathcal{O}\left(\mathcal{V}^{1/6}\right)\tilde{\Phi} + \mathcal{O}\left(\mathcal{V}^{2/3}\right)\tilde{\chi}\,, \tag{4.39}$$

$$\delta\tilde{\tau}_s = \left(\frac{2\sqrt{6}}{3}\langle\tau_b\rangle^{3/4}\langle\tau_s\rangle^{1/4}\right)\frac{\tilde{\Phi}}{\sqrt{2}} + \left(\frac{\sqrt{3}}{a_s}\right)\frac{\tilde{\chi}}{\sqrt{2}} \sim \mathcal{O}\left(\mathcal{V}^{1/2}\right)\tilde{\Phi} + \mathcal{O}\left(1\right)\tilde{\chi}. \tag{4.40}$$

We focus now on the modulini mass spectrum. We recall that in LVS the minimum is non-supersymmetric, and so the Goldstino is eaten by the gravitino via the super-Higgs effect. The Goldstino is the supersymmetric partner of the scalar field, which is responsible for SUSY breaking. In our case this is the modulus related to the overall volume of the Calabi-Yau, as can be checked by studying the order of magnitude of the various F-terms. Therefore, the volume modulino is the Goldstino. More precisely, in the $\mathbb{C}P^4_{[1,1,1,6,9]}$ case, $\tilde{\chi}$ is eaten by the gravitino, whereas the mass of $\tilde{\Phi}$ can be derived as follows:

$$m^2_{\tilde{\Phi}} = \mathrm{Tr}M_f^2 = \langle e^G K^{i\bar{j}}K^{l\bar{m}}(\nabla_i G_l + \frac{G_i G_l}{3})(\nabla_{\bar{j}}G_{\bar{m}} + \frac{G_{\bar{j}}G_{\bar{m}}}{3})\rangle, \tag{4.41}$$

where the function $G = K + \ln|W|^2$ is the supergravity Kähler invariant potential, and $\nabla_i G_j = G_{ij} - \Gamma^l_{ij}G_l$, with the connection $\Gamma^l_{ij} = K^{l\bar{m}}\partial_i K_{j\bar{m}}$. Equation (4.41) at

leading order in a large volume expansion, can be approximated as

$$m_{\tilde{\Phi}}^2 \simeq \langle e^G | (K^{s\bar{s}}(\nabla_s G_s + \frac{G_s G_s}{3})|^2 \rangle \tag{4.42}$$

where $\nabla_s G_s \simeq G_{ss} - \Gamma^s_{ss} G_s$ and $\Gamma^s_{ss} \simeq K^{s\bar{s}} \partial_s K_{s\bar{s}}$. In the single-hole Swiss-cheese case, for $a_s \tau_s \gg 1$, we obtain:

$$m_{\tilde{\Phi}}^2 \simeq \langle \frac{g_s e^{K_{cs}} M_P^2}{\pi} \left(36 a_s^4 A_s^2 \tau_s e^{-2a_s\tau_s} - \frac{6\sqrt{2} a_s^2 A_s W_0}{\mathcal{V}} \sqrt{\tau_s} e^{-a_s \tau_s} + \frac{W_0^2}{2\mathcal{V}^2} \right) \rangle. \tag{4.43}$$

Evaluating (4.43) at the minimum, we find that the mass of the modulino $\tilde{\Phi}$ is of the same order of magnitude as the mass of its supersymmetric partner Φ:

$$m_{\tilde{\Phi}}^2 \simeq \frac{a_s^2 \langle \tau_s \rangle^2 W_0^2}{\mathcal{V}^2} M_P^2 \sim \left(\frac{\ln \mathcal{V}}{\mathcal{V}} \right)^2 M_P^2 \sim m_{\Phi}^2. \tag{4.44}$$

Similarly, it can be checked that, in the general case of multiple-hole Swiss-cheese Calabi-Yaus and K3 fibrations, the masses of the modulini also keep being of the same order of magnitude as the masses of the corresponding supersymmetric partners.

We now turn to the computation of the modulini couplings. In fact, we are interested only in the modulino-gaugino-gauge boson coupling since, as we shall see in section 4.4, this is the relevant interaction through which the modulini reach thermal equilibrium with the MSSM thermal bath. This coupling can be worked out by recalling that the small modulus τ_s couples to gauge bosons X as (see appendix 4.A.1):

$$\mathcal{L}_{gauge} \sim \frac{\tau_s}{M_P} F_{\mu\nu} F^{\mu\nu} \,. \tag{4.45}$$

The supersymmetric completion of this interaction term contains the following modulino-gaugino-gauge boson coupling:

$$\mathcal{L} \sim \frac{\tilde{\tau}_s}{M_P} \sigma^{\mu\nu} \lambda' F_{\mu\nu} \,. \tag{4.46}$$

Now, expanding $\tilde{\tau}_s$ around its minimum and going to the canonically normalised fields $G_{\mu\nu}$ and λ defined as (see appendices 4.A.1 and 4.A.2):

$$G_{\mu\nu} = \sqrt{\langle \tau_s \rangle} F_{\mu\nu} \,, \quad \lambda = \sqrt{\langle \tau_s \rangle} \lambda' \,, \tag{4.47}$$

we obtain:

$$\mathcal{L} \sim \frac{\delta\tilde{\tau}_s}{M_P\langle\tau_s\rangle}\sigma^{\mu\nu}\lambda G_{\mu\nu}\,. \tag{4.48}$$

Hence, by means of (4.40), we end up with the following *dimensionful* couplings:

$$\mathcal{L}_{\tilde{\chi}\tilde{X}X} \sim \left(\frac{1}{M_P \ln\mathcal{V}}\right)\tilde{\chi}\sigma^{\mu\nu}\lambda G_{\mu\nu}\,, \tag{4.49}$$

$$\mathcal{L}_{\tilde{\Phi}\tilde{X}X} \sim \left(\frac{\sqrt{\mathcal{V}}}{M_P}\right)\tilde{\Phi}\sigma^{\mu\nu}\lambda G_{\mu\nu}\,. \tag{4.50}$$

4.4 Study of moduli thermalisation

Using the general discussion of section 2.3.2 and the explicit expressions for the moduli masses and couplings of section 4.3, we can now study in detail which particles form the thermal bath. Consequently, in section 4.4 we will be able to write down the general form of the finite temperature corrections in the LVS.

We shall start by focusing on the simple $\mathbb{C}P^4_{[1,1,1,6,9]}$ geometry, and then extend our analysis to more general Swiss-cheese and fibred CY manifolds. We will show below that, unlike previous expectations in the literature, the moduli corresponding to small cycles that support chiral matter can reach thermal equilibrium with the matter fields.

4.4.1 Single-hole Swiss-cheese

As we have seen in section 2.3.2, both $2 \leftrightarrow 2$ and $1 \leftrightarrow 2$ processes can establish and maintain thermal equilibrium. Let us now apply the general conditions of section 2.3.2 to our case.

As we have already pointed out, scattering and annihilation processes involving strong interactions will establish thermal equilibrium between MSSM particles for temperatures $T < 10^{15}$ GeV [67]. Let us now concentrate on the moduli.

Small modulus Φ

From section 4.3.1, we know that the largest coupling of the small canonical modulus Φ is with the non-abelian gauge bosons denoted by X:

$$\mathcal{L}_{\Phi XX} = g_{\Phi XX}\Phi F_{\mu\nu}F^{\mu\nu}, \quad g_{\Phi XX} \sim \frac{\sqrt{\mathcal{V}}}{M_P} \sim \frac{1}{M_s}. \tag{4.51}$$

Therefore according to (2.68), scattering or annihilation and pair production processes with two gravitational vertices like $X+X \leftrightarrow \Phi+\Phi$, $X+\Phi \leftrightarrow X+\Phi$, or $X+X \leftrightarrow X+X$, can establish thermal equilibrium between Φ and X for temperatures:

$$T > T_f^{(1)} \equiv g_*^{1/6} \frac{M_P}{\mathcal{V}^{2/3}}, \tag{4.52}$$

where $T_f^{(1)}$ denotes the freeze-out temperature of the modulus. Taking the number of degrees of freedom g_* to be $\mathcal{O}(100)$, as in the MSSM, we find that (4.52) implies $T > 5 \times 10^8$ GeV for $\mathcal{V} \sim 10^{15}$, whereas $T > 10^{16}$ GeV for $\mathcal{V} \sim 10^4$.[9]

In fact, for a typically large volume ($\mathcal{V} > 10^{10}$) a more efficient $2 \leftrightarrow 2$ process is $X + X \leftrightarrow X + \Phi$ with one gravitational and one renormalisable vertex with coupling constant g. Indeed, according to (2.69), such scattering processes maintain thermal equilibrium for temperatures:

$$T > T_f^{(2)} \equiv \frac{g_*^{1/2} M_P}{g^2 \mathcal{V}} \sim 10^3 \frac{M_P}{\mathcal{V}} \quad \text{for} \quad g_* \sim 100 \quad \text{and} \quad g \sim 0.1\,, \tag{4.53}$$

which for $\mathcal{V} \sim 10^{15}$ gives $T > 10^6$ GeV while for $\mathcal{V} \sim 10^4$ it gives $T > 10^{17}$ GeV.

Finally, let us investigate the role played by decay and inverse decay processes of the form $\Phi \leftrightarrow X + X$. We recall that such processes can, in principle, maintain thermal equilibrium only for temperatures:

$$T > m_\Phi \sim \frac{\ln \mathcal{V}}{\mathcal{V}} M_P, \tag{4.54}$$

because the energy of the gauge bosons is given by $E_X \sim T$ and hence for $T < m_\Phi$ it is insufficient for the inverse decay process to occur. However, for $T > m_\Phi$ the process $X + X \to \Phi$ does take place and so one only needs to know the rate of the decay $\Phi \to X + X$ in order to find out whether thermal equilibrium is achieved. According to (2.80) with $D \sim g^2_{\Phi XX}/4\pi \sim \mathcal{V}/4\pi$, where we have also used (4.51), the condition for equilibrium is that:

$$T < T_{eq} \equiv \left(\frac{\mathcal{V} m_\Phi}{4\pi g_*^{1/2} M_P} \right)^{1/3} m_\Phi \sim \left(\frac{\ln \mathcal{V}}{4\pi g_*^{1/2}} \right)^{1/3} m_\Phi \equiv \kappa m_\Phi\,. \tag{4.55}$$

Hence thermal equilibrium between Φ and X can be maintained by $1 \leftrightarrow 2$ processes only if $\kappa > 1$.[10] However, estimating the total number of degrees of freedom as $g_* \sim$

[9] Recall that M_P here is the reduced Planck mass, which equals $(8\pi G_N)^{-1/2} = 2.4 \times 10^{18}$ GeV.

[10] The exact value of κ can be worked out via a more detailed calculation, very similar to the one that

$\mathcal{O}(100)$, and writing the volume as $\mathcal{V} \sim 10^x$, we obtain that $\kappa > 1 \Leftrightarrow x > 55$. Such a large value is unacceptable, as it makes the string scale too small to be compatible with observations. Therefore, we conclude that in LVS the small modulus Φ never thermalises via decay and inverse decay processes.

The final picture is the following:

- For $\mathcal{V}$ of order 10^{15} (10^{10}), as in typical LVS, from (4.53) we deduce that the modulus Φ is in thermal equilibrium with MSSM particles for temperatures $T > T_f^{(2)} \simeq 10^6$ GeV ($T > T_f^{(2)} \simeq 10^{11}$ GeV) due to $X + X \leftrightarrow \Phi + X$ processes.
- On the other hand, for $\mathcal{V} < 10^{10}$, as for LVS that allow gauge coupling unification, the main processes that maintain thermal equilibrium of the modulus Φ with MSSM particles are purely gravitational: $X+X \leftrightarrow \Phi+\Phi$, $\Phi+X \leftrightarrow \Phi+X$ or $X+X \leftrightarrow X+X$ and the freeze-out temperature is given by (4.52). For example for $\mathcal{V} \sim 10^4$ ($\Leftrightarrow M_s \sim 10^{16}$ GeV), Φ is in thermal equilibrium for temperatures $T > T_f^{(1)} \simeq 5 \times 10^{15}$ GeV.

We stress that this is the first example in the literature of a modulus that reaches thermal equilibrium with ordinary particles for temperatures significantly less than M_P, and so completely within the validity of the low energy effective theory. Note that we did not focus on the interactions of Φ with other ordinary and supersymmetric particles, since the corresponding couplings, derived in Appendix 4.A, are not large enough to establish thermal equilibrium.

Large modulus χ

As summarised in section 4.3.1, the coupling of the large modulus χ with gauge bosons is given by

$$\mathcal{L}_{\chi XX} = g_{\chi XX} \chi F_{\mu\nu} F^{\mu\nu}, \quad g_{\chi XX} \sim \frac{1}{M_P \ln \mathcal{V}}. \tag{4.56}$$

Consequently purely gravitational $2 \leftrightarrow 2$ processes like $X+X \leftrightarrow \chi+\chi$, $X+\chi \leftrightarrow X+\chi$, or $X + X \leftrightarrow X + X$, could establish thermal equilibrium between χ and X for temperatures:

$$T > T_f^{(1)} \equiv g_*^{1/6} M_P \left(\ln \mathcal{V}\right)^{4/3}. \tag{4.57}$$

we will carry out in section 4.5.4. It turns out that this value differs from the '$\sim$' estimate in (4.55) just by a multiplicative factor $c^{1/3}$ of $\mathcal{O}(1)$. More precisely, $c = 18(\pi\langle\tau_s\rangle)^{-3/2} e^{K_{\rm cs}/2} W_0 \sqrt{10 g_s}$ and so, for natural values of all the parameters: $W_0 = 1$, $g_s = 0.1$, $\langle\tau_s\rangle = 5$, $K_{\rm cs} = 3$, we obtain $c^{1/3} = 1.09$.

On the other hand, scattering processes like $X + X \leftrightarrow X + \chi$ with one gravitational and one renormalisable vertex with coupling constant g, could maintain thermal equilibrium for temperatures:

$$T > T_f^{(2)} \equiv \frac{g_*^{1/2} M_P}{g^2} \left(\ln \mathcal{V}\right)^2 \sim 10^3 M_P \left(\ln \mathcal{V}\right)^2 , \quad \text{for} \quad g_* \sim 100 \quad \text{and} \quad g \sim 0.1 \,. \quad (4.58)$$

Clearly, both $T_f^{(1)}$ and $T_f^{(2)}$ are greater than M_P and so we conclude that χ can never thermalise via $2 \leftrightarrow 2$ processes. It is also immediate to notice that thermal equilibrium cannot be maintained by $1 \leftrightarrow 2$ processes, like $\chi \leftrightarrow X + X$, either. The reason is that, as derived in [92], for typical LARGE values of the volume $\mathcal{V} \sim 10^{10} - 10^{15}$, the lifetime of the large modulus χ is greater than the age of the Universe. Hence this modulus could contribute to dark matter and its decay to photons or electrons could be one of the smoking-gun signal of LVS.

Furthermore, as can be seen from section 4.3.1, the couplings of χ to other MSSM particles are even weaker than its coupling to gauge bosons. So χ cannot thermalise via any other kind of interaction. Finally, one can also verify that thermal equilibrium between χ and Φ can never be maintained via $1 \leftrightarrow 2$ and $2 \leftrightarrow 2$ processes involving only the moduli, which processes arise due to the moduli triple self-couplings computed in Appendix 4.A.3. Therefore, χ behaves as a typical modulus studied in the literature.

4.4.2 Multiple-hole Swiss-cheese

We shall now extend the previous results to the more general case of CY three-folds with one large cycle and several small ones. We discuss only qualitatively the generic behaviour of small moduli in the case of 'multiple-hole Swiss-cheese' CY manifolds without focusing on explicit models.

As we have seen in Section 4.3.1, the couplings with MSSM particles of all the small cycles wrapped by MSSM branes have the same volume scaling as the corresponding couplings of the single small modulus in the $\mathbb{C}P^4_{[1,1,1,6,9]}$ case. Moreover, in the previous section we have learned that Φ can thermalise via its interaction with gauge bosons. Hence, we conclude that the same arguments as in Section 4.4.1 can be applied for $h_{1,1} > 2$ and so all small cycles, that support MSSM chiral matter, reach thermal equilibrium with the gauge bosons.

However, as we already pointed out in section 4.3.1, the situation may be more complicated in concrete phenomenological models due to the possibility that non-

perturbative effects may be incompatible with MSSM branes, which are localized on the same 4-cycle [94] supporting non-perturbative corrections. Whether or not such an incompatibility arises depends on the particular features of the model one considers, including the presence or absence of charged matter fields with non-vanishing VEVs. As a consequence of these subtleties, the issue of moduli thermalisation is highly dependent on the possible underlying brane set-ups. To gain familiarity with the outcome, let us explore in more detail several brane set-ups in the case of only two small moduli. At the end we will comment on the generalization of these results to the case of arbitrary $h_{1,1}$ Kähler moduli.

We will focus on the case $h_{1,1} = 3$ with two small moduli τ_1 and τ_2, that give the volumes of the two rigid divisors Γ_1 and Γ_2. The results of the previous section imply the following for the different brane setups below:

1. If Γ_1 is wrapped by an ED3 instanton and Γ_2 is wrapped by MSSM branes:
   - τ_1 couples to MSSM gauge bosons with strength $g \sim 1/(\sqrt{\mathcal{V}}M_P) \Rightarrow \tau_1$ does not thermalise.[11]
   - τ_2 couples to MSSM gauge bosons with strength $g \sim \sqrt{\mathcal{V}}/M_P \Rightarrow \tau_2$ thermalises.
2. If Γ_1 is wrapped by an ED3 instanton and $\Gamma_1 + \Gamma_2$ is wrapped by MSSM branes with chiral intersections on Γ_2:[12]
   - τ_1 couples to MSSM gauge bosons with strength $g \sim \sqrt{\mathcal{V}}/M_P \Rightarrow \tau_1$ thermalises.
   - τ_2 couples to MSSM gauge bosons with strength $g \sim \sqrt{\mathcal{V}}/M_P \Rightarrow \tau_2$ thermalises.
3. If Γ_1 is supporting a pure $SU(N)$ theory, that undergoes gaugino condensation, and Γ_2 is wrapped by MSSM branes:
   - τ_1 couples to MSSM gauge bosons with strength $g \sim 1/(\sqrt{\mathcal{V}}M_P)$ and to hidden sector gauge bosons with strength $g \sim \sqrt{\mathcal{V}}/M_P \Rightarrow \tau_1$ thermalises via its interaction with hidden sector gauge bosons.

[11] The coupling $g \sim 1/(\sqrt{\mathcal{V}}M_P)$ can be worked out by substituting the expression (4.21b) in (4.130). As pointed out in point 1 at the end of subsection 4.3.2, the weakness of this coupling is due to the mixing term in (4.21b) being highly suppressed by inverse powers of $\mathcal{V}$.

[12] We assume that a single D7 brane is wrapping Γ_2 in order to get chirality from the intersection with the MSSM branes. The same assumption applies throughout the paper everywhere we use the expression 'chiral intersections on some divisor'.

- τ_2 couples to MSSM gauge bosons with strength $g \sim \sqrt{\mathcal{V}}/M_P$ and to hidden sector gauge bosons with strength $g \sim 1/(\sqrt{\mathcal{V}}M_P) \Rightarrow \tau_2$ thermalises via its interaction with MSSM gauge bosons.

Hence in this case there are two separate thermal baths: one contains τ_1 and the hidden sector gauge bosons at temperature T_1, whereas the other one is formed by τ_2 and the MSSM particles at temperature T_2. Generically, we would expect that $T_1 \neq T_2$ since the two thermal baths are not in contact with each other.

4. If Γ_1 is supporting a pure $SU(N)$ theory, that undergoes gaugino condensation, and $\Gamma_1 + \Gamma_2$ is wrapped by MSSM branes with chiral intersections on Γ_2:

   - τ_1 couples both to MSSM and hidden sector gauge bosons with strength $g \sim \sqrt{\mathcal{V}}/M_P \Rightarrow \tau_1$ thermalises.
   - τ_2 couples to MSSM gauge bosons with strength $g \sim \sqrt{\mathcal{V}}/M_P$ and to hidden sector gauge bosons with strength $g \sim 1/(\sqrt{\mathcal{V}}M_P) \Rightarrow \tau_2$ thermalises via its interaction with MSSM gauge bosons.

   Unlike the previous case, now there is only one thermal bath, which contains both τ_1 and τ_2 together with the MSSM particles and the hidden sector gauge bosons, since in the present case τ_1 interacts strongly enough with the MSSM gauge bosons.

We can now extend these results to the general case with $h_{1,1} > 3$ by noticing that a small 4-cycle wrapped by MSSM branes will always thermalise via its interaction with MSSM gauge bosons. On the other hand, for a 4-cycle that is not wrapped by MSSM branes there are the following two options. If it is wrapped by an ED3 instanton, it will not thermalise. If instead it is supporting gaugino condensation, it will reach thermal equilibrium with the hidden sector gauge bosons.

4.4.3 K3 Fibration

Let us now turn to the issue of moduli thermalisation for K3 fibrations. As we have seen in subsection 4.3.3, there is an essential difference between the cases when the K3 fiber is stabilized at a large and at a small value. Let us consider separately each of these two situations.

Large K3 fiber

As we have already stressed in subsection 4.3.3, in the case 'LV' where the K3 divisor is stabilised large, the small modulus Φ plays exactly the same role as the small modulus of the single-hole Swiss-cheese case, whereas both χ_1 and χ_2 behave as the single large modulus. Hence we can repeat the same analysis as in subsection 4.4.1 and conclude that only Φ will reach thermal equilibrium with the MSSM particles via its interaction with the gauge bosons.

Small K3 fiber

The study of moduli thermalisation in the case of small K3 fiber is more complicated. We shall first focus on CY three-folds with just one blow-up mode and later on will infer the general features of the situation with several blow-ups.

K3 fibrations with $h_{1,1} = 3$ are characterised by two small moduli: τ_1 that gives the volume of the K3 divisor Γ_1, and τ_s which is the volume of the rigid divisor Γ_s. The canonically normalised fields χ_1 and Φ are defined by (4.33) and (4.35). We recall that one has to be careful about the possible incompatibility of MSSM branes on Γ_s with the non-perturbative effects that this cycle supports. Hence, to avoid dealing with such subtleties, below we will assume that the MSSM branes are not wrapping Γ_s. Again, using the results of Subsection 4.4.1, we infer the following for the different brane set-ups below:

1. If Γ_s is wrapped by an ED3 instanton and Γ_1 is wrapped by MSSM branes:
   - χ_1 couples to MSSM gauge bosons with strength $g \sim 1/M_P \Rightarrow \chi_1$ does not thermalise.
   - Φ couples to MSSM gauge bosons more weakly than $\chi_1 \Rightarrow \Phi$ does not thermalise.
2. If Γ_s is wrapped by an ED3 instanton and $\Gamma_s + \Gamma_1$ is wrapped by MSSM branes with chiral intersections on Γ_1:
   - χ_1 couples to MSSM gauge bosons with strength $g \sim \sqrt{\mathcal{V}}/M_P \Rightarrow \chi_1$ thermalises.
   - Φ couples to MSSM gauge bosons with strength $g \sim \sqrt{\mathcal{V}}/M_P \Rightarrow \Phi$ thermalises.
3. If Γ_s is supporting a pure $SU(N)$ theory, that undergoes gaugino condensation, and Γ_1 is wrapped by MSSM branes:

- χ_1 couples to MSSM gauge bosons with strength $g \sim 1/M_P$ and to hidden sector gauge boson with strength $g \sim \sqrt{\mathcal{V}}/M_P \Rightarrow \chi_1$ thermalises via its interaction with hidden sector gauge bosons.
- Φ couples to MSSM gauge bosons more weakly than χ_1 and to hidden sector gauge bosons with strength $g \sim \sqrt{\mathcal{V}}/M_P \Rightarrow \Phi$ thermalises via its interaction with hidden sector gauge bosons.

In this case, two separate thermal baths are established: one contains χ_1, Φ and the hidden sector gauge bosons at temperature T_1, whereas the other one is formed by the MSSM particles at temperature T_2. Generically, we expect that $T_1 \neq T_2$ since the two thermal baths are not in contact with each other.

4. If Γ_s is supporting a pure $SU(N)$ theory, that undergoes gaugino condensation, and $\Gamma_s + \Gamma_1$ is wrapped by MSSM branes with chiral intersections on Γ_1:

   - χ_1 couples both to MSSM and hidden sector gauge bosons with strength $g \sim \sqrt{\mathcal{V}}/M_P \Rightarrow \chi_1$ thermalises.
   - Φ couples both to MSSM and hidden sector gauge bosons with strength $g \sim \sqrt{\mathcal{V}}/M_P \Rightarrow \Phi$ thermalises.

   Now only one thermal bath is established containing χ_1, Φ, the hidden sector gauge bosons and the MSSM particles, since both moduli interact with equal strength with the gauge bosons of the MSSM and of the hidden sector.

It is interesting to notice that both moduli χ_1 and Φ thermalise in all situations, except when the blow-up mode is wrapped by an ED3 instanton only. In this particular case, no modulus thermalises. It is trivial to generalise these conclusions for more than one blow-up mode and the MSSM still localised on the K3 fiber.

On the other hand, if the MSSM is localised on one of the rigid divisors, then for the case of more than one blow-up mode one can repeat the same general conclusions as at the end of subsection 4.4.2, with in addition the fact that χ_1 will always thermalise as soon as one of the blow-up modes thermalises. This is due to the leading order mixing between Φ and any other small modulus, as can be seen explicitly in (4.36) and (4.37).

4.4.4 Modulini thermalisation

The study of modulini thermalisation is straightforward since, as we have seen in subsection 4.3.4, the canonical normalisation for the modulini takes exactly the same

form as the canonical normalisation for the moduli. This implies that, after supersymmetrisation, the small modulino-gaugino-gauge boson coupling has the same strength as the small modulus-gauge boson-gauge boson coupling. Given that this is the relevant interaction for moduli thermalisation, we can repeat the same considerations as those in subsections 4.4.1-4.4.3 and conclude that the modulini thermalise every time, when their supersymmetric partners reach thermal equilibrium with the MSSM thermal bath. Note however that, if for the moduli the relevant processes are $2 \leftrightarrow 2$ interactions with gauge bosons, the crucial $2 \leftrightarrow 2$ processes for the modulini are:

- $2 \leftrightarrow 2$ processes with two gravitational vertices dominant for $\mathcal{V} < 10^{10}$: $\tilde{X}+\tilde{X} \leftrightarrow \tilde{\Phi}+\tilde{\Phi}$, $X+X \leftrightarrow \tilde{\Phi}+\tilde{\Phi}$, $\tilde{X}+\tilde{\Phi} \leftrightarrow \tilde{X}+\tilde{\Phi}$, $X+\tilde{\Phi} \leftrightarrow X+\tilde{\Phi}$, $\tilde{X}+\tilde{X} \leftrightarrow X+X$, $\tilde{X}+X \leftrightarrow \tilde{X}+X$.
- $2 \leftrightarrow 2$ processes with one gravitational and one renormalisable vertex dominant for $\mathcal{V} > 10^{10}$: $X+\tilde{\Phi} \leftrightarrow \tilde{X}+\tilde{X}$, $\tilde{X}+\tilde{\Phi} \leftrightarrow X+X$.

4.5 Finite temperature corrections in LVS

In this section we study the finite temperature effective potential in LVS. We show that it has runaway behaviour at high T and compute the decompactification temperature T_{max}. We also investigate the cosmological implications of the small modulus decay. By imposing that the temperature just after its decay be less than T_{max}, in order to avoid decompactification of the internal space, we find important restrictions on the range of svalues of the CY volume.

4.5.1 Effective potential

We shall now derive the explicit form of the finite temperature effective potential for LVS, following the analysis of moduli thermalisation performed in the previous section. We will study in detail the behaviour of thermal corrections to the $T = 0$ potential of the simple $\mathbb{C}P^4_{[1,1,1,6,9]}$ model, and then realise that the single-hole Swiss-cheese case already incorporates all the key properties of the general LVS.

Single-hole Swiss-cheese

As we have seen in Section 4.4.1, not only ordinary MSSM particles thermalise via Yang-Mills interactions but also the small modulus and modulino reach thermal equilibrium with matter via their interactions with the gauge bosons. Therefore, the

general expression (2.53) for the 1-loop finite temperature effective potential, takes the following form:

$$V_T^{1-loop} = -\frac{\pi^2 T^4}{90}\left(g_B + \frac{7}{8}g_F\right) + \frac{T^2}{24}\left(m_\Phi^2 + m_{\tilde{\Phi}}^2 + \sum_i M_{\rm SOFT,i}^2\right) + \dots . \tag{4.59}$$

We recall that (4.59) is a high temperature expansion of the general 1-loop integral (2.51), and so it is valid only for $T \gg m_\Phi, m_{\tilde{\Phi}}, M_{\rm SOFT,i}$. The general moduli-dependent expression for the modulino mass-squared $m_{\tilde{\Phi}}^2$ is given by (4.43) without the vacuum expectation value. On the other hand, in the limit $\tau_b \gg \tau_s$, m_Φ^2 can be estimated as follows:

$$m_\Phi^2 \simeq {\rm Tr} M_b^2 = \frac{K^{ij}}{2}\frac{\partial^2 V_0}{\partial\tau_i\partial\tau_j} \simeq \frac{K^{ss}}{2}\frac{\partial^2 V_0}{\partial\tau_s^2}. \tag{4.60}$$

For $a_s\tau_s \gg 1$, the previous expression (4.60), at leading order, becomes:

$$m_\Phi^2 \simeq \frac{A_s a_s^3 g_s e^{K_{cs}} M_P^2}{\pi}\left(72 A_s a_s \tau_s e^{-2a_s\tau_s} - \frac{3W_0\tau_s^{3/2}e^{-a_s\tau_s}}{\sqrt{2}\mathcal{V}}\right). \tag{4.61}$$

It can be shown that the gaugino and scalar masses arising from gravity mediated SUSY breaking[13] are always parametrically smaller than m_Φ and $m_{\tilde{\Phi}}$, and so we shall neglect them. Moreover we shall drop also the $\mathcal{O}(T^4)$ term in (4.59) since it has no moduli dependence. Therefore, the relevant 1-loop finite-temperature effective potential reads:

$$V_T^{1-loop} = \frac{T^2}{24}\left(m_\Phi^2 + m_{\tilde{\Phi}}^2\right) + \dots , \tag{4.62}$$

which using (4.43) and (4.61), takes the form:

$$V_T^{1-loop} = \frac{T^2}{24}\left(\frac{g_s e^{K_{cs}} M_P^2}{\pi}\right)\left[\lambda_1\tau_s e^{-2a_s\tau_s} - \lambda_2\left(4 + a_s\tau_s\right)\frac{\sqrt{\tau_s}e^{-a_s\tau_s}}{\mathcal{V}} + \frac{W_0^2}{2\mathcal{V}^2}\right] + \dots , \tag{4.63}$$

with

$$\lambda_1 \equiv 108 A_s^2 a_s^4, \qquad \lambda_2 \equiv 3 a_s^2 A_s W_0/\sqrt{2}. \tag{4.64}$$

Given that the leading contribution in (4.59), namely the $\mathcal{O}(T^4)$ term, does not bring in any moduli dependence, we need to go beyond the ideal gas approximation and consider the effect of 2-loop thermal corrections, as the latter could in principle

[13] The contribution from anomaly mediation is subleading with respect to gravity mediation as shown in [98].

compete with the terms in (4.63). The high temperature expansion of the 2-loop contribution looks like:

$$V_T^{2-loops} = T^4 \left(\kappa_1 g_{MSSM}^2 + \kappa_2 g_{\Phi XX}^2 m_\Phi^2 + \kappa_3 g_{\tilde{\Phi}\tilde{X}X}^2 m_{\tilde{\Phi}}^2 + ... \right) + ... \, , \tag{4.65}$$

where the κ's are $\mathcal{O}(1)$ coefficients and:

- the $\mathcal{O}(g_{MSSM}^2)$ contribution comes from two loops involving MSSM particles,
- the $\mathcal{O}(g_{\Phi XX}^2)$ contribution is due to two loop diagrams with Φ and two gauge bosons,
- the $\mathcal{O}(g_{\tilde{\Phi}\tilde{X}X}^2)$ contribution comes from two loops involving the modulino $\tilde{\Phi}$, the gaugino $\tilde{X}$ and the gauge boson X,
- all the other two loop diagrams give rise to subdominant contributions, and so they have been neglected. Such diagrams are the ones with Φ or $\tilde{\Phi}$ plus other MSSM particles, the self-interactions of the moduli and of the modulini, and two loops involving both Φ and $\tilde{\Phi}$. For example, the subleading contribution originating from the two-loop vacuum diagram due to the Φ^3 self-interaction takes the form: $\delta V_T^{2-loops} = \kappa_4 T^4 \frac{g_{\Phi^3}^2}{m_\Phi^2} \sim T^4 \frac{const}{\mathcal{V}(\ln \mathcal{V})^2}$.

Note that in (4.65) we have neglected the $\mathcal{O}(T^2)$ term since it is subleading compared to both the $\mathcal{O}(T^4)$ 2-loop term and the $\mathcal{O}(T^2)$ 1-loop one. Now, the relevant gauge couplings in (4.65), have the following moduli dependence:

- $g_{MSSM}^2 = 4\pi/\tau_s$ since we assume that the MSSM is built via magnetised D7 branes wrapping the small cycle. In the case of a supersymmetric $SU(N_c)$ gauge theory with N_f matter multiplets, the coefficient κ_1 reads [99]:

$$\kappa_1 = \frac{1}{64} \left(N_c^2 - 1 \right) (N_c + 3N_f) > 0. \tag{4.66}$$

- $g_{\Phi XX}^2 \sim g_{\tilde{\Phi}\tilde{X}X}^2 \sim \frac{\sqrt{\mathcal{V}}}{M_P}$ as derived in (4.50) and (4.131).

Adding (4.62) and (4.65) to the $T = 0$ potential V_0, we obtain the full finite temperature effective potential:

$$V_{TOT} = V_0 + T^4 \left(\kappa_1 g_{MSSM}^2 + \kappa_2 g_{\Phi XX}^2 m_\Phi^2 + \kappa_3 g_{\tilde{\Phi}\tilde{X}X}^2 m_{\tilde{\Phi}}^2 \right) + \frac{T^2}{24} \left(m_\Phi^2 + m_{\tilde{\Phi}}^2 \right) + ... \, . \tag{4.67}$$

Despite the thermalisation of Φ and $\tilde{\Phi}$, which in principle leads to a modification of V_{TOT} compared to previous expectations in the literature, we shall now show that the thermal corrections due to Φ and $\tilde{\Phi}$ are, in fact, negligible compared to the other contributions in (4.67), everywhere in the moduli space of these models. In particular, the 2-loop MSSM effects dominate the temperature-dependent term.[14]

Let us start by arguing that the $\mathcal{O}(T^4)$ corrections arising from the modulus Φ and the modulino $\tilde{\Phi}$ are subleading compared to the 1-loop $\mathcal{O}(T^2)$ term. Indeed, the relevant part of the effective scalar potential (4.67) may be rewritten as:

$$T^4\left(\kappa_2 g^2_{\Phi XX} m^2_\Phi + \kappa_3 g^2_{\tilde{\Phi}\tilde{X}X} m^2_{\tilde{\Phi}}\right) \sim T^2\left(m^2_\Phi + m^2_{\tilde{\Phi}}\right) \underbrace{T^2\frac{\mathcal{V}}{M_P^2}}_{\left(\frac{T}{M_s}\right)^2 \ll 1}, \tag{4.68}$$

where the $\ll$ inequality is due to the fact that our effective field theory treatment makes sense only at energies lower than the string scale M_s. Therefore, we can neglect the effect of 2-loop thermal corrections involving Φ and $\tilde{\Phi}$. So we see that, although the interactions of Φ and $\tilde{\Phi}$ with gauge bosons and gauginos are strong enough to make them thermalise, they are not sufficient to produce thermal corrections large enough to affect the form of the total effective potential. Let us also stress that this result is valid everywhere in moduli space, i.e. for each value of m^2_Φ and $m^2_{\tilde{\Phi}}$, not just in the region around the zero-temperature minimum.

We now turn to the study of the general behaviour of the 1-loop $\mathcal{O}(T^2)$ term arising from Φ and $\tilde{\Phi}$. We shall show that it is always subdominant compared to the zero-temperature potential (4.2), and so it can be safely neglected. In fact, the two relevant terms (4.2) and (4.63) can be written as (ignoring the subleading loop corrections in V_0):

$$V_0 + \frac{T^2}{24}\left(m^2_\Phi + m^2_{\tilde{\Phi}}\right) = \frac{g_s e^{K_{cs}} M_P^4}{8\pi}\left[p_1 A_1 \sqrt{\tau_s}\frac{e^{-2a_s\tau_s}}{\mathcal{V}} - p_2 A_2 \frac{\tau_s e^{-a_s\tau_s}}{\mathcal{V}^2} + p_3 A_3 \frac{1}{\mathcal{V}^3}\right], \tag{4.69}$$

with

$$p_1 = 36 a_s^4 A_s^2, \qquad p_2 = 4 a_s A_s W_0, \qquad p_3 = W_0^2/6, \tag{4.70}$$

[14] Note that this is consistent with the results of the previous chapter and with the ones of [1, 2] in the context of the O'KKLT model, where it was also found that the T-dependent contribution of moduli, that were assumed to be in thermal equilibrium, is negligible compared to the dominant contribution of the rest of the effective potential.

and

$$A_1 \equiv \frac{2\sqrt{2}}{3a_s^2} + \underbrace{\frac{T^2\mathcal{V}\sqrt{\tau_s}}{M_P^2}}_{\left(\frac{T}{M_{KK}}\right)^2 \ll 1}, \quad A_2 \equiv 1 + \frac{a_s^2}{4\sqrt{2}} \underbrace{\frac{T^2\mathcal{V}\sqrt{\tau_s}}{M_P^2}}_{\left(\frac{T}{M_{KK}}\right)^2 \ll 1} \left(1 + \frac{4}{a_s\tau_s}\right), \quad A_3 \equiv \frac{9\hat{\xi}}{2} + \underbrace{\frac{T^2\mathcal{V}}{M_P^2}}_{\left(\frac{T}{M_s}\right)^2 \ll 1}.$$

where the appearance of the Kaluza-Klein scale comes from the assumption that the MSSM branes are wrapping the small cycle τ_s:

$$M_{KK} \sim \frac{M_s}{\tau_s^{1/4}} \simeq \frac{M_P}{\sqrt{\mathcal{V}}\tau_s^{1/4}}\,. \tag{4.71}$$

Therefore, we can see that the 1-loop $\mathcal{O}(T^2)$ thermal corrections can never compete with V_0 for temperatures below the compactification scale $M_{KK} < M_s$, where our low energy effective field theory is trustworthy. Once again, we stress that the previous considerations are valid in all the moduli space (within our large volume approximations) and not just in the vicinity of the $T = 0$ minimum. We have seen that the only finite-temperature contribution that can compete with V_0 is the 2-loop $T^4 g_{MSSM}^2$ term, and so we can only consider from now on the following potential:

$$\begin{aligned} V_{TOT} &= V_0 + 4\pi\kappa_1 \frac{T^4}{\tau_s} \\ &= M_P^4 \left(\frac{g_s e^{K_{cs}}}{8\pi}\right) \left[\frac{\lambda\sqrt{\tau_s}e^{-2a_s\tau_s}}{\mathcal{V}} - \frac{\mu\tau_s e^{-a_s\tau_s}}{\mathcal{V}^2} + \frac{\nu}{\mathcal{V}^3} + \frac{4\pi\tilde{\kappa}_1}{\tau_s}\left(\frac{T}{M_P}\right)^4\right], \end{aligned} \tag{4.72}$$

valid for temperatures $T \gg M_{SOFT}$, and with the constants given in (4.3) and (4.66)[15]. We realize that the leading moduli-dependent finite temperature contribution to the effective potential comes from 2-loops instead of 1-loop. This, however, does not mean that perturbation theory breaks down, since 1-loop effects still dominate when one takes into account the moduli independent $\mathcal{O}(T^4)$ piece that we dropped.

Now, from (4.72) it is clear that the thermal correction cannot induce any new T-dependent extremum of the effective potential. Its presence only leads to destabilization of the $T = 0$ minimum at a certain temperature, above which the potential has a runaway behaviour. Therefore, we are led to the following qualitative picture. Let us assume that at the end of inflation the system is sitting at the $T = 0$ minimum. Then, after reheating the MSSM particles thermalise and the thermal correction $T^4 g_{MSSM}^2 \sim T^4/\tau_s$ gets switched on. As a result, the system starts running

[15]For convenience, here we have redefined $\tilde{\kappa}_1 \equiv 8\pi\kappa_1 g_s^{-1} e^{-K_{cs}}$.

away along the τ_s direction only, since V_T does not depend on $\mathcal{V}$. However, as soon as τ_s becomes significantly larger than its $T = 0$ VEV, the two exponential terms in (4.72) become very suppressed with respect to the $\mathcal{O}(\mathcal{V}^{-3})$ α' correction (the ν term). Hence, the potential develops a run-away behaviour also along the $\mathcal{V}$-direction, thus allowing the Kähler moduli to remain within the Kähler cone.

In section 4.5.2, we shall compute the decompactification temperature, at which the $T = 0$ minimum gets destabilised. Hence we shall focus on the region in the vicinity of the zero-temperature minimum, where the regime of validity of the expression (4.72) takes the form:

$$M_{SOFT} \ll T \ll M_{KK} \qquad \Leftrightarrow \qquad \frac{1}{\mathcal{V}\ln\mathcal{V}} \ll \frac{T}{M_P} \ll \frac{1}{\sqrt{\mathcal{V}}\tau_s^{1/4}}. \tag{4.73}$$

In the typical LVS where $\mathcal{V} \sim 10^{14}$ allows low energy SUSY, we get $M_{SOFT} \sim 10^3$ GeV and $M_{KK} \sim 10^{11}$ GeV; thus, in that case, eq. (4.72) makes sense only for energies 10^3 GeV $\ll T \ll 10^{11}$ GeV. On the other hand, for LVS that allow GUT string scenarios, $\mathcal{V} \sim 10^4$, which implies $M_{SOFT} \sim 10^{13}$ GeV and $M_{KK} \sim 10^{16}$ GeV; thus, in that case, (4.73) becomes 10^{13} GeV $\ll T \ll 10^{16}$ GeV.

General LARGE Volume Scenario

As we have seen in section 4.2, one of the conditions on an arbitrary Calabi-Yau to obtain LVS, is the presence of a blow-up mode resolving a point-like singularity (del Pezzo 4-cycle). The moduli scaling of the scalar potential, at leading order and in the presence of N_{small} blow-up modes τ_{s_i}, $i = 1, ..., N_{small}$, is still of the form (4.2) (neglecting loop corrections):

$$V_0 = \left(\frac{g_s e^{K_{cs}} M_P^4}{8\pi}\right)\left[\sum_{i=1}^{N_{small}}\left(\frac{\lambda\sqrt{\tau_{s_i}}e^{-2a_{s_i}\tau_{s_i}}}{\mathcal{V}} - \frac{\mu\tau_{s_i}e^{-a_{s_i}\tau_{s_i}}}{\mathcal{V}^2}\right) + \frac{\nu}{\mathcal{V}^3}\right]. \tag{4.74}$$

All the other moduli which are neither the overall volume nor a blow-up mode will appear in the scalar potential at subleading order. Moreover, due to the topological nature of $\tau_{s,i}$, $K^{-1}_{s_i s_i} \sim \mathcal{V}\sqrt{\tau_{s_i}}$ $\forall i = 1, ..., N_{small}$ [91].

As derived in section 4.3.1, these blow-up modes correspond to the heaviest moduli and modulini, which play the same role as Φ and $\tilde{\Phi}$ in the single-hole Swiss-cheese case. Hence the leading order behaviour of the mass-squareds of the blow-up moduli τ_{s_i} and the corresponding modulini $\tilde{\tau}_{s_i}$ are still given by (4.43) and (4.61) $\forall i = 1, ..., N_{small}$. Therefore we can repeat the same considerations made in the previous paragraph and

conclude that, for a general LVS, the 1-loop $\mathcal{O}(T^2)$ thermal corrections are always subdominant with respect to V_0 for temperatures below the compactification scale[16]. The only finite-temperature contribution that can compete with V_0 is again the 2-loop $T^4 g^2_{MSSM}$ term.

4.5.2 Decompactification temperature

As we saw in the previous subsection, the finite temperature corrections destabilize the large volume minimum in a general LVS. In this subsection we will derive the decompactification temperature T_{max}, that is the temperature above which the full effective potential has no other minima than the one at infinity.

Before performing a detailed calculation of T_{max}, let us present a qualitative argument that gives a good intuition for its magnitude. Let us denote by V_b the height of the potential barrier that separates the supersymmetric minimum at infinity from the zero temperature SUSY breaking one. Now, in order for the moduli to overcome the potential barrier and run away to infinity, one needs to supply energy of at least the same order of magnitude as V_b. In our case, the source of energy is provided by the finite-temperature effects, which give a contribution to the scalar potential of the order $V_T \sim T^4$. Hence a very good estimate for the decompactification temperature is given by $T_{max} \sim V_b^{1/4}$.

It is instructive to compare the implications of this estimate for the KKLT and LVS cases. In the simplest KKLT models the potential reads:

$$V_{KKLT} = \lambda_1 \frac{e^{-2a\tau}}{\tau} - \lambda_2 W_0 \frac{e^{-a\tau}}{\tau^2}, \tag{4.75}$$

where λ_1 and λ_2 are constants of order unity. The minimum is achieved by fine-tuning the flux parameter $W_0 \sim \tau e^{-a\tau}$ and so the height of the barrier is given by

$$V_b \sim \langle V_{KKLT} \rangle \sim \frac{W_0^2}{\mathcal{V}^2} M_P^4 \sim m_{3/2}^2 M_P^2, \tag{4.76}$$

where we have used the fact that $\mathcal{V} = \tau^{3/2}$ and $m_{3/2} = W_0 M_P / \mathcal{V}$. Therefore the decompactification temperature becomes $T_{max} \sim \sqrt{m_{3/2} M_P} \sim 10^{10}$ GeV, as estimated in [78, 79].

In the case of LVS, the height of the barrier is lower and so we expect a lower

[16] As we have seen in section 4.4.2, if all the τ_{s_i} are wrapped by ED3 instantons then they do not thermalise. Only the moduli corresponding to 4-cycles wrapped by MSSM branes would then thermalise but, since they are lighter than the ED3 moduli, our argument is still valid. The same is true for all the possible scenarios outlined for the K3 fibration case in section 4.4.3.

decompactification temperature T_{max}. Indeed, to leading order the potential is given by

$$V_{LVS} = \lambda_1 \sqrt{\tau_s} \frac{e^{-2a_s\tau_s}}{\mathcal{V}} - \lambda_2 W_0 \tau_s \frac{e^{-a_s\tau_s}}{\mathcal{V}^2} + \lambda_3 \frac{W_0^2}{\mathcal{V}^3} \tag{4.77}$$

with λ_1, λ_2 and λ_3 being constants of order one, as reviewed in section 4.2. The minimum is achieved for natural values of the flux parameter $W_0 \sim \mathcal{O}(1)$ and at exponentially large values of the overall volume $\mathcal{V} \sim W_0 \sqrt{\tau_s} e^{a_s\tau_s}$. Hence the height of the barrier can be estimated as:

$$V_b \sim \langle V_{LVS} \rangle \sim \frac{W_0^2}{\mathcal{V}^3} M_P^4 \sim m_{3/2}^3 M_P, \tag{4.78}$$

which gives a decompactification temperature of the order:

$$T_{max} \sim \left(m_{3/2}^3 M_P \right)^{1/4} \sim \frac{M_P}{\mathcal{V}^{3/4}}. \tag{4.79}$$

Let us now turn to a more precise computation. Without loss of generality, we shall focus here on the effective potential (4.72), valid for the single-hole Swiss-cheese case, and look for its extrema. Given that the thermal contribution does not depend on the volume, the derivative of the potential with respect to $\mathcal{V}$ gives the same result as in the $T = 0$ case:

$$\frac{\partial V_{TOT}}{\partial \mathcal{V}} = 0 \qquad \Longrightarrow \qquad \mathcal{V}_* = \frac{\mu}{\lambda} A(\tau_s) \sqrt{\tau_s} e^{a_s\tau_s}, \tag{4.80}$$

where[17]

$$A(\tau_s) \equiv 1 - \sqrt{1 - \frac{3}{4} \left(\frac{\langle \tau_s \rangle}{\tau_s} \right)^{3/2}}, \tag{4.81}$$

and $\langle \tau_s \rangle \simeq \left(4\lambda\nu/\mu^2 \right)^{2/3}$ is the $T = 0$ VEV of τ_s. Substituting (4.80) in the derivative of V_{TOT} with respect to τ_s and working in the limit $a_s\tau_s \gg 1$, in which one can neglect higher order instanton corrections, we obtain:

$$\left. \frac{\partial V_{TOT}}{\partial \tau_s} \right|_{\mathcal{V}=\mathcal{V}_*} = 0 \quad \Longrightarrow \quad 4\pi\tilde{\kappa}_1 \frac{\mu e^{3a_s\tau_s}}{\lambda^2 a_s \tau_s^2} \left(\frac{T}{M_P} \right)^4 A(\tau_s)^2 + 2A(\tau_s) - 1 = 0. \tag{4.82}$$

Notice that at zero temperature (4.82) simplifies to $A(\tau_s) = 1/2$, which from (4.81) correctly implies $\tau_s = \langle \tau_s \rangle$. Now, since equation (4.82) is transcendental, one can-

[17] We discard the solution with the positive sign in front of the square root in (4.81) since, upon its substitution one finds that the other extremum condition, $\partial V_{TOT}/\partial \tau_s = 0$, does not have any solution.

not write down an analytical solution, that gives the general relation between the location of the τ_s extrema and the temperature. Nevertheless, we will see shortly that it is actually possible to extract an analytic estimate for the decompactification temperature. To understand why, let us gain insight into the behaviour of the function on the LHS of (4.82) by plotting it and looking at its intersections with the τ_s-axis. We plot the LHS of equation (4.82) on Figure 4.1 for several values of the

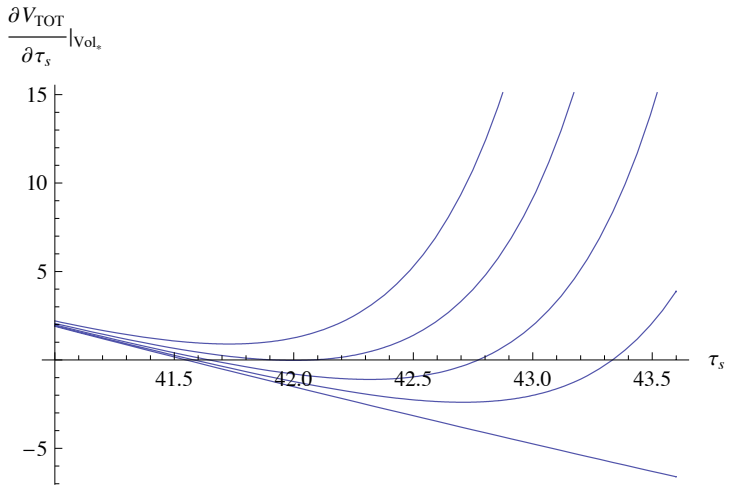

Figure 4.1: The LHS of eq. (4.82) is plotted versus τ_s. The temperature increases from right to left. The straight line represents the zero temperature case. The other values of the temperature are $T/M_P = 0.8 \cdot 10^{-10}$, $1.0 \cdot 10^{-10}$, $1.2 \cdot 10^{-10}$, $1.4 \cdot 10^{-10}$. To obtain the plots we used the following numerical values: $\xi = 1.31$, $A_s = 1$, $W_0 = 1$, $a_s = \pi/4$, $e^{K_{cs}} = 8\pi/g_s$, $g_s = 0.1$, $N_c = 5$, $N_f = 7$. With these values one has that $\langle \tau_s \rangle = 41.55$ and $\langle \mathcal{V} \rangle = 7.02 \cdot 10^{13}$, which implies that $T_{max} = 1.58 \cdot 10^{-10} M_P \simeq 3.79 \cdot 10^8$ GeV according to (4.87). Note that the numerically found value of the decompactification temperature is $T_{max,num} = 1.20 \cdot 10^{-10} M_P$.

temperature; T increases from right to left. From this figure it is easy to see that the temperature-dependent correction to V_{TOT} behaves effectively as an up-lifting term. Namely, the finite-temperature contribution lifts the potential, giving rise to a local maximum (the right intersection with the τ_s axis) in addition to the $T = 0$ minimum (the left intersection). As the temperature increases, the maximum increases as well and shifts towards smaller values of τ_s. On the other hand, the minimum remains very close to the zero-temperature one at all temperatures. Clearly, the decompactification temperature T_{max} is reached when the two extrema coincide. The key observation here is that this happens in a small neighborhood of the $T = 0$ minimum, located at $\langle \tau_s \rangle \simeq \left(4\lambda\nu/\mu^2\right)^{2/3}$.

In view of the considerations of the previous paragraph, to find an analytic estimate

for T_{max} we shall utilize the following strategy. We will Taylor-expand the function $F(\tau_s)$, defined by the LHS of equation (4.82), to second order in a small neighborhood of the point $\tau_s = \langle\tau_s\rangle$. Then we will use the resulting quadratic function $f(\delta)$, where $\delta \equiv \tau_s - \langle\tau_s\rangle$, as an approximation of $F(\tau_s)$ in a larger neighborhood and will look for the zeros of $f(\delta)$. Requiring that the two roots of $f(\delta)$ coincide, will give us an estimate for the decompactification temperature. Clearly, this procedure is not exact. In particular, the function $F(\tau_s)$ is better approximated by keeping higher orders in the Taylor expansion. In our case, we have checked numerically that a really good approximation is obtained by going to at least sixth order. However, in doing so one again ends up with an equation that cannot be solved analytically. So the key point is that the systematic error introduced by the quadratic approximation is rather small (we have checked that the analytical results obtained by following the above procedure are in very good agreement with the exact numerical values).

Now let us substitute $\tau_s = \langle\tau_s\rangle + \delta$ in (4.82) and read off the terms up to order δ^2. The result is:

$$a\,\delta^2 + b\,\delta + c = 0, \tag{4.83}$$

where the corresponding coefficients, in the limit $a_s\langle\tau_s\rangle \gg 1$, take the form:

$$a \simeq \frac{9}{2}\mathcal{T}a_s^2 + \frac{171}{8}\lambda^2 a_s, \quad b \simeq 3\mathcal{T}a_s - 9\lambda^2 a_s\langle\tau_s\rangle, \quad c \simeq \mathcal{T}, \tag{4.84}$$

and we have set

$$\mathcal{T} \equiv 4\pi\tilde{\kappa}_1 \left(\frac{T}{M_P}\right)^4 \mu e^{3a_s\langle\tau_s\rangle}. \tag{4.85}$$

Finally, to find the decompactification temperature, we require that the two solutions δ_1 and δ_2 coincide: which, for $a_s\langle\tau_s\rangle \gg 1$, gives:

$$\mathcal{T}_{max} = 3(\sqrt{2}-1)\lambda^2\langle\tau_s\rangle \quad \Longleftrightarrow \quad T_{max}^4 = \frac{3(\sqrt{2}-1)\lambda^2\langle\tau_s\rangle}{4\pi\tilde{\kappa}_1\mu} e^{-3a_s\langle\tau_s\rangle} M_P^4. \tag{4.86}$$

Notice that we can rewrite the decompactification temperature in terms of $\mathcal{V}$ as:

$$T_{max}^4 = \frac{3(\sqrt{2}-1)}{32\pi}\frac{\mu^2}{\lambda\tilde{\kappa}_1}\frac{\langle\tau_s\rangle^{5/2}}{\mathcal{V}^3} M_P^4 \quad \Longrightarrow \quad T_{max} \sim \left(m_{3/2}^3 M_P\right)^{1/4} \sim \frac{M_P}{\mathcal{V}^{3/4}}, \tag{4.87}$$

where we have used the relation between the $T = 0$ VEV of the volume and $\langle\tau_s\rangle$, which is given by (4.80) with $\tau_s = \langle\tau_s\rangle$ and $A = 1/2$. It is reassuring that (4.87) is of the same form as the result (4.79), obtained from the intuitive arguments based on the height of the potential barrier.

4.5.3 Small moduli cosmology

Clearly, the decompactification temperature (4.87) sets an upper bound on the temperature in the early Universe, in particular on the reheating temperature, T^0_{RH}, at the end of inflation. We will investigate now how this constraint affects the moduli thermalisation picture studied in subsection 4.4.1.[18] Before that, let us define here for clarity the following temperatures:

- T_{max}: the decompactification temperature;
- T_f^{SV}, T_f^{LV}: the freeze-out temperature for the modulus Φ in the small volume and large volume scenario, respectively. Below those temperatures the Φ drops out from the thermal bath;
- T^0_{RH}: the initial reheating temperature, namely the reheating temperature set by the decay of the inflaton field;
- T_{dom}: the temperature at which the energy density of the modulus Φ dominates over the radiation energy;
- T_D: the decay temperature for the modulus Φ;
- T_{RH}: the temperature at which the decay of Φ reheats the Universe.

Furthermore, recall that we derived the following freeze-out temperatures:

- For small values of the volume ($\mathcal{V} < 10^{10}$), the freeze-out temperature for the small modulus Φ is given by (4.52): $T_f^{SV} \sim M_P \mathcal{V}^{-2/3}$.
- For large values of the volume ($\mathcal{V} > 10^{10}$), the freeze-out temperature for Φ is given by (4.53): $T_f^{LV} \sim 10^3 M_P \mathcal{V}^{-1}$.

Note also that, in both cases, the condition $T_f < T^0_{RH} < T_{max}$ has to be satisfied in order for the modulus to reach equilibrium with the MSSM thermal bath. Now, for small values of $\mathcal{V}$ we have that:

$$\frac{T_{max}}{T_f^{SV}} \sim \frac{\mathcal{V}^{2/3}}{\mathcal{V}^{3/4}} = \mathcal{V}^{-1/12} < 1, \tag{4.88}$$

[18] Similar considerations apply for the more general multiple-hole Swiss-cheese and K3 fibration cases.

which implies that Φ actually never thermalises. On the other hand, for large values of $\mathcal{V}$ we have that (writing $\mathcal{V} \sim 10^x$):

$$\frac{T_{max}}{T_f^{LV}} \sim \frac{\mathcal{V}^{1/4}}{10^3} = 10^{x/4-3} > 1 \quad \Leftrightarrow \quad x > 12. \tag{4.89}$$

Hence, for $\mathcal{V} > 10^{12}$, Φ can reach thermal equilibrium with the MSSM plasma, as long as T_{RH}^0 is such that $T_f^{LV} < T_{RH}^0 < T_{max}$. Let us stress, however, that if $T_{RH}^0 < T_f^{LV}$ the modulus will never thermalise even though $T_f^{LV} < T_{max}$. Note that, since the temperature T_{RH}^0 depends on the concrete realization of inflation and the details of the initial reheating process, its determination is beyond the scope of the present work. So we will treat it as a free parameter, satisfying only the constraint $T_{RH}^0 < T_{max}$.

We would like now to study the cosmological history of Φ which, in our case, presents two possibilities:

1. The modulus Φ decays at the end of inflation and is the main responsible for the initial reheating. After Φ decays, its energy density is converted into radiation. The decay products thermalise rapidly and re-heat the Universe to a temperature $T_{RH} = T_{RH}^0$. The latter can be computed by noticing that the Φ energy density $\rho_\Phi \sim \Gamma^2_{\Phi\to XX} M_P^2$ will be converted into radiation energy density $\rho_R \sim g_* T^4$. Hence T_{RH}^0 can be obtained by comparing $\Gamma_{\Phi\to XX}$ with the value of H, given by the Friedmann equation for radiation dominance:

$$\begin{aligned} \Gamma_{\Phi\to XX} \simeq H \Leftrightarrow \frac{\ln\mathcal{V}}{16\pi}\frac{m_\Phi^2}{M_P} \sim g_*^{1/2}\frac{\left(T_{RH}^0\right)^2}{M_P} \\ \Leftrightarrow \quad T_{RH}^0 \simeq \left(\frac{\ln\mathcal{V}}{16\pi\sqrt{g_*}}\right)^{1/2} m_\Phi = \frac{(\ln\mathcal{V})^{3/2}}{4\sqrt{\pi}g_*^{1/4}}\frac{M_P}{\mathcal{V}}. \end{aligned} \tag{4.90}$$

   In order for this picture to be compatible with the presence of a decompactification temperature (4.87), that sets the maximal temperature of the Universe, we need to require that $T_{RH}^0 < T_{max}$. As we shall see in subsection 4.5.4, this requirement can be translated into a constraint on the values that the internal volume can take.

2. The modulus Φ is not the main source of initial reheating, which we suppose to be the inflaton. After the inflaton decays, the Universe is re-heated to a temperature T_{RH}^0 and an epoch of radiation dominance begins. The modulus Φ will only thermalise if $\mathcal{V} > 10^{12}$ and $T_f^{LV} < T_{RH}^0$. However, T_f^{LV} is rather close to T_{max} and so, even when Φ thermalises, it will drop out of equilibrium

very quickly at T_f^{LV}. Then, for general values of $\mathcal{V}$, the modulus Φ will decay out of equilibrium at a temperature $T_D < T_{RH}^0$. As we shall show below, this decay will occur during radiation domination, since $T_D > T_{dom}$, with T_{dom} being the temperature at which the modulus energy density would dominate over the radiation energy density. So the temperature T_D at which Φ decays, is still given by (4.90) upon replacing T_{RH}^0 with T_D:

$$T_D \simeq \frac{(\ln \mathcal{V})^{3/2}}{4\sqrt{\pi} g_*^{1/4}} \frac{M_P}{\mathcal{V}}. \tag{4.91}$$

Note that the above expression satisfies $T_D < T_f^{SV,LV}$, as should be the case for consistency. Another important observation is that (4.91) is also the usual expression for the temperature T_{RH}, to which the Universe is re-heated by the decay of a particle releasing its energy to the thermal bath. In other words, for us $T_{RH} = T_D$ since the modulus Φ decays during radiation domination. On the contrary, if a modulus decays when its energy density is dominating the energy density of the Universe, then $T_D < T_{RH}$ and the decay produces an increase in the entropy density S, which is determined by:

$$\Delta \equiv \frac{S_{fin}}{S_{in}} \sim \left(\frac{T_{RH}}{T_D}\right)^3. \tag{4.92}$$

As already mentioned, since for us $T_{RH} = T_D$, the decay of Φ does not actually lead to reheating or, equivalently, to an increase in the entropy density, given that from (4.92) we have $\Delta = 1$. As a consequence, Φ cannot dilute any unwanted relics, like for example the large modulus χ which suffers from the cosmological moduli problem.[19] To recapitulate, in the present case we have the following system of inequalities among the different temperatures:

$$\text{for } \mathcal{V} < 10^{12}: \quad T_{dom} < T_D < T_{RH}^0 < T_{max}, \tag{4.93}$$

$$\text{for } \mathcal{V} > 10^{12}: \quad T_{dom} < T_D < T_f^{LV} < T_{RH}^0 < T_{max}. \tag{4.94}$$

In this case the condition $T_D < T_{max}$ (similarly to the previous condition $T_{RH}^0 < T_{max}$) implies a constraint on $\mathcal{V}$, that we will derive in subsection 4.5.4. We underline again that this condition is necessary but not sufficient, since for us T_{RH}^0 is an undetermined parameter when Φ is not the inflaton. In concrete

[19] This kind of solution of the cosmological moduli problem, i.e. dilution via saxion or modulus decay, is used both in [72] and in [71].

models, in which one could compute T^0_{RH}, the condition $T^0_{RH} < T_{max}$ might lead to further restrictions.

Let us now prove our claim above that, when the modulus Φ is not responsible for the initial reheating (case 2), it will decay before its energy density begins to dominate the energy density of the Universe. Φ will start oscillating around its VEV when $H \sim m_\Phi$ at a temperature T_{osc} given by:

$$T_{osc} \sim g_*^{-1/4}\sqrt{m_\Phi M_P}. \tag{4.95}$$

The energy density ρ_Φ stored by Φ and the ratio between ρ_Φ and the radiation energy density at T_{osc} read as follows:

$$\rho_\Phi|_{T_{osc}} \sim m_\Phi^2\langle\tau_s\rangle^2 \quad \Rightarrow \quad \left(\frac{\rho_\Phi}{\rho_r}\right)\Big|_{T_{osc}} \sim \frac{m_\Phi^2\langle\tau_s\rangle^2}{g_* T_{osc}^4} \sim \frac{\langle\tau_s\rangle^2}{M_P^2}. \tag{4.96}$$

By definition, the temperature T_{dom}, at which ρ_Φ becomes comparable to ρ_r and hence Φ begins to dominate the energy density of the Universe, is such that:

$$\left(\frac{\rho_\Phi}{\rho_r}\right)\Big|_{T_{dom}} \sim 1. \tag{4.97}$$

Now, given that ρ_Φ redshifts as T^3 whereas ρ_r scales as T^4, we can relate T_{dom} with T_{osc}:

$$T_{dom}\left(\frac{\rho_\Phi}{\rho_r}\right)\Big|_{T_{dom}} \sim T_{osc}\left(\frac{\rho_\Phi}{\rho_r}\right)\Big|_{T_{osc}} \quad \Leftrightarrow \quad T_{dom} \sim g_*^{-1/4}\frac{\langle\tau_s\rangle^2}{M_P^2}\sqrt{m_\Phi M_P}. \tag{4.98}$$

We shall show now that $T_{dom} < T_D$ with T_D being the decay temperature during radiation dominance, which is obtained by comparing H with $\Gamma_{\Phi\to XX}$:

$$T_D \sim g_*^{-1/4}\sqrt{\Gamma_{\Phi\to XX} M_P}. \tag{4.99}$$

The ratio of (4.99) and (4.98) gives:

$$\frac{T_D}{T_{dom}} \sim \frac{\sqrt{\Gamma_{\Phi\to XX}}}{\sqrt{m_\Phi}}\frac{M_P^2}{\langle\tau_s\rangle^2}. \tag{4.100}$$

Using that $\Gamma_{\Phi\to XX} \sim \mathcal{V} m_\Phi^3 M_P^{-2}$ and $\langle\tau_s\rangle \sim 10 M_s \sim 10 M_P \mathcal{V}^{-1/2}$, the last relation becomes:

$$\frac{T_D}{T_{dom}} \sim \frac{(\ln\mathcal{V})\sqrt{\mathcal{V}}}{100} > 1 \quad \text{for} \quad \mathcal{V} > 10^{2.5}. \tag{4.101}$$

Hence, we conclude that $T_D > T_{dom}$ and, therefore, Φ decays before it can begin to dominate the energy density of the Universe. The main consequence of this is that Φ cannot dilute unwanted relics via its decay.

4.5.4 Lower bound on $\mathcal{V}$

As we saw in the previous subsection, there are two possible scenarios for the cosmological evolution of the small modulus Φ. However, since the RHS of (4.90) and (4.91) coincide, in both cases the crucial quantity is the same, although with a different physical meaning. Let us denote this quantity by $T_* \sim (\Gamma_\Phi M_P)^{1/2}$. We shall impose that $T_* < T_{max}$ and shall show below that from this requirement one can derive a lower bound on the possible values of $\mathcal{V}$ in a general LVS. Before we begin, let us first recall that:

1. If Φ is responsible for the initial reheating via its decay, then $T_* = T^0_{RH}$.
2. If Φ decays after the original reheating in a radiation dominated era, then $T_* = T_D < T^0_{RH}$.

Regardless of which of these two situations we consider, T_* is the temperature of the Universe after Φ decays. Then, in order to prevent decompactification of the internal space, we need to impose $T_* < T_{max}$. In general, this condition is necessary but not sufficient because in case 2 one must ensure also that $T^0_{RH} < T_{max}$. This is a constraint that we cannot address given that in this case T^0_{RH} is an undetermined parameter for us.

Let us now compute T_* precisely. We start by using the exact form of the decay rate $\Gamma_{\Phi\to XX}$:

$$\Gamma_{\Phi\to XX} = \frac{g^2_{\Phi XX} m^3_\Phi}{64\pi M_P^2}, \tag{4.102}$$

where

$$g_{\Phi XX} = \frac{2^{5/4}\sqrt{3}}{\langle\tau_s\rangle^{3/4}}\sqrt{\mathcal{V}}. \tag{4.103}$$

The mass of Φ is given by:

$$m_\Phi = \sqrt{P}\frac{2a_s\langle\tau_s\rangle W_0}{\mathcal{V}} M_P, \tag{4.104}$$

where we are denoting with P the prefactor of the scalar potential: $P \equiv g_s e^{K_{cs}}/(8\pi)$. From the minimisation of the scalar potential we have that

$$a_s\langle\tau_s\rangle = \ln(p\mathcal{V}) = \ln p + \ln\mathcal{V}, \tag{4.105}$$

where

$$p \equiv \frac{12\sqrt{2}a_s A_s}{W_0\sqrt{\tau_s}} \sim \mathcal{O}(1) \quad \Rightarrow \quad a_s\langle\tau_s\rangle \simeq \ln\mathcal{V}, \tag{4.106}$$

and so

$$m_\Phi = \sqrt{P}\frac{2W_0\ln\mathcal{V}}{\mathcal{V}}M_P. \tag{4.107}$$

Therefore, the decay rate $\Gamma_{\Phi\to XX}$ turns out to be:

$$\Gamma_{\Phi\to XX} = P^{3/2}\frac{3W_0^3(\ln\mathcal{V})^3}{\sqrt{2}\pi\langle\tau_s\rangle^{3/2}}\frac{M_P}{\mathcal{V}^2}. \tag{4.108}$$

Finally, in order to obtain the total decay rate, we need to multiply $\Gamma_{\Phi\to XX}$ by the total number of gauge bosons for the MSSM $N_X = 12$:

$$\Gamma^{TOT}_{\Phi\to XX} = P^{3/2}\frac{36W_0^3(\ln\mathcal{V})^3}{\sqrt{2}\pi\langle\tau_s\rangle^{3/2}}\frac{M_P}{\mathcal{V}^2}. \tag{4.109}$$

Now, we can find T_* by setting $4\left(\Gamma^{TOT}_{\Phi\to XX}\right)^2/3$ equal to $3H^2$, with H read off from the Friedmann equation for radiation dominance:

$$T_* = \left(\frac{40}{\pi^2 g_*}\right)^{1/4}\sqrt{\Gamma^{TOT}_\Phi M_P} = P^{3/4}\frac{6}{\pi}\left(\frac{20}{g_*}\right)^{1/4}\frac{(W_0\ln\mathcal{V})^{3/2}}{\langle\tau_s\rangle^{3/4}}\frac{M_P}{\mathcal{V}}. \tag{4.110}$$

We are finally ready to explore the constraint $T_* < T_{max}$. Recall that the maximal temperature is given by the decompactification temperature (4.87):

$$T_{max} = \left(\frac{P}{4\pi\kappa_1}\right)^{1/4}\left[\frac{(\sqrt{2}-1)}{4\sqrt{2}}\right]^{1/4}\frac{\sqrt{W_0}\langle\tau_s\rangle^{5/8}}{\mathcal{V}^{3/4}}M_P. \tag{4.111}$$

Let us now consider the ratio T_{max}/T_* and impose that it is larger than unity (using $g_*(MSSM) = 228.75$):

$$R \equiv \frac{T_{max}}{T_*} = c\frac{\mathcal{V}^{1/4}}{(\ln\mathcal{V})^{3/2}} \quad \text{with} \quad c \equiv J\left[\frac{(\sqrt{2}-1)g_*}{80\sqrt{2}}\right]^{1/4}\frac{\pi\langle\tau_s\rangle^{11/8}}{6W_0} \simeq \frac{\langle\tau_s\rangle^{11/8}}{2W_0}, \tag{4.112}$$

where we have defined:

$$J \equiv \left(4\pi\kappa_1 P^2\right)^{-1/4} = \frac{8.42}{\kappa_1^{1/4}} e^{-K_{\rm cs}/2} \quad \text{for} \quad g_s = 0.1, \tag{4.113}$$

and in the last approximation in (4.112) we have set $J = 1$.[20] Let us consider now the maximum and minimum values that the parameter c can take for natural values of $\langle\tau_s\rangle$ and W_0:

$$\begin{cases} \langle\tau_s\rangle_{max} = 100 \\ W_{0,min} = 0.01 \end{cases} \implies c_{max} \simeq 10^4, \tag{4.114}$$

$$\begin{cases} \langle\tau_s\rangle_{min} = 2 \\ W_{0,max} = 100 \end{cases} \implies c_{min} \simeq 10^{-2}. \tag{4.115}$$

Now writing $\mathcal{V} \simeq 10^x$, R becomes a function of x and c. Finally, we can make a 3D plot of R with $c_{min} < c < c_{max}$ and $2 < x < 15$, and see in which region $R > 1$. This is done in Figure 4.2. In order to understand better what values of $\mathcal{V}$ are disfavoured, we also plot in Figure 4.3, as the shaded region, the region in the (x,c)-plane below the curve $R = 1$, which represents the phenomenologically forbidden area for which $T_{max} < T_*$. We conclude that small values of the volume, which would allow the

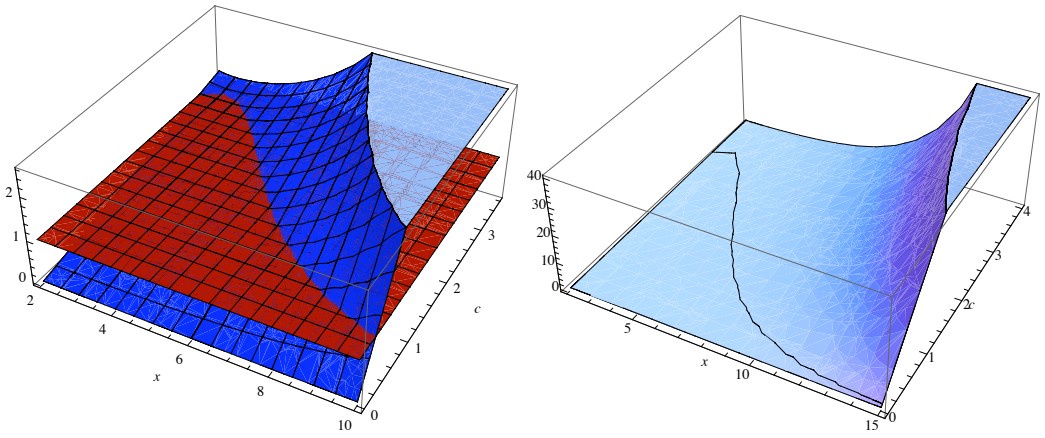

Figure 4.2: Plots of the ratio $R \equiv T_{max}/T_*$ as a function of $\mathcal{V} = 10^x$ and the parameter $c_{min} < c < c_{max}$ as defined in (4.112), (4.114) and (4.115). In the left plot, the red surface is the constant function $R = 1$, whereas in the right plot the black line denotes the curve in the (x,c)-plane for which $R = 1$.

[20] In fact, from (4.66), we find that in the case of SQCD with $N_c = 3$ and $N_f = 6$, $\kappa_1 = 2.625$. However for the MSSM we expect a larger value of κ_1 which we assume to be of the order $\kappa_1 = 10$. Then for natural values of $K_{\rm cs}$ like $K_{\rm cs} = 3$, from (4.113), we find $J = 1.05$.

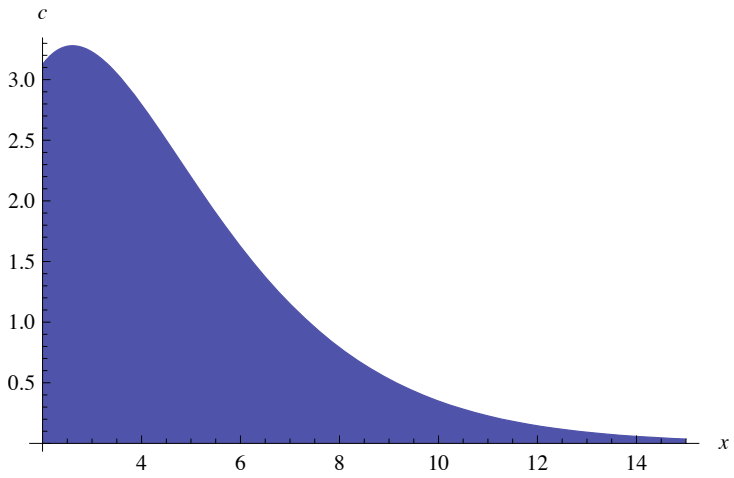

Figure 4.3: Plot of the $R = 1$ curve in the (x,c)-plane. The shaded region represents the phenomenologically forbidden area, in which the values of x and c are such that $R < 1 \Leftrightarrow T_{max} < T_*$.

standard picture of gauge coupling unification and GUT theories, are disfavoured compared to larger values of $\mathcal{V}$, that naturally lead to TeV-scale SUSY and are thus desirable to solve the hierarchy problem. In Table 4.4, we show explicitly how the lower bound on the volume, for some benchmark scenarios, favours LVS with larger values of $\mathcal{V}$.

	$R > 1 \Leftrightarrow$ $T_{max} > T_*$
$c = 4$	$\forall x$
$c = 3$	$x > 2.1$
$c = 2$	$x > 3.8$
$c = 1$	$x > 5.9$
$c = 0.5$	$x > 7.6$
$c = 0.1$	$x > 11.3$
$c = 0.05$	$x > 12.8$
$c = 0.01$	$x > 16.1$

Table 4.4: Lower bounds on the volume in the string frame $\mathcal{V}_s \sim 10^{x-3/2}$ for some benchmark scenarios.

From the definition (4.112) of the parameter c, it is interesting to notice that for values of $\langle \tau_s \rangle$ far from the edge of consistency of the supergravity approximation $\langle \tau_s \rangle \sim \mathcal{O}(10)$, c should be fairly large, and hence the bound very weak, for natural

values of $W_0 \sim \mathcal{O}(1)$, while c should get smaller for larger values of W_0 that lead to a stronger bound. In addition, it is reassuring to notice that for typical values of $\mathcal{V} \sim 10^{15}$, $T_{max} > T_*$ except for a tiny portion of the (x,c)-space. It also important to recall that the physical value of the volume as seen by the string is the one expressed in the string frame $\mathcal{V}_s$, while we are working in the Einstein frame where $\mathcal{V}_s = g_s^{3/2}\mathcal{V}_E$. Hence if we write $\mathcal{V}_E \sim 10^x$, then we have that $\mathcal{V}_s = 10^{x-3/2}$, upon setting $g_s = 0.1$.

General LARGE Volume Scenario

Let us now generalise our lower bound on $\mathcal{V}$ to the four cases studied in subsections 4.4.2 and 4.4.3 for the multiple-hole Swiss-cheese and K3 fibration case (focusing on the small K3 fiber scenario) respectively.

First of all, we note that, since in all the cases the 4-cycle supporting the MSSM is stabilised by string loop corrections [91], we can estimate the actual height of the barrier seen by this modulus as (see (4.7)):

$$V_b \sim \frac{W_0^2}{\mathcal{V}^3\sqrt{\tau}}, \tag{4.116}$$

where we are generically denoting any small cycle (either a blow-up or a K3 fiber divisor) as τ, given that the values of the VEV of all these 4-cycles will have the same order of magnitude. Then setting $V_b \sim T_{max}^4/\tau$, we obtain:

$$T_{max}^4 \sim \frac{\sqrt{\tau}W_0^2}{\mathcal{V}^3}. \tag{4.117}$$

We notice that (4.117) is a bit lower than (4.87) but the two expressions for T_{max} share the same leading order $\mathcal{V}$-dependence.

Let us now examine the 4 cases of subsection 4.4.2 in more detail, keeping the same notation and denoting as Φ the small modulus of the single-hole Swiss-cheese scenario studied above:

1. The relevant decay is the one of τ_2 to MSSM gauge bosons. The order of magnitude of the mass of τ_2 is:

$$m_{\tau_2}^2 \sim \frac{(\ln \mathcal{V})^2 W_0^2}{\mathcal{V}^2\tau^2}, \tag{4.118}$$

   and so τ_2 is lighter than Φ, and, in turn, T_* will be smaller. In fact, plugging

(4.118) in (4.102), we end up with (ignoring numerical prefactors):

$$T_* \sim \frac{(\ln \mathcal{V})^{3/2} W_0^{3/2}}{\mathcal{V}\tau^{9/4}}. \tag{4.119}$$

Hence we obtain

$$R^{(1)} \equiv \frac{T_{max}}{T_*} = c^{(1)} \frac{\mathcal{V}^{1/4}}{(\ln \mathcal{V})^{3/2}} \quad \text{with} \quad c^{(1)} \sim \frac{\tau^{19/8}}{W_0}. \tag{4.120}$$

Comparing this result with (4.112), we realise that $R^{(1)} \sim R\,\tau$ and so the lower bound on $\mathcal{V}$ turns out to be less stringent. The final results can still be read from Table 4.4 upon replacing c with $c^{(1)}$.

2. The relevant decay is the one of τ_1 to MSSM gauge bosons since $m_{\tau_1} \sim m_\Phi$, and so τ_1 is heavier than τ_2. Therefore T_* will still be given by (4.110). Hence we obtain

$$R^{(2)} \equiv \frac{T_{max}}{T_*} = c^{(2)} \frac{\mathcal{V}^{1/4}}{(\ln \mathcal{V})^{3/2}} \quad \text{with} \quad c^{(2)} \sim \frac{\tau^{7/8}}{W_0}. \tag{4.121}$$

Comparing this result with (4.112), we realise that $R^{(2)} \sim R\,\tau^{-1/2}$ and so the lower bound on $\mathcal{V}$ turns out to be more stringent. The final results can still be read from Table 4.4 upon replacing c with $c^{(2)}$.

3. The relevant decay is the one of τ_1 to hidden sector gauge bosons. Hence we point out that the considerations of case 2 apply also for this case.

4. The relevant decay is the one of τ_1 to MSSM gauge bosons, and so we can repeat the same considerations of case 2.

The final picture is that for all cases the $\mathcal{V}$-dependence of the ratio T_{max}/T_* is the same as in (4.112). The only difference is a rescaling of the parameter c. Thus we conclude that, as far as the lower bound on $\mathcal{V}$ is concerned, the single-hole Swiss-cheese case shows all the qualitative features of a general LVS.

Finally, we mention that in the case of a K3 fibration with small K3 fiber, cases 2, 3, and 4 of subsection 4.4.3 have the same behaviour as case 2 of the multiple-hole Swiss-cheese, so giving a more stringent lower bound on $\mathcal{V}$. We should note though that this lower bound does not apply to case 1 of subsection 4.4.3, since both of the moduli have an M_P-suppressed, instead of M_s-suppressed, coupling to MSSM gauge bosons. However, these kinds of models tend to prefer larger values of $\mathcal{V}$ (due to the

fact that $a_s = 2\pi$ for an ED3 instanton) which are not affected by the lower bound that we derived.

4.6 Discussion

In this section we shall discuss some of the possible applications of these results and at the same time give some indications for future works on this subject. As we have emphasized throughout the chapter, there are two kinds of LVS, depending on the magnitude of the value of the internal volume $\mathcal{V}$. We now outline their main cosmological characteristics.

4.6.1 LV case

In this case the volume is stabilised at large values of the order $\mathcal{V} \sim 10^{15}$ which allows to solve the hierarchy problem yielding TeV scale SUSY naturally. Here are the main cosmological features of these scenarios:

- The moduli spectrum includes a light field χ related to the overall volume. This field is a source for the cosmological moduli problem (CMP) as long as $M_s < 10^{13}$ GeV, corresponding to $\mathcal{V} > 10^{10}$. In fact, in this case the modulus χ is lighter than 10 TeV and, coupling with gravitational strength interactions, it would overclose the Universe or decay so late to ruin Big-Bang nucleosynthesis. There are two main possible solutions to this CMP:

  1. The light modulus χ gets diluted due to an increase in the entropy that occurs when a short-lived modulus decays out of equilibrium and while dominating the energy density of the Universe [71, 72];
  2. The volume modulus gets diluted due to a late period of low energy inflation caused by thermal effects [69, 70].

  Assuming this problem is solved, the volume modulus becomes a dark matter candidate (with a mass $m \sim 1$ MeV, if $\mathcal{V} \sim 10^{15}$) and its decay to e^+e^- could be one of the sources that contribute to the observed 511 KeV line, coming from the centre of our galaxy.[21] The light modulus χ can also decay into photons, producing a clean monochromatic line that would represent a clear astrophysical

[21] However, recently it has been discovered with the INTEGRAL spectrometer SPI [100] that the 511 KeV line emission appears to be asymmetric. This distribution of positron annihilation resembles that of low mass X-ray binaries, suggesting that these systems may be the dominant origin of the positrons and so reducing the need for more exotic explanations, such as the one presented above.

smoking-gun signal for these scenarios [92]. We point out that in the case of K3 fibrations, where the K3 fiber is stabilised large [91], the spectrum of moduli fields includes an additional light field. This field is also a potential dark matter candidate with a mass $m \sim 10$ keV, that could produce another monochromatic line via its decay to photons.

- At present, there are no known models of inflation in LVS with intermediate scale M_s. However, the Fibre Inflation model of [97] can give rise to inflation for every value of $\mathcal{V}$. The only condition, which fixes $\mathcal{V} \sim 10^3$, and so $M_s \sim M_{GUT}$, is the matching with the COBE normalisation for the density fluctuations. Such a small value of $\mathcal{V}$ is also necessary to have a very high inflationary scale (close to the GUT scale) which, in turn, implies detectable gravity waves. However, in principle it is possible that the density perturbations could be produced by another scalar field (not the inflaton), which is playing the role of a curvaton. In such a case, one could be able to get inflation also for $\mathcal{V} \sim 10^{15}$. In this way, both inflation and TeV scale SUSY would be achieved within the same model, even though gravity waves would not be observable. It would be interesting to investigate whether such scenarios are indeed realisable.

- As derived in Section 4.5.2, if the volume is stabilised such that $\mathcal{V} \sim 10^{15}$, the decompactification temperature is rather low: $T_{max} \sim 10^7$ GeV.

4.6.2 SV case

In this case the volume is stabilised at smaller values of the order $\mathcal{V} \sim 10^4$, which allows to reproduce the standard picture of gauge coupling unification with $M_s \sim M_{GUT}$. Here are the main cosmological features of these scenarios:

- Given that in this case $\mathcal{V} < 10^{13}$, all the moduli have a mass $m > 10$ TeV, and so they decay before Big-Bang nucleosynthesis. Hence these scenarios are not plagued by any CMP.

- As we have already pointed out in the LV case above, smaller values of $\mathcal{V}$ give rise to the inflationary model presented in [97].

- Fixing the volume at small values of the order $\mathcal{V} \sim 10^3$, the decompactification temperature turns out to be extremely high: $T_{max} \sim 10^{15}$ GeV.

According to the discussion above, it would seem that cosmology tends to prefer smaller values of $\mathcal{V}$. The reason is that in the SV case there is no CMP and at least

one model of inflation is known, whereas for $\mathcal{V} \sim 10^{15}$ the light modulus suffers from the CMP and no model of inflation has been found yet. Interestingly enough, the lower bound on $\mathcal{V}$, derived in this chapter, suggests exactly the opposite. Namely, larger values of $\mathcal{V}$ are favoured since, writing the volume as $\mathcal{V} \sim 10^x$ and recalling the definition (4.112) of the parameter c, the constraint $T_* < T_{max}$ rules out a relevant portion of the (x, c)-parameter space, that corresponds to the SV case.

We shall not discuss further the realization of inflation in the LV scenario, however, we would like to comment on the cosmological moduli problem which is present in this scenario for $\mathcal{V} > 10^{10}$. The results of this paper pose a challenge for the solution of the problem. Indeed, as we have shown in subsection 4.5.3, the CMP cannot be solved by diluting the volume modulus via the entropy increase caused by the decay of the small moduli. The reason is that the latter decay before they can begin to dominate the energy density of the Universe. So let us now discuss in more detail the prospects of the other main possible solution of the CMP in LVS which was first suggested in [92], namely, thermal inflation.

4.6.3 Thermal Inflation

Thermal inflation has been studied in the literature from the field theoretic point of view [69, 70]. The basic idea is that a field ϕ, whose VEV is much larger than its mass (and so is called flaton) can be trapped by thermal corrections at a false vacuum at the origin of the field space. At a certain temperature, its vacuum energy density starts dominating over the radiation one thus leading to a short period of inflation. This period ends when the temperature drops enough to destabilise the local minimum the flaton was trapped in.

Since the flaton ϕ has a VEV $\langle\phi\rangle \gg m_\phi$, it is assumed that the quartic piece in its potential is absent. However, in this way, the 1-loop thermal corrections cannot trap the flaton in the origin because they go like

$$V_T \sim T^2 m_\phi^2 = T^2 \frac{d^2 V}{d\phi^2}, \tag{4.122}$$

and there is no quartic term in V that would give rise to a term like $T^2\phi^2$. Instead, it is usually assumed that there is an interaction of the flaton with a very massive field, say a scalar ψ, of the form $g\psi^2\phi^2$, where $g \sim 1$ so that ψ thermalises at a relatively low temperature. At this point, a 1-loop thermal correction due to ψ would give the required term

$$V_T \sim T^2 m_\psi^2 = gT^2\phi^2. \tag{4.123}$$

The interaction term $g\psi^2\phi^2$ generates a mass term for ψ of the order $m_\psi \sim \langle\phi\rangle$. Hence, when ϕ is trapped in the origin at high T, ψ becomes very light. Close to the origin, the potential looks like:

$$V = V_0 + (gT^2 - m_\phi^2)\phi^2 + \dots, \tag{4.124}$$

where V_0 is the height of the potential in the origin. A period of thermal inflation takes place in the temperature window $T_c < T < T_{in}$, where $T_{in} \sim V_0^{1/4}$ is the temperature at which the flaton starts to dominate the energy density of the Universe (beating the radiation energy density $\rho_r \sim T^4$) and $T_c \sim m_\phi/g$ is the critical temperature at which the flaton undergoes a phase transition rolling towards the $T = 0$ minimum. The number of e-foldings of thermal inflation is given by:

$$N_e \sim \ln\left(\frac{T_{in}}{T_c}\right) \sim \ln\sqrt{\frac{\langle\phi\rangle}{m_\phi}}. \tag{4.125}$$

Let us see how the above picture relates to the LVS. In the case of $\mathcal{V} \sim 10^{15}$, the modulus τ_s has the right mass scale and VEV to produce $N_e \sim 10$ e-foldings of inflation, which would solve the CMP without affecting the density perturbations generated during ordinary high-energy inflation. However, in subsection 4.5.1 we derived the relevant 1-loop temperature corrections to the scalar potential and showed that they are always subleading with respect to the $T = 0$ potential, for temperatures below the Kaluza-Klein scale. Hence, since thermal inflation requires the presence of new minima at finite-temperature, we would be tempted to conclude that it does not take place in the LVS. In fact, this was to be expected also for the following reason. According to the field theoretic arguments above, in order for thermal inflation to occur, it is crucial that the flaton be coupled to a very massive field ψ. However, in our model there is no particle, which is heavier than the flaton candidate τ_s.

Let us now discuss possible extensions of our model that could, perhaps, allow for thermal inflation to occur, as well as the various questions that they raise.

1. Since in our case τ_s is the candidate flaton field, the necessary ψ field would have a mass of the order $m_\psi \sim \langle\tau_s\rangle M_s$, and so it is likely to be a stringy mode. In such a case, it is not a priori clear how to compute thermal corrections to V_T due to the presence of ψ in the thermal bath.

2. Even if we can compute V_T, it is not clear why these corrections should trap τ_s at the origin. Note, however, that this is not implausible, as the origin is a

special point in moduli space, where new states may become massless or the local symmetry may get enhanced. Any such effect might turn out to play an important role.

3. Even assuming that V_T does trap τ_s in the origin, one runs into another problem. Namely, the corresponding small cycle shrinks below M_s and so we cannot trust our low-energy EFT. For a full description, we should go to the EFT that applies close to the origin. The best known examples of these are EFTs for blow-up fields at the actual orbifold point. In addition, one should verify that $\mathcal{V}$ stays constant when the τ_s cycle shrinks to zero size.

4. When τ_s goes to zero, the field ψ should become massless, according to the comparison with the field theoretic argument (if this comparison is valid). So possible candidates for the role of the ψ field could be winding strings or D1-branes wrapping a 1-cycle of the collapsing 4-cycle.

5. If ψ corresponds to a winding string, the interaction of the flaton τ_s with ψ cannot be seen in the EFT and it would be very difficult to have a detailed treatment of this issue.

6. The field ψ could also be a right handed neutrino, or sneutrino, heavier than τ_s. The crucial question would still be if it would be possible to see ψ in our EFT description. In addition, one would need to write down m_ψ as a function of τ_s and $\mathcal{V}$. It goes without saying that this issue is highly dependent on the particular mechanism for the generation of neutrino masses.

7. Besides the small modulus τ_s, another possible flaton candidate could be a localised matter field such as an open string mode. However we notice that the main contribution to the scalar potential of this field should come from D-terms, and that a D-term potential usually gives rise to a mass of the same order of the VEV. Hence it may be difficult to find an open string mode with the typical behaviour of a flaton field.

In general, all of the above open questions are rather difficult to address. This poses a significant challenge for the derivation of thermal inflation in LVS and the corresponding solution of the CMP. However, let us note that the CMP could also be solved by finding different models of low-energy inflation, which do not rely on thermal effects.

4.7 Conclusions

In this chapter, we studied how finite-temperature corrections affect the $T = 0$ effective potential of type IIB LVS and what are the subsequent cosmological implications in this context.

We showed that the small moduli and modulini can reach thermal equilibrium with the MSSM particles. Despite that, we were able to prove that their thermal contribution to the effective potential is always subleading compared to the $T = 0$ potential, for temperatures below the Kaluza-Klein scale. As a result, the leading temperature-dependent part of the effective potential is due only to the MSSM thermal bath and it turns out to have runaway behaviour at high T. We derived the decompactification temperature T_{max}, above which the $T = 0$ minimum is completely erased and the volume of the internal space starts running towards infinity. Clearly, in this class of IIB compactifications the temperature T_{max} represents the maximal allowed temperature in the early Universe. Hence, in particular, it gives an upper bound on the initial reheating temperature after inflation: $T^0_{RH} < T_{max}$.[22] The temperature T^0_{RH} is highly dependent on the details of the concrete inflationary model and re-heating process, and so in principle its determination is beyond the scope of our paper. Nevertheless, we can compute the temperature of the Universe after the small moduli decay. They are rather short-lived and their decay can either be the main source of initial reheating (in which case the temperature after their decay is exactly T^0_{RH}) or it can occur during a radiation dominated epoch, after initial reheating has already taken place. In both cases, the resulting temperature of the Universe T_* has to satisfy $T_* < T_{max}$, which implies a lower bound on the allowed values of $\mathcal{V}$. We were able to derive this bound and show that it rules out a large range of smaller $\mathcal{V}$ values (which lead to standard GUT theories), while favouring greater values of $\mathcal{V}$ (that lead to TeV scale SUSY). Note though, that the condition $T_* < T_{max}$ is both necessary and sufficient in the case the decay of the small moduli is the origin of initial reheating, whereas it is just necessary but not sufficient in the case the small moduli decay below T^0_{RH}.

Finally, we discussed possible cosmological applications of our work. In particular, we argued that, to realize thermal inflation in this type of compactifications, one needs to go beyond the current effective field theory description of the closed string moduli sector.

[22] Note, however, that it may be possible to relax this constraint to a certain degree by studying the dynamical evolution of the moduli in presence of finite temperature corrections, as in [73] for the KKLT set-up.

Appendix 4.A Moduli couplings

We shall now assume that the MSSM is built via magnetised D7 branes wrapping an internal 4-cycle within the framework of 4D $\mathcal{N}=1$ supergravity. The full Lagrangian of the system can be obtained by expanding the superpotential W, the Kähler potential K and the gauge kinetic functions f_i as a power series in the matter fields:

$$W = W_{mod}(\varphi) + \mu(\varphi) H_u H_d + \frac{Y_{ijk}(\varphi)}{6} C^i C^j C^k + ..., \tag{4.126a}$$

$$K = K_{mod}(\varphi, \bar{\varphi}) + \tilde{K}_{i\bar{j}}(\varphi, \bar{\varphi}) C^i C^{\bar{j}} + [Z(\varphi, \bar{\varphi}) H_u H_d + h.c.] + ..., \tag{4.126b}$$

$$f_i = \frac{T_{MSSM}}{4\pi} + h_i(F) S. \tag{4.126c}$$

In the previous expressions, φ denotes globally all the moduli fields, and W_{mod} and K_{mod} are the superpotential and the Kähler potential for the moduli, which we have discussed in depth in Section 4.2. H_u and H_d are the two Higgs doublets of the MSSM, and the C's denote collectively all the matter fields. In the expression for the gauge kinetic function (4.126), T_{MSSM} is the modulus related to the 4-cycle wrapped by the MSSM $D7$ branes, and $h_i(F)$ are 1-loop topological functions of the world-volume fluxes F on different branes (the index i runs over the three MSSM gauge group factors). Finally the moduli scaling of the Kähler potential for matter fields $\tilde{K}_{i\bar{j}}(\varphi, \bar{\varphi})$ and $Z(\varphi, \bar{\varphi})$, for LVS with the small cycle τ_s supporting the MSSM, has been derived in [101] and looks like:[23]

$$\tilde{K}_{i\bar{j}}(\varphi, \bar{\varphi}) \sim \frac{\tau_s^{1/3}}{\tau_b} k_{i\bar{j}}(U) \quad \text{and} \quad Z(\varphi, \bar{\varphi}) \sim \frac{\tau_s^{1/3}}{\tau_b} z(U). \tag{4.127}$$

4.A.1 Moduli couplings to ordinary particles

We now review the derivation of the moduli couplings to gauge bosons, matter particles and Higgs fields for high temperatures $T > M_{EW}$. In this case all the gauge bosons and matter fermions are massless.

Couplings to Gauge Bosons

The coupling of the gauge bosons X to the moduli arise from the moduli dependence of the gauge kinetic function (4.126). We shall assume that the MSSM $D7$ branes are

[23] Note that, in the case of more than one small cycle supporting the MSSM, these expressions would be more complicated.

wrapping the small cycle[24], and so we identify $T_{MSSM} \equiv T_s$. We also recall that the gauge couplings of the different MSSM gauge groups are given by the real part of the gauge kinetic function, and that one obtains different values by turning on different fluxes. Thus the coupling of τ_s with the gauge bosons is the same for $U(1)$, $SU(2)$ and $SU(3)$. We now focus on the $U(1)$ factor without loss of generality. The kinetic terms read (neglecting the τ_s-independent 1-loop contribution)

$$\mathcal{L}_{gauge} = -\frac{\tau_s}{M_P} F_{\mu\nu} F^{\mu\nu}. \tag{4.128}$$

We then expand τ_s around its minimum and go to the canonically normalised field strength $G_{\mu\nu}$ defined as

$$G_{\mu\nu} = \sqrt{\langle \tau_s \rangle} F_{\mu\nu}, \tag{4.129}$$

and obtain

$$\mathcal{L}_{gauge} = -G_{\mu\nu} G^{\mu\nu} - \frac{\delta\tau_s}{M_P \langle \tau_s \rangle} G_{\mu\nu} G^{\mu\nu}. \tag{4.130}$$

Now by means of (4.17b) we end up with the following *dimensionful* couplings

$$\mathcal{L}_{\chi XX} \sim \left(\frac{1}{M_P \ln \mathcal{V}} \right) \chi G_{\mu\nu} G^{\mu\nu}, \tag{4.131a}$$

$$\mathcal{L}_{\Phi XX} \sim \left(\frac{\sqrt{\mathcal{V}}}{M_P} \right) \Phi G_{\mu\nu} G^{\mu\nu}. \tag{4.131b}$$

Couplings to matter fermions

The terms of the supergravity Lagrangian which are relevant to compute the order of magnitude of the moduli couplings to an ordinary matter fermion ψ are its kinetic and mass terms[25]:

$$\mathcal{L} = \tilde{K}_{\bar{\psi}\psi} \bar{\psi} i \gamma^\mu \partial_\mu \psi + e^{K/2} \lambda H \bar{\psi} \psi, \tag{4.132}$$

where H is the corresponding Higgs field (either H_u or H_d). The moduli scaling of $\tilde{K}_{\bar{\psi}\psi}$ is given in (4.127), whereas $e^{K/2} = \mathcal{V}^{-1}$. Expanding the moduli and the Higgs

[24] The large cycle would yield an unrealistically small gauge coupling: $g^2 \sim \langle \tau_b \rangle^{-1} \sim 10^{-10}$.

[25] Instead of the usual 2-component spinorial notation, we are using here the more convenient 4-component spinorial notation.

around their VEVs, we obtain

$$\begin{aligned}\mathcal{L} &= \frac{\langle\tau_s\rangle^{1/3}}{\langle\tau_b\rangle}\left(1+\frac{1}{3}\frac{\delta\tau_s}{\langle\tau_s\rangle}-\frac{\delta\tau_b}{\langle\tau_b\rangle}+...\right)\bar{\psi}i\gamma^\mu\partial_\mu\psi \\ &\quad+\frac{1}{\langle\tau_b\rangle^{3/2}}\left(1-\frac{3}{2}\frac{\delta\tau_b}{\langle\tau_b\rangle}+...\right)\lambda\left(\langle H\rangle+\delta H\right)\bar{\psi}\psi. \end{aligned} \tag{4.133}$$

We now canonically normalise the ψ kinetic terms ($\psi \to \psi_c$) and rearrange the previous expression as

$$\begin{aligned}\mathcal{L} &= \bar{\psi}_c\left(i\gamma^\mu\partial_\mu+m_\psi\right)\psi_c+\left(\frac{1}{3}\frac{\delta\tau_s}{\langle\tau_s\rangle}-\frac{\delta\tau_b}{\langle\tau_b\rangle}\right)\bar{\psi}_c\left(i\gamma^\mu\partial_\mu+m_\psi\right)\psi_c \\ &\quad-\left(\frac{1}{3}\frac{\delta\tau_s}{\langle\tau_s\rangle}+\frac{1}{2}\frac{\delta\tau_b}{\langle\tau_b\rangle}\right)m_\psi\bar{\psi}_c\psi_c+\mathcal{L}_{\delta H}, \end{aligned} \tag{4.134}$$

where

$$m_\psi \equiv \frac{\lambda\langle H\rangle}{\langle\tau_s\rangle^{1/3}\langle\tau_b\rangle^{1/2}}, \tag{4.135}$$

and

$$\mathcal{L}_{\delta H}=\left(\frac{\lambda}{\langle\tau_b\rangle^{1/2}\langle\tau_s\rangle^{1/3}}\right)\delta H\bar{\psi}_c\psi_c-\left(\frac{3\lambda}{2\langle\tau_b\rangle^{3/2}\langle\tau_s\rangle^{1/3}}\right)\delta\tau_b\delta H\bar{\psi}_c\psi_c. \tag{4.136}$$

The second term of (4.134) does not contribute to the moduli interactions since Feynman amplitudes vanish for on-shell final states satisfying the equations of motion. Writing everything in terms of Φ and χ, we end up with the following *dimensionless* couplings

$$\mathcal{L}_{\chi\bar{\psi}_c\psi_c} \sim \left(\frac{m_\psi}{M_P}\right)\chi\bar{\psi}_c\psi_c, \tag{4.137a}$$

$$\mathcal{L}_{\Phi\bar{\psi}_c\psi_c} \sim \left(\frac{m_\psi\sqrt{\mathcal{V}}}{M_P}\right)\Phi\bar{\psi}_c\psi_c. \tag{4.137b}$$

Moreover the first term in the Higgs Lagrangian (4.136) gives rise to the usual Higgs-fermion-fermion coupling, whereas the second term yields a modulus-Higgs-fermion-

fermion vertex:

$$\mathcal{L}_{\delta H\bar{\psi}_c\psi_c} \sim \left(\frac{1}{\mathcal{V}^{1/3}}\right)\delta H\bar{\psi}_c\psi_c, \tag{4.138a}$$

$$\mathcal{L}_{\chi\delta H\bar{\psi}_c\psi_c} \sim \left(\frac{1}{M_P\mathcal{V}^{1/3}}\right)\chi\delta H\bar{\psi}_c\psi_c, \tag{4.138b}$$

$$\mathcal{L}_{\Phi\delta H\bar{\psi}_c\psi_c} \sim \left(\frac{1}{M_P\mathcal{V}^{5/6}}\right)\Phi\delta H\bar{\psi}_c\psi_c. \tag{4.138c}$$

We notice that for $T > M_{EW}$ the fermions are massless since $\langle H\rangle = 0$, and so the two direct moduli couplings to ordinary matter particles (4.137a) and (4.137b) are absent.

Couplings to Higgs Fields

The form of the un-normalised kinetic and mass terms for the Higgs from the supergravity Lagrangian, reads:

$$\mathcal{L}_{Higgs} = \tilde{K}_{\bar{H}H}\partial_\mu H\partial^\mu\bar{H} - \tilde{K}_{\bar{H}H}\left(\hat{\mu}^2 + m_0^2\right)H\bar{H}, \tag{4.139}$$

where H denotes a Higgs field (either H_u or H_d), and $\hat{\mu}$ and m_0 are the canonically normalised supersymmetric μ-term and SUSY breaking scalar mass respectively. Their volume dependence, in the dilute flux limit, is [98]:

$$|\hat{\mu}| \sim m_0 \sim \frac{M_P}{\mathcal{V}\ln\mathcal{V}}. \tag{4.140}$$

In addition to (4.139), there is also a mixing term of the form

$$\mathcal{L}_{Higgs\ \ mix} = Z\left(\partial_\mu H_d\partial^\mu H_u + \partial_\mu\bar{H}_d\partial^\mu\bar{H}_u\right) - \tilde{K}_{\bar{H}H}B\hat{\mu}\left(H_dH_u + \bar{H}_d\bar{H}_u\right), \tag{4.141}$$

with

$$B\hat{\mu} \sim m_0^2. \tag{4.142}$$

However given that we are interested only in the leading order volume scaling of the Higgs coupling to the moduli, we can neglect the $\mathcal{O}(1)$ mixing of the *up* and *down*

components, and focus on the simple Lagrangian:

$$\begin{aligned}\mathcal{L}_{Higgs} &= \tilde{K}_{\bar{H}H}\left(\partial_\mu H\partial^\mu\bar{H} - \frac{M_P^2}{(\mathcal{V}\ln\mathcal{V})^2}H\bar{H}\right)\\ &= -\frac{1}{2}\tilde{K}_{\bar{H}H}\left[\bar{H}\left(\Box + \frac{M_P^2}{(\mathcal{V}\ln\mathcal{V})^2}\right)H + H\left(\Box + \frac{M_P^2}{(\mathcal{V}\ln\mathcal{V})^2}\right)\bar{H}\right]\end{aligned} \tag{4.143}$$

where we have integrated by parts. We now expand $\tilde{K}_{\bar{H}H}$ and $(\mathcal{V}\ln\mathcal{V})^{-2}$ and get:

$$\begin{aligned}\mathcal{L}_{Higgs} \simeq\ & -\frac{1}{2}K_0\left(1 + \frac{1}{3}\frac{\delta\tau_s}{\langle\tau_s\rangle} - \frac{\delta\tau_b}{\langle\tau_b\rangle}\right)\left[\bar{H}\left(\Box + m_H^2\left(1 - 3\frac{\delta\tau_b}{\langle\tau_b\rangle}\right)\right)H + \right.\\ & \left. H\left(\Box + m_H^2\left(1 - 3\frac{\delta\tau_b}{\langle\tau_b\rangle}\right)\right)\bar{H}\right],\end{aligned} \tag{4.144}$$

where $K_0 = \langle\tau_s\rangle^{1/3}\langle\mathcal{V}\rangle^{-2/3}$ and the Higgs mass is given by

$$m_H \simeq \frac{M_P}{\langle\mathcal{V}\rangle\ln\langle\mathcal{V}\rangle}. \tag{4.145}$$

Now canonically normalising the scalar kinetic terms $H \to H_c = \sqrt{K_0}H$, we obtain

$$\begin{aligned}\mathcal{L}_{Higgs} =\ & -\frac{1}{2}\left[\bar{H}_c\left(\Box + m_H^2\right)H_c + H_c\left(\Box + m_H^2\right)\bar{H}_c\right]\\ & -\frac{1}{2}\left(\frac{1}{3}\frac{\delta\tau_s}{\langle\tau_s\rangle} - \frac{\delta\tau_b}{\langle\tau_b\rangle}\right)\left[\bar{H}_c\left(\Box + m_H^2\right)H_c + H_c\left(\Box + m_H^2\right)\bar{H}_c\right]\\ & +3\frac{\delta\tau_b}{\langle\tau_b\rangle}m_H^2\bar{H}_cH_c.\end{aligned}$$

The second term in the previous expression does not contribute to scattering amplitudes since Feynman amplitudes vanish for final states satisfying the equations of motion. Thus the *dimensionful* moduli couplings to Higgs fields arise only from the third term once we express $\delta\tau_b$ in terms of Φ and χ using (4.17a). The final result is

$$\mathcal{L}_{\Phi\bar{H}_cH_c} \sim \left(\frac{m_H^2}{M_P\sqrt{\mathcal{V}}}\right)\Phi\bar{H}_cH_c \sim \left(\frac{M_P}{\mathcal{V}^{5/2}(\ln\mathcal{V})^2}\right)\Phi\bar{H}_cH_c, \tag{4.146a}$$

$$\mathcal{L}_{\chi\bar{H}_cH_c} \sim \left(\frac{m_H^2}{M_P}\right)\chi\bar{H}_cH_c \sim \left(\frac{M_P}{\mathcal{V}^2(\ln\mathcal{V})^2}\right)\chi\bar{H}_cH_c. \tag{4.146b}$$

4.A.2 Moduli couplings to supersymmetric particles

We shall now work out the moduli couplings to gauginos, SUSY scalars and Higgsinos. Given that we are interested in thermal corrections at high temperatures, we shall

focus on $T > M_{EW}$. Thus we can neglect the mixing of Higgsinos with gauginos into charginos and neutralinos, which takes place at lower energies due to EW symmetry breaking.

Couplings to Gauginos

The relevant part of the supergravity Lagrangian involving the gaugino kinetic terms and their soft masses looks like

$$\mathcal{L}_{gaugino} \simeq \frac{\tau_s}{M_P}\bar{\lambda}' i\bar{\sigma}^\mu \partial_\mu \lambda' + \frac{F^s}{2}\left(\lambda'\lambda' + h.c.\right), \tag{4.147}$$

where in the limit of dilute world-volume fluxes on the D7-brane, the gaugino mass is given by $M_{1/2} = \frac{F^s}{2\tau_s}$, [98]. Now if the small modulus supporting the MSSM is stabilised via non-perturbative corrections, then the corresponding F-term scales as

$$F^s \simeq \frac{\tau_s}{\mathcal{V}\ln\mathcal{V}}. \tag{4.148}$$

Notice that the suppression factor $\ln\mathcal{V} \sim \ln(M_P/m_{3/2})$ in (4.148) would be absent in the case of perturbative stabilisation of the MSSM cycle [91]. Let us expand τ_s around its VEV and get:

$$\begin{aligned}\mathcal{L}_{gaugino} \;\simeq\; & \langle\tau_s\rangle\left[\bar{\lambda}' i\bar{\sigma}^\mu\partial_\mu\lambda' + \frac{1}{2}\frac{M_P}{\mathcal{V}\ln\mathcal{V}}\left(\lambda'\lambda' + h.c.\right)\right] \\ & + \frac{\delta\tau_s}{M_P}\left[\bar{\lambda}' i\bar{\sigma}^\mu\partial_\mu\lambda' + \frac{M_P}{\langle\mathcal{V}\rangle\ln\langle\mathcal{V}\rangle}\frac{(\lambda'\lambda' + h.c.)}{2}\right].\end{aligned} \tag{4.149}$$

We need now to expand also τ_b around its VEV in the first term of (4.149):

$$\frac{1}{\mathcal{V}\ln\mathcal{V}} \simeq \frac{1}{\tau_b^{3/2}\ln\mathcal{V}} \simeq \frac{1}{\langle\mathcal{V}\rangle\ln\langle\mathcal{V}\rangle}\left(1 - \frac{3}{2}\frac{\delta\tau_b}{\langle\tau_b\rangle} + ...\right), \tag{4.150}$$

and canonically normalise the gaugino kinetic terms $\lambda' \to \lambda = \sqrt{\langle\tau_s\rangle}\lambda'$. At the end we obtain:

$$\begin{aligned}\mathcal{L}_{gaugino} \;\simeq\; & \bar{\lambda} i\bar{\sigma}^\mu\partial_\mu\lambda + \frac{\delta\tau_s}{\langle\tau_s\rangle M_P}\bar{\lambda} i\bar{\sigma}^\mu\partial_\mu\lambda \\ & + \frac{M_P}{\langle\mathcal{V}\rangle\ln\langle\mathcal{V}\rangle}\frac{(\lambda\lambda + h.c.)}{2} + \frac{(\lambda\lambda + h.c.)}{2\langle\mathcal{V}\rangle\ln\langle\mathcal{V}\rangle}\left(\frac{\delta\tau_s}{\langle\tau_s\rangle} - \frac{3}{2}\frac{\delta\tau_b}{\langle\tau_b\rangle}\right).\end{aligned} \tag{4.151}$$

From (4.151) we can immediately read off the gaugino mass:

$$M_{1/2} \simeq \frac{M_P}{\langle\mathcal{V}\rangle \ln\langle\mathcal{V}\rangle} \simeq \frac{F^s}{\tau_s} \sim \frac{m_{3/2}}{\ln\left(M_P/m_{3/2}\right)}. \tag{4.152}$$

Let us now rewrite (4.151) as:

$$\mathcal{L}_{gaugino} \simeq \left(1 + \frac{\delta\tau_s}{\langle\tau_s\rangle M_P}\right)\left[\bar{\lambda} i\bar{\sigma}^\mu \partial_\mu \lambda + \frac{M_{1/2}}{2}\left(\lambda\lambda + h.c.\right)\right] - \frac{3}{4}\frac{\delta\tau_b}{\langle\tau_b\rangle}\frac{M_{1/2}}{M_P}\left(\lambda\lambda + h.c.\right). \tag{4.153}$$

We shall now focus only on the last term in (4.153) since it is the only one that contributes to decay rates. In fact, Feynman amplitudes with on-shell final states that satisfy the equations of motion, are vanishing. Using (4.17a), we finally obtain the following *dimensionless* couplings:

$$\mathcal{L}_{\Phi\lambda\lambda} \sim \left(\frac{M_{1/2}}{M_P\sqrt{\mathcal{V}}}\right)\Phi\lambda\lambda \sim \left(\frac{1}{\mathcal{V}^{3/2}\ln\mathcal{V}}\right)\Phi\lambda\lambda, \tag{4.154a}$$

$$\mathcal{L}_{\chi\lambda\lambda} \sim \left(\frac{M_{1/2}}{M_P}\right)\chi\lambda\lambda \sim \left(\frac{1}{\mathcal{V}\ln\mathcal{V}}\right)\chi\lambda\lambda. \tag{4.154b}$$

Couplings to SUSY Scalars

The form of the un-normalised kinetic and soft mass terms for SUSY scalars from the supergravity Lagrangian, reads:

$$\mathcal{L}_{scalars} = \tilde{K}_{\alpha\bar{\beta}}\partial_\mu C^\alpha \partial^\mu \bar{C}^{\bar{\beta}} - \frac{\tilde{K}_{\alpha\bar{\beta}}}{\left(\mathcal{V}\ln\mathcal{V}\right)^2} C^\alpha \bar{C}^{\bar{\beta}}. \tag{4.155}$$

Assuming diagonal Kähler metric for matter fields

$$\tilde{K}_{\alpha\bar{\beta}} = \tilde{K}_\alpha \delta_{\alpha\bar{\beta}}, \tag{4.156}$$

the initial Lagrangian (4.155) simplifies to

$$\begin{aligned}\mathcal{L}_{scalars} &= \tilde{K}_\alpha\left(\partial_\mu C^\alpha \partial^\mu \bar{C}^{\bar{\alpha}} - \frac{1}{\left(\mathcal{V}\ln\mathcal{V}\right)^2} C^\alpha \bar{C}^{\bar{\alpha}}\right) \\ &= -\frac{1}{2}\tilde{K}_\alpha\left[\bar{C}^{\bar{\alpha}}\left(\Box + \frac{1}{\left(\mathcal{V}\ln\mathcal{V}\right)^2}\right)C^\alpha + C^\alpha\left(\Box + \frac{1}{\left(\mathcal{V}\ln\mathcal{V}\right)^2}\right)\bar{C}^{\bar{\alpha}}\right]\end{aligned} \tag{4.157}$$

We note that (4.157) is of exactly the same form as the Higgs Lagrangian (4.143). This is not surprising since for temperatures $T > M_{EW}$, the Higgs behaves effectively as a SUSY scalar with mass of the order the scalar soft mass: $m_H \sim m_0$. Thus we can

read off immediately the *dimensionful* moduli couplings to the canonically normalised SUSY scalars φ from (4.146a) and (4.146b):

$$\mathcal{L}_{\Phi\bar{\varphi}\varphi} \sim \left(\frac{m_0^2}{M_P\sqrt{\mathcal{V}}}\right)\Phi\bar{\varphi}\varphi \sim \left(\frac{M_P}{\mathcal{V}^{5/2}(\ln\mathcal{V})^2}\right)\Phi\bar{\varphi}\varphi, \tag{4.158a}$$

$$\mathcal{L}_{\chi\bar{\varphi}\varphi} \sim \left(\frac{m_0^2}{M_P}\right)\chi\bar{\varphi}\varphi \sim \left(\frac{M_P}{\mathcal{V}^{2}(\ln\mathcal{V})^2}\right)\chi\bar{\varphi}\varphi. \tag{4.158b}$$

Couplings to Higgsinos

The relevant part of the supergravity Lagrangian involving the Higgsino kinetic terms and their supersymmetric masses looks like:

$$\mathcal{L}_{Higgsino} \simeq \tilde{K}_{\bar{\tilde{H}}\tilde{H}}\left[\bar{\tilde{H}}_u i\bar{\sigma}^\mu\partial_\mu\tilde{H}_u + \bar{\tilde{H}}_d i\bar{\sigma}^\mu\partial_\mu\tilde{H}_d + \hat{\mu}\left(\tilde{H}_u\tilde{H}_d + h.c.\right)\right]. \tag{4.159}$$

After diagonalising the supersymmetric Higgsino mass term, we end up with a usual Lagrangian of the form:

$$\mathcal{L}_{Higgsino} \simeq \tilde{K}_{\bar{\tilde{H}}\tilde{H}}\left[\bar{\tilde{H}} i\bar{\sigma}^\mu\partial_\mu\tilde{H} + \hat{\mu}\left(\tilde{H}\tilde{H} + h.c.\right)\right], \tag{4.160}$$

where $\tilde{H}$ denotes collectively both the Higgsino mass eigenstates, which are the result of a mixing between the *up* and *down* gauge eigenstates. We recall also that since we are focusing on temperatures above the EWSB scale, we do not have to deal with any mixing between Higgsinos and gauginos to give neutralinos and charginos. Expanding the Kähler metric (4.127) and the μ-term (4.140), we obtain:

$$\mathcal{L}_{Higgsino} \simeq K_0\left(1 + \frac{1}{3}\frac{\delta\tau_s}{\langle\tau_s\rangle} - \frac{\delta\tau_b}{\langle\tau_b\rangle}\right)\left[\bar{\tilde{H}} i\bar{\sigma}^\mu\partial_\mu\tilde{H} + \frac{m_{\tilde{H}}}{2}\left(1 - \frac{3}{2}\frac{\delta\tau_b}{\langle\tau_b\rangle}\right)\left(\tilde{H}\tilde{H} + h.c.\right)\right], \tag{4.161}$$

where $K_0 = \langle\tau_s\rangle^{1/3}\langle\mathcal{V}\rangle^{-2/3}$ and the physical Higgsino mass is of the same order of magnitude of the soft SUSY masses:

$$m_{\tilde{H}} \simeq \frac{M_P}{\langle\mathcal{V}\rangle\ln\langle\mathcal{V}\rangle} \simeq M_{1/2}. \tag{4.162}$$

Now canonically normalising the scalar kinetic terms $\tilde{H} \to \tilde{H}_c = \sqrt{K_0}\tilde{H}$, we end up with:

$$\begin{aligned}\mathcal{L}_{Higgsino} &= \left(1 + \frac{1}{3}\frac{\delta\tau_s}{\langle\tau_s\rangle} - \frac{\delta\tau_b}{\langle\tau_b\rangle}\right)\left[\bar{\tilde{H}}_c i\bar{\sigma}^\mu \partial_\mu \tilde{H}_c + \frac{m_{\tilde{H}}}{2}\left(\tilde{H}_c\tilde{H}_c + h.c.\right)\right] \\ &\quad -\frac{3}{4}\frac{\delta\tau_b}{\langle\tau_b\rangle} m_{\tilde{H}}\left(\tilde{H}_c\tilde{H}_c + h.c.\right). \end{aligned} \tag{4.163}$$

Writing everything in terms of Φ and χ, from the last term of (4.163), we obtain the following *dimensionless* couplings:

$$\mathcal{L}_{\chi\tilde{H}_c\tilde{H}_c} \sim \left(\frac{m_{\tilde{H}}}{M_P}\right)\chi\tilde{H}_c\tilde{H}_c \sim \left(\frac{1}{\mathcal{V}\ln\mathcal{V}}\right)\chi\tilde{H}_c\tilde{H}_c, \tag{4.164a}$$

$$\mathcal{L}_{\Phi\tilde{H}_c\tilde{H}_c} \sim \left(\frac{m_{\tilde{H}}}{M_P\sqrt{\mathcal{V}}}\right)\Phi\tilde{H}_c\tilde{H}_c \sim \left(\frac{1}{\mathcal{V}^{3/2}\ln\mathcal{V}}\right)\Phi\tilde{H}_c\tilde{H}_c. \tag{4.164b}$$

4.A.3 Moduli self couplings

In this section we shall investigate if moduli reach thermal equilibrium among themselves. In order to understand this issue, we need to compute the moduli self interactions, which can be obtained by first expanding the moduli fields around their VEV

$$\tau_i = \langle\tau_i\rangle + \delta\tau_i, \tag{4.165}$$

and then by expanding the potential around the LARGE Volume vacuum as follows:

$$V = V(\langle\tau_s\rangle, \langle\tau_b\rangle) + \frac{1}{2}\left.\frac{\partial^2 V}{\partial\tau_i\partial\tau_j}\right|_{\min}\delta\tau_i\delta\tau_j + \frac{1}{3!}\left.\frac{\partial^3 V}{\partial\tau_i\partial\tau_j\partial\tau_k}\right|_{\min}\delta\tau_i\delta\tau_j\delta\tau_k + ... \tag{4.166}$$

We then concentrate on the trilinear terms which can be read off from the third term of (4.166). We neglect the $\mathcal{O}(\delta\tau_i^4)$ terms since the strength of their couplings will be subleading with respect to the $\mathcal{O}(\delta\tau_i^3)$ terms since one has to take a further derivative which produces a suppression factor. Taking the third derivatives and then expressing these self-interactions in terms of the canonically normalised fields

$$\begin{aligned}\delta\tau_b &\sim \mathcal{O}\left(\mathcal{V}^{1/6}\right)\Phi + \mathcal{O}\left(\mathcal{V}^{2/3}\right)\chi, \\ \delta\tau_s &\sim \mathcal{O}\left(\mathcal{V}^{1/2}\right)\Phi + \mathcal{O}\left(1\right)\chi,\end{aligned}$$

we end up with the following Lagrangian terms at leading order in a large volume expansion:

$$\mathcal{L}_{\Phi^3} \simeq \frac{M_P}{\mathcal{V}^{3/2}}\Phi^3, \qquad \mathcal{L}_{\Phi^2\chi} \simeq \frac{M_P}{\mathcal{V}^2}\chi\Phi^2, \tag{4.167}$$

$$\mathcal{L}_{\chi^2\Phi} \simeq \frac{M_P}{\mathcal{V}^{5/2}}\Phi\chi^2, \qquad \mathcal{L}_{\chi^3} \simeq \frac{M_P}{\mathcal{V}^3}\chi^3. \tag{4.168}$$

5 D-anti-D branes at finite temperature

Summary. In this chapter we consider a pair of parallel Dp and anti-Dp branes in flat space, with a finite separation d along some perpendicular spatial direction and at finite temperature. If this spatial direction is compactified on a circle then by T-duality, the system is equivalent to a D(p+1) anti-D(p+1) pair wrapped around the dual circle with a constant Wilson line $A \sim d$ on one of the branes. We focus in particular on the p = 8 case and compute the free energy of this system and study the occurrence of second order phase transitions as both the temperature and Wilson line (brane-antibrane separation) are varied. In the limit of vanishing Wilson line we recover the previous results obtained in the literature, whereby the open string vacuum is stabilized at sufficiently high temperature. For sufficiently large Wilson line, we find new second order phase transitions corresponding to the existence of two minima in the tachyon effective potential at finite temperature and tachyon field value.

5.1 Introduction

In the previous chapters we considered type IIB flux compactification at finite temperature and concluded that the inclusion of temperature corrections do no alter significantly the zero temperature scenario. In this final chapter we study a system in which the inclusion of thermal corrections modify the picture at zero temperature, namely, we consider a pair of separated parallel brane-antibrane at finite temperature. This configuration is unstable to decay through the open string tachyon field T rolling down to its minimum.Whilst the above behaviour of the open string tachyon is true for a system at zero temperature, it can become stable once finite temperature corrections are switched on. The study of such corrections is interesting because it is possible that such brane configurations could survive in the early universe.

Separated brane-antibrane system at zero temperature have been considered in the context warped type IIB flux compactification as a way of obtaining inflation [102], see also [103, 104] for a review on the subject.

In this chapter we will work in flat space instead. There have been several papers discussing the situation if the brane-antibrane pair is considered as part of a thermodynamic system at finite temperature [105–109].

In [106], Hotta investigated the phase structure of a finite temperature Dp and anti-Dp brane pair where the branes were assumed to be coincident and in flat space. Using the framework of *boundary string field theory* (BSFT) he showed that in the p = 9 case, a phase transition occurs just below the string Hagedorn temperature, whereas for p < 9 there is no phase transition. In the p = 9 case, the zero temperature minimum of the tachyon effective potential was shown to shift from $T \to \infty$ towards $T \to 0$ as the temperature approached criticality. Thus the interpretation is that the open string vacuum is stabilized at sufficiently high temperature (but below the Hagedorn transition) in the case of D9-$\overline{\text{D9}}$ whereas for pairs of lower dimensionality, no such transition occurs and the point $T = 0$ remains unstable at high temperature.

These results are in broad agreement with those of Danielsson et al. [105] who investigated the same system but rather than including the full set of string states, in computing the free energy they focussed on the truncation to the tachyonic sector only.

In this chapter we wish to generalize the results above to the case where the D(p-1)-$\overline{\text{D}}(p-1)$ pair is separated along some perpendicular spatial direction, but still parallel and in flat space. We shall assume that the pair has a finite separation d along a perpendicular spatial direction which is compactified on a circle S^1. Then by T-duality, the system is equivalent to a Dp-$\overline{\text{Dp}}$ pair wrapped around the dual circle $\tilde{S}^1$, with a constant Wilson line $A \sim d$ turned on one of the branes [108], [110].

At zero temperature, one may extend the BSFT results to include Wilson lines and obtain an expression for the effective potential at 1-loop $V_{eff}(T, A)$ depending on T and the Wilson line A. At tree level, the extrema of this potential depend on the size of A: for $A < \frac{1}{\sqrt{2\alpha'}}$ the potential has a local maximum at $T = 0$ as in the case of a coincident brane-antibrane. If $A > \frac{1}{\sqrt{2\alpha'}}$, $T = 0$ becomes a local minimum and so the open string vacuum is metastable [108]. We shall see that when we consider this latter situation at finite temperature, we have an interesting situation whereby the effective potential (in the canonical ensemble) has two local minima at finite values of T. Thus we can ask the same question again, about what vacuum the tachyon field will likely be found, i.e., which vacuum is thermodynamically favoured over the other. Also, it is interesting to ask what is the likelihood of a first order phase transition occurring since we anticipate that the two minima might well become degenerate at some particular temperature, so that quantum tunnelling may become important.

The structure of this chapter is as follows. In section 5.2 we review the two derivative BSFT action to studying the tachyon potential for coincident D(p-1)-$\overline{\text{D}}(p-1)$ system [111–117] and its extension to the case of finite separation. In section 5.3 we consider the 1-loop (annulus or cylinder) computations of the free energy of open strings stretched between separated D(p-1)-$\overline{\text{D}}(p-1)$ pair. In section 5.4 we then investigate the critical points of the free energy and determine the nature of the phase transitions as the temperature approaches the Hagedorn temperature from below. In particular we compare the situation when the Wilson line modulus A is greater than or less than its critical value $A_{crit} = \frac{1}{\sqrt{2\alpha'}}$. Finally in section 5.5 we draw some conclusions from our results.

5.2 BSFT action for the D-anti-D brane pair

In string theory a pair of parallel Dp-$\overline{\text{Dp}}$ pair constitutes an unstable object. To study the dynamics of unstable D-branes, the BSFT [111–117] is a useful tool and it has provided a good understanding of tachyon condensation at the classical level. It describes the off-shell dynamics of open strings in a fixed on-shell background of closed strings in which an open string field configuration corresponds to a boundary term in the world-sheet action of the string. Therefore, specifying a boundary term means giving the background values of the various modes of the open string.

The BSFT action of a single D9-$\overline{\text{D9}}$ brane pair was derived in [118, 119]. In the case of vanishing gauge fields and linear tachyon profile, it is given by

$$S = 2T_9 \int d^{10}X \, e^{-2\pi\alpha' T\bar{T}} F(4\pi\alpha'^2 \partial_\mu T \partial^\mu \bar{T}) \tag{5.1}$$

where

$$F(x) = \frac{4^x x \Gamma(x)^2}{2\Gamma(2x)} \tag{5.2}$$

As it is explained in [118, 119], the previous action is ambiguous in the sense that any term with at least second derivatives action on T can be added. However, at quadratic order the result is unambiguous:

$$S \sim 2T_9 \int d^{10}x \, e^{-2\pi\alpha' T\bar{T}} \left[1 + 8\pi\alpha'^2 \ln(2) \, \partial^\mu \bar{T} \partial_\mu T + \ldots\right] \tag{5.3}$$

where the expansion

$$F(x) = 1 + 2\ln(2)\, x + \mathcal{O}(x^2), \quad x \to 0 \tag{5.4}$$

has been used. Now, consider the case where one of the spatial directions, y, is wrapped on a circle of radius $\tilde{R} \leq \sqrt{\alpha'}$ and that we have a constant Wilson line A wrapping the compact direction on say the D9-brane. Since the gauge field strength vanishes, the only dependence on the gauge field comes from the covariant derivative of the tachyon. We can lift the expression in (5.3) by simply changing the argument of the function F to include the covariant derivative.
Applying a T-duality transformation along y, the gauge field is mapped to the Higgs field which measures the distance d between a D8-$\overline{\text{D8}}$ pair, separated along the dual coordinate $\tilde{y}$ with $d \sim |A|$.

Adopting the normalization of the tachyon field used in [108], the action (5.3) becomes

$$S = 2T_9 \int d^9x\, dy\, e^{-|T|^2} \left[1 + 2\alpha' |\partial_\mu T|^2 + 2\alpha' A^2 |T|^2\right] \tag{5.5}$$

The potential term is

$$V_0(T) = 2T_9\, e^{-|T|^2} \left[1 + 2\alpha' A^2 |T|^2\right] \tag{5.6}$$

The extrema are

$$|T| = 0, \quad |T| = +\infty, \quad \text{and} \quad |T| = \frac{\sqrt{2A^2\alpha' - 1}}{\sqrt{2\alpha'} A} \tag{5.7}$$

To study the nature of these extrema, we need to compute the second derivative: around $|T| = 0$ we have

$$\frac{\partial^2 V_0(T)}{\partial^2 |T|}|_{|T|=0} = m^2 = 4T_9 \left(2\alpha' A^2 - 1\right) \ . \tag{5.8}$$

Therefore, we see that this potential has a minimum at $|T| = 0$ if $A > \sqrt{\frac{1}{2\alpha'}}$ or it has a true tachyonic instability if $A < \sqrt{\frac{1}{2\alpha'}}$. Figure 5.1 shows the different cases.
This behavior has a clear physical interpretation: recall that our model is equivalent to the case of a parallel D8-$\overline{\text{D8}}$ pair separated by a distance d. If the distance d is "large enough", then the tachyon mode between the two should go away, since the tachyon field comes from the open string suspended between the two branes and thus that string acquires a mass lift when two branes are distant.
Notice also that in order to get a canonical kinetic term in the BSFT action we must

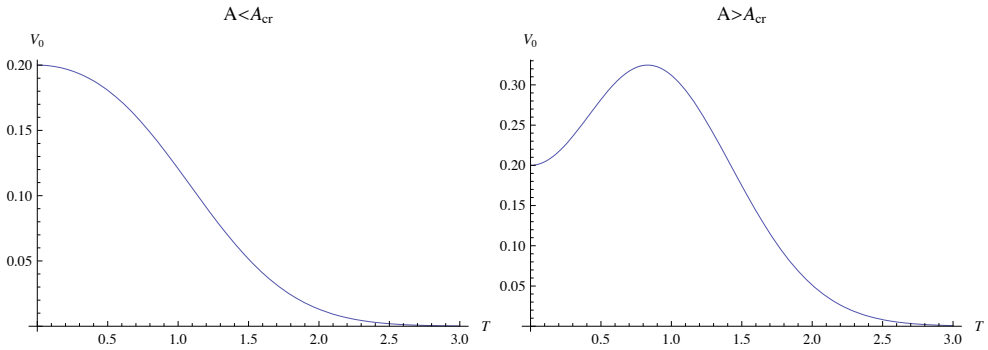

Figure 5.1: Left: Tachyon potential for $0 \leq A < A_{cr}$. Right: $A > \frac{1}{\sqrt{2\alpha'}}$. In all the plots $T_9 = 0.1$, $\alpha' = 1/2$.

perform the following redefinition of the tachyon field: $T = T(\phi)$ with

$$\phi = \sqrt{8\alpha' T_9} \int_0^{|T|} ds\, e^{-s^2/2} \tag{5.9}$$

With this redefinition, the action (5.5) becomes

$$S = \int d^9x\, dy\, \left(\frac{1}{2}(\partial\phi)^2 + V_0(T(\phi)) \right) \tag{5.10}$$

and the tachyon vacuum at infinity is placed at a finite value of the new field ϕ. Indeed, the two local minima are

$$\phi_0 = 0\,, \quad \phi_1 = \sqrt{4\pi\alpha' T_9}. \tag{5.11}$$

This redefinition allows us to compute the mass of the tachyon. In the presence of a Wilson line A it is given by

$$M^2 = \frac{\partial^2 V(\phi)}{\partial\phi^2} = \frac{1}{\alpha'} \left[\frac{|T|^2 - 1}{2} + \alpha' A^2 \left(|T|^4 - 4|T|^2 + 1 \right) \right] \tag{5.12}$$

whereas if $A = 0$ we have

$$M^2_{A=0} = \frac{1}{\alpha'} \frac{|T|^2 - 1}{2} \tag{5.13}$$

Notice that the same results were found in [120] but with different methods.
Henceforth, we will consider only the real part of the tachyon field: this is consistent with the tachyon equations of motion and it is also a natural setup since we are not interested in lower dimensional D-brane left after the tachyon condensation which

needs complex tachyon configurations.

5.3 Free energy of open strings in between a D-anti-D brane pair

Before we discuss the free energy of strings stretched between a Dp-$\overline{\text{Dp}}$ pair, let us first comment on the issue, raised by Hotta in [106], concerning the microcanonical ensemble versus the canonical ensemble framework for the computation of the tachyon finite temperature potential. It was shown in [106] that whilst in principle, the microcanonical picture is more trustworthy as we approach the Hagedorn temperature, in fact for the case of a coincident D9-$\overline{\text{D9}}$ pair, the micro and canonical ensembles agree in the nature and existence of the second order phase transition of the tachyon effective potential near the origin. For the case p $<$ 9 the case is less clear as the predictions for phase transitions do not entirely overlap for the various values of 'p' in the two formalisms. In this case it is better to adopt the microcanonical ensemble as in [106, 107].

Since we wish to consider the case where we turn on constant Wilson lines around a compact spatial S^1 in the Dp-$\overline{\text{Dp}}$ system, we should consider how this affects the predictions made in both frameworks. In fact in all cases, the additional terms in the free energy (the singular part of which is used in [106, 107] to extract the density of states in the microcanonical ensemble) coming from the Wilson line A can be computed. As we shall see below, the Wilson line only appears as an effective shift in the tachyon mass term when one considers the sums over all states contributing to the 1-loop partition. As such one can verify that at least in the p = 9 case, the canonical and microcanonical formalism will agree with respect to the nature of the phase transitions in the tachyon effective potential even with $A \neq 0$. For p $<$ 9 and $A \neq 0$ one should again adopt the microcanonical ensemble too. It is straightforward to extend the techniques and results in [106] to include A but for brevity we will simply use the canonical ensemble in this paper, in which the one-loop part of the tachyon effective potential is given by the free energy of open strings.

Thus we will primarily focus on the p = 9 case and do all computations in the canonical ensemble. By T-duality this is equivalent to separated D8-$\overline{\text{D8}}$ pair with separation $d \sim A$. It is interesting to see whether the finite temperature could drastically modify the tachyon potential: in the case of zero Wilson line this is motivated by the fact that the tachyon field at $T = 0$ can become stable and there is no tachyon condensation [105, 106]. In the presence of a brane separation, we might also be

interested in the fate of the metastable minimum at $T = 0$ (see Figure 5.1).

Temperature corrections to the potential (5.6) come from the evaluation of the path integral for the $\mathrm{D}\overline{\mathrm{D}}$ system over all connected graphs of strings on the space where the Euclidean time direction is compactified on a circle of radius β proportional to the inverse of the temperature. We will consider the weak coupling approximation in which the strings can be thought as an ideal gas, that is to say, ignoring the interactions of open strings. We take into account only one-loop amplitude by considering only zero-genus oriented Riemann surfaces.

Let us first quickly review the situation for a coincident Dp-$\overline{\mathrm{Dp}}$ pair (though following our discussion above we will ultimately focus on the case p = 9). The effective potential at finite temperature is given by

$$V_{eff}(T, \beta) = V_0(T) + V_1(T, \beta) \tag{5.14}$$

where $V_1(T, \beta)$ is the one-loop finite temperature potential. Since we work in the canonical ensemble the one-loop part of the effective potential above is related to the free energy $F(T, \beta)$ of open strings:

$$V_{eff}(T, \beta) = V_0(T) + \mathcal{V}^{-1} F(T, \beta) \tag{5.15}$$

where $\mathcal{V}$ is the volume of the system, the Dp-$\overline{\mathrm{Dp}}$ pair in our case.

At this point, one immediately faces difficulties: in order to compute $V_1(T, \beta)$ or F, we need to include quantum corrections to the BSFT. Since at tree level the BSFT action is essentially given by the partition function on the disk, at one loop one might expect that the first loop correction corresponds to the partition function on a world-sheet of cylinder or annulus topology. However, because the boundary interactions break conformal invariance this result would depend on the choice of the Weyl factor. Nevertheless, there have been several attempts to generalize the BSFT to the one-loop amplitude in the Dp-$\overline{\mathrm{Dp}}$ system [121–126]. In [127], for example, the partition function on the annulus and cylinder were computed in the presence of a constant tachyon profile. To fix the problems coming from the breaking of conformal invariance, they proposed to use a comparison with field theory results [128–130]. Indeed, given the partition function, one can in principle extract the contribution due to the tachyon and fix the background by comparison with the corresponding field theory results computed from the tree level effective action. This leads to equivalent expressions for the partition functions computed for the annulus and cylinder. The

one-loop amplitude on the cylinder in such background is given by

$$Z_1 = -\frac{16\, i\, \pi^4 \mathcal{V}_p}{(2\pi\alpha')^{\frac{p}{2}}} \qquad \int_0^\infty \frac{d\tau}{\tau}\, (4\pi\tau)^{-\frac{p+1}{2}}\, e^{-2\pi T^2 \tau} \times \left[\left(\frac{\theta_3(0|i\tau)}{\theta_1'(0|i\tau)} \right)^4 - \left(\frac{\theta_2(0|i\tau)}{\theta_1'(0|i\tau)} \right)^4 \right] \tag{5.16}$$

where $\mathcal{V}_p$ is the volume of the Dp-brane. In [106], it was noted that the previous one-loop amplitude (5.16) can be obtained by considering the free energy of strings stretching between the coincident Dp-$\overline{\text{Dp}}$ pair[1]

$$\begin{aligned} F(\beta) &= -\frac{\mathcal{V}_p}{(2\pi\alpha')^{\frac{p+1}{2}}} \int_0^\infty \frac{d\tau}{\tau} (4\pi\tau)^{-\frac{p+1}{2}} \sum_{M_{NS}^2} \sum_{r=1}^{\infty} \exp\left(-2\pi\alpha' M_{NS}^2 \tau - \pi \frac{r^2\beta^2}{\beta_H^2 \tau} \right) \\ &+ \frac{\mathcal{V}_p}{(2\pi\alpha')^{\frac{p+1}{2}}} \int_0^\infty \frac{d\tau}{\tau} (4\pi\tau)^{-\frac{p+1}{2}} \sum_{M_R^2} \sum_{r=1}^{\infty} (-1)^r \exp\left(-2\pi\alpha' M_R^2 \tau - \pi \frac{r^2\beta^2}{\beta_H^2 \tau} \right) \end{aligned} \tag{5.17}$$

with the following mass spectrum

$$M_{NS}^2 = \frac{1}{\alpha'} \left(N_B + N_{NS} + \frac{T}{2}^2 - \frac{1}{2} \right) \tag{5.18}$$

$$M_R^2 = \frac{1}{\alpha'} \left(N_B + N_R + \frac{T}{2}^2 \right) \tag{5.19}$$

where M_{NS} and M_R are the masses of the Neveu-Schwarz and Ramond sectors, respectively, whereas N_B, N_{NS} and N_R are the oscillation modes of the bosons, Neveu-Schwarz fermion and Ramond fermions. Notice that the lowest mode of the NS sector (5.18) coincides with the mass of the tachyon field (5.13) of the coincident Dp-$\overline{\text{Dp}}$ pair.

This suggests a straightforward generalization of eqs. (5.18) and (5.19) to the case of separated D(p-1)-$\overline{\text{D}}(p-1)$. The only difference with the case described above is that in our model we have a constant Wilson line turned on on a circle of radius close to the string scale. Therefore, in general, we have to include quantized momenta in the direction parallel to the Dp-$\overline{\text{Dp}}$ system, and winding modes in the direction transverse to it. As for the presence of the Wilson line, notice that in the T-dual picture, the dependence on the constant Wilson line A in the tachyon mass (5.12) factorizes out, so we require that the lowest mode of the NS sector coincides with the tachyon mass. In the general case of D toroidal-compactified directions and d

[1] We adopt the following definition for the Hagedorn temperature $\beta_H^2 = 8\pi^2\alpha'$.

non-compact ones, the mass spectrum is given by [107]

$$M_{NS}^2 = \sum_{I=1}^{p-d}\left(\frac{m_I}{R_I}\right)^2 + \sum_{i=p-d+1}^{D}\left(\frac{n_i R_i}{\alpha'}\right)^2 + \frac{1}{\alpha'}\left(N_B + N_{NS} + \frac{T}{2}^2 - \frac{1}{2} + M_A^2\right) \quad (5.20)$$

$$M_R^2 = \sum_{I=1}^{p-d}\left(\frac{m_I}{R_I}\right)^2 + \sum_{i=p-d+1}^{D}\left(\frac{n_i R_i}{\alpha'}\right)^2 + \frac{1}{\alpha'}\left(N_B + N_R + \frac{T}{2}^2 + M_A^2\right) \quad (5.21)$$

where we have defined

$$M_A^2 = \alpha' A^2\left(T^4 - 4T^2 + 1\right) \quad (5.22)$$

Inserting these two expressions into eq. (5.17) and expressing the sums in terms of the θ-functions using the conventions of [106], the free energy can be written in the following way:

$$\begin{aligned} F(T,\beta) = & -\frac{16\pi^4\mathcal{V}_d}{(\beta_H)^{d+1}}\int_0^\infty \frac{d\tau}{\tau^{\frac{d+3}{2}}}\exp^{-\pi[T^2+2M_A^2]\tau}\prod_{I=1}^{p-d}\theta_3\left(0\middle|\frac{2i\alpha'\tau}{R_I^2}\right)\prod_{i=p-d+1}^{D}\theta_3\left(0\middle|\frac{2iR_i^2\tau}{\alpha'}\right) \\ & \times\left[\left(\frac{\theta_3(0|i\tau)}{\theta_1'(0|i\tau)}\right)^4\left(\theta_3\left(0\middle|\frac{i\beta^2}{\beta_H^2\tau}\right)-1\right)\right. \\ & \left.-\left(\frac{\theta_2(0|i\tau)}{\theta_1'(0|i\tau)}\right)^4\left(\theta_4\left(0\middle|\frac{i\beta^2}{\beta_H^2\tau}\right)-1\right)\right] \end{aligned} \quad (5.23)$$

where $\mathcal{V}_d$ is the volume in the non-compact directions parallel to the Dp-$\overline{\text{Dp}}$ system. This expression for the open string free energy will be our starting point in order to compute the phase transitions in the model under consideration.

5.4 Phase transitions at finite temperature

Given the explicit form of the effective potential in eq. (5.15), it is interesting to see whether temperature corrections could modify the tachyon potential. We expect that at high temperature the system is in a local minimum of the temperature-dependent part of eq. (5.15). Then, as the temperature decreases, a point will be reached at which a second order phase transition will occur. The critical temperature $\mathcal{T}_c$ for this to happen, as well as the relevant field space position T_c can be found by solving the following set of equations:

$$V'_{eff}(\mathcal{T}_c, T_c) = 0 \quad \text{and} \quad V''_{eff}(\mathcal{T}_c, T_c) = 0 \quad (5.24)$$

where V_{eff} is given in eq. (5.15), and the $'$ denotes d/dT_c.

In particular, in the case $A = 0$ we expect that temperature corrections should lead to an effective potential in which the location of the minimum has shifted away from infinity. The physical reason for this is that moving towards $T = 0$ can be thermodynamically favorable: it costs energy, but it also reduces the mass of the tachyon and therefore increases the entropy of the tachyon gas [105, 106]. We will show explicitly that for temperature near the Hagedorn temperature the minimum will be shifted all the way to $T = 0$, in which case the open string vacuum would be stable. In the presence of a separation, it is interesting to see whether as the temperature decreases the system will start rolling towards one or other of the zero temperature minima.

5.4.1 Low Temperature

As a warm up calculation and in order to check that our expression for the free energy of open strings in eq. (5.23), reproduces known results in the limit of small separation between the D(p-1)-$\overline{\text{D}}(p-1)$ pair (equivalently small A in the Dp-$\overline{\text{Dp}}$ T-dual system), let us study the low temperature approximation of eq. (5.23).
In [105, 106] it is shown that starting at zero temperature with the minimum of the potential at $T = \infty$, as the temperature increases the vacuum is shifted from $T = \infty$ to $T = 0$. In particular, it is shown that the position of the tachyon minimum, $T_{\min}$, moves almost linearly towards $T = 0$ as the temperature increases.

In this subsection we will recover this result in the more general background in which a Wilson line is present. In the large β limit, we can approximate the free energy (5.23) by the large τ contributions to the integral. In this limit the θ-functions become

$$\begin{aligned}
\theta_1'(0|i\tau) &\sim 2e^{-\frac{\pi\tau}{4}} \\
\theta_2(0|i\tau) &\sim 2e^{-\frac{\pi\tau}{4}} \\
\theta_3(0|i\tau) &\sim 1 + 2e^{-\pi\tau} \\
\theta_4(0|i\tau) &\sim 1 - 2e^{-\pi\tau}
\end{aligned}$$

Using the above expressions, the free energy becomes

$$F(T,\beta) \sim -\frac{16\pi^4\mathcal{V}_d}{\beta_H^{d+1}} \int_0^\infty d\tau\, \tau^{-\frac{d+3}{2}} \exp\left[-\pi\left(T^2 + 2\alpha' A^2\left(T^4 - 4T^2 + 1\right) - 1\right)\tau - \pi\frac{\beta^2}{\beta_H^2\tau}\right] \tag{5.25}$$

This integral can be rewritten in terms of the modified K-Bessel function as

$$F(T,\beta) = -4\mathcal{V}_d \left(\frac{\pi\sqrt{2f(T,A)-1}}{\beta_H \beta}\right)^{\frac{d+1}{2}} K_{\frac{d+1}{2}}\left(\frac{2\pi\sqrt{2f(T,A)-1}}{\beta_H}\beta\right) \tag{5.26}$$

where we defined

$$f(T,A) = \frac{T}{2}^2 + \alpha' A^2 \left(T^4 - 4T^2 + 1\right)$$

In the limit in which both T and β are very large the free energy becomes

$$F(T,\beta) \sim -\frac{2^{\frac{d}{2}}\pi^{\frac{d+1}{2}}\mathcal{V}_d}{\beta_H^{\frac{d}{2}}\beta^{\frac{d}{2}+1}} \exp\left(-\frac{2\pi\beta}{\beta_H}\sqrt{2f(T,A)}\right)\ f(T,A)^{\frac{d}{2}} \tag{5.27}$$

Inserting this expression in the effective potential (5.15) and minimizing it w.r.t. T leads to the following condition

$$T_{\min}^2 - \frac{2\pi\beta}{\beta_H}\sqrt{2f(T_{\min},A)} = 0 \tag{5.28}$$

In the case $A = 0$ we simply have $f(T, A = 0) = \frac{T}{2}^2$ and therefore we get:

$$T_{\min} = 2\pi\tfrac{\beta}{\beta_H}. \tag{5.29}$$

If $A \neq 0$, let's assume that its absolute value is $A < \frac{1}{\sqrt{2\alpha}}$: we are in the regime in which $T = 0$ is a maximum of the potential and the tachyon has negative mass near the origin. Then, if T is large but $(A^2\,T^2) \ll 1$, the minimum is found by requiring that

$$T_{\min}^2 - \frac{2\pi\beta\,T_{\min}}{\beta_H}\sqrt{1 + 2\alpha' A^2 T_{\min}^2} \sim 0$$

and by expanding the square root

$$T_{\min}^2 - \frac{2\pi\beta\,T_{\min}}{\beta_H}\left(1 + \alpha' A^2 T_{\min}^2 + \mathcal{O}(A^4\,T_{\min}^4)\right) \sim 0. \tag{5.30}$$

The solution of the previous equation is either $T_{\min} = 0$, which is not in the $T \gg 1$ approximation, or

$$T_{\pm\,,\min} = \frac{\beta_H \pm \sqrt{\beta_H^2 - 16\pi^2\alpha' A^2\beta^2}}{4\alpha' A^2\pi\beta} \tag{5.31}$$

Again here we assume that β is large, but $\beta\,A \ll 1$ thus the square root can be

expanded in terms of $(\beta^2\, A^2)$

$$\begin{aligned} T_- &= 2\pi\frac{\beta}{\beta_H} + 8\alpha' A^2\pi^3\frac{\beta^3}{\beta_H^3} + \mathcal{O}(\alpha'^2 A^4\,\frac{\beta^4}{\beta_H^4}) \\ T_+ &= \frac{\beta_H}{4\pi\alpha' A^2\beta} - \frac{2\pi\beta}{\beta_H} - \frac{8A^2\pi^3\beta^3}{\beta_H^3} + \mathcal{O}(\alpha'^2 A^4\,\frac{\beta^4}{\beta_H^4}) \end{aligned} \tag{5.32}$$

T_- is the solution we announced at the beginning of this section and it is in agreement with [105] and [106]. We see that, as the temperature increases, this minimum shifts almost linearly towards $T = 0$.[2]

The other solution T_+ has an opposite behaviour compared to the previous results, namely, the minimum increases as the temperature increases. In fact, we see that this solution violates the approximation we made, namely $A^2T^2 << 1$ and $\beta\, A \ll 1$. For example, for $A = 10^{-7}$ and $\beta \sim \mathcal{O}(10^3)$ we get $T_+ \sim 10^{11}$ which gives $A^2T^2 >> 1$.

At low temperature, no phase transition occurs regardless of the value of A. To see this, expand eq. (5.28) around large T, this time taking $A = \mathcal{O}(1)$. Then

$$\frac{\partial V_{eff}(T,\beta)}{\partial T} = 0 \to T^\star = \left(\frac{2}{\alpha'}\right)^{1/4} \frac{\sqrt{\pi\beta\,(1-4A^2\alpha')}}{\sqrt{A\left(\beta_H - 2\sqrt{2}A\beta\pi\sqrt{\alpha'}\right)}} \tag{5.33}$$

Computing the second derivative of the potential in this point, we have:

$$\frac{\partial^2 V_{eff}(T,\beta)}{\partial T^2}|_{T=T^\star} = 0 \to \beta_{cr} = -\frac{\beta_H}{2\sqrt{2\alpha'}\pi A} \tag{5.34}$$

which is negative and clearly indicates the absence of a second order phase transition at low temperature.

Finally, before moving on to consider the high temperature regime, notice that these results can also be found by considering the tachyon field alone, ignoring the contribution of all other open string modes to the free energy of the system [105]. The reason is that as long as the temperature is low compared to the Hagedorn temperature, the tachyon has the lowest mass and its contribution is dominant.
In this setup, the effective potential, e.g. of a D9-$\overline{\text{D9}}$ system is given by the sum of the zero temperature tachyon potential and the free energy of the brane-antibrane system at finite temperature $\mathcal{T} = \beta^{-1}$. The one-loop free energy density for the tachyonic

[2]Note that the coefficient of the linear term in β in eq. (5.31) differs from [106] due to the different normalization we adopted in eq. (5.23).

degree of freedom in $9+1$-dimensional space is given by

$$\mathcal{F}(T,\beta) = \frac{1}{\beta}\int \frac{d^9k}{(2\pi)^9}\log\left(1-e^{-\beta u_k}\right) \tag{5.35}$$

where $u_k = \sqrt{k^2+\tilde{M}_{NS}^2}$, and $\tilde{M}_{NS}$ is given by eq. (5.20) in which the bosonic degrees of freedom N_B and N_{NS} are set to zero. Expanding the logarithm and performing the integration one gets:

$$\mathcal{F}(T,\beta) = -\sum_{n=1}^{\infty}(\beta n)^5\pi^{-5}2^{-4}\tilde{M}_{NS}^5 K_5(n\beta\tilde{M}_{NS}) \tag{5.36}$$

where $K_5(z)$ is the modified Bessel function. At low temperature (large β) we keep only the first term in the previous sum, obtaining

$$\mathcal{F}(T,\beta) \sim -2(2\pi)^{-5}(\tilde{M}_{NS}/\beta)^5 K_5(\beta\tilde{M}_{NS}) \tag{5.37}$$

which agrees with the free energy eq. (5.27) after we expand it in the limit in which both T and β are very large.

5.4.2 High Temperature

We will now use the expression for the free energy eq. (5.23) in order to investigate the behavior of the model at high temperature, that is to say, at a temperature close to, but below, the Hagedorn temperature. As we discussed earlier in section 5.3, in this case the canonical ensemble is generally not reliable and we should adopt the microcanonical description in order to compute thermodynamical quantities. However, as we argued there, for the case of D9-$\overline{\text{D9}}$ pairs with constant Wilson line, the canonical ensemble agrees with the computations made in the microcanonical ensemble. Thus we will focus our attention on the D9-$\overline{\text{D9}}$ system with $A \neq 0$.

In contrast to the low temperature case discussed before, we now want to expand the integral in eq. (5.23) near $\tau = 0$. To facilitate this, it is convenient to introduce the variable

$$t = \frac{1}{\tau}$$

and consider the large t region expansion.
Using the modular transformation of θ functions and extracting the leading term in

the large t region near the Hagedorn singularity, we obtain from (5.23)

$$\begin{aligned} F(T,x) &\sim -\frac{\alpha'^{\,d-p+\frac{D}{2}}\mathcal{V}_d}{2^{\frac{D}{2}-2}\beta_H^{d+1}}\left(\frac{\prod_{I=1}^{p-d}R_I^2}{\prod_{i=p-d+1}^{D}R_i^2}\right)\times \\ &\int_\Lambda^\infty dt\, t^{\frac{D+d-9}{2}}\exp\left[-\frac{\pi\left(T^2+2M_A^2\right)}{t}-\pi\left(x^2-1\right)t\right]\times \\ &\prod_{I=1}^{p-d}\theta_3\left(0\middle|\frac{iR_I^2t}{2\alpha'}\right)\prod_{i=p-d+1}^{D}\theta_3\left(0\middle|\frac{i\alpha' t}{2R_i^2}\right) \end{aligned} \tag{5.38}$$

where Λ is a cutoff and we have defined $x=\frac{\beta}{\beta_H}$. In (5.38) we have in mind the case p = 9, $d=8$, $D=1$.

We are interested in the behaviour of the system at the origin of field space, namely near $T=0$, therefore, we expand the previous expression around this limit and we keep only the lower order terms. As shown in [107], the additional contributions from the quantized winding and momenta in (5.38) may modify the leading order Hagedorn singularity if the compactification radii are much bigger than the string scale. In the case where p = 9, d=8, D=1 there is only quantized momenta on the circle (since it necessarily lies in a direction parallel to the D9). If the radius of this circle is close to the string scale then as shown in [107] the Hagedorn singularity is dominant and the expression (5.38) becomes

$$\begin{aligned} F(T,x) &\sim -\frac{CV_p}{\beta_H}\int_\Lambda^\infty dt\exp\left[-\pi\left(x^2-1\right)t-\frac{2\alpha' A^2\pi}{t}\right]\times \\ &\times\left[t^{\frac{p-9}{2}}+-\pi\left(T^2+2\alpha' A^2\left(T^4-4T^2\right)\right)t^{\frac{p-11}{2}}\right] \end{aligned} \tag{5.39}$$

where we have replaced $p=d+D$ and defined

$$\begin{aligned} C &= \frac{\alpha'^{\,d-p+\frac{D}{2}}}{2^{\frac{D}{2}-2}\beta_H^d\prod_{i=p-d+1}^{D}R_i} \\ \mathcal{V}_p &= \mathcal{V}_d\prod_{I=1}^{p-d}R_I \end{aligned} \tag{5.40}$$

On the other hand the same will be true if we take the radius $R_1\leq\sqrt{\alpha'}$ and assume that the energy of our system is sufficient to excite the quantized momentum modes along the S^1. For the case p = 9, d=8, D=1 the latter condition means we may consider small R_1 and large t such that $R_1^2 t$ is still sufficiently large to allow us to

approximate $\theta_3\left(0\left|\frac{i\,R_1^2 t}{2\alpha'}\right.\right)$ by unity.

Under this assumption, we can expand the exponential containing A in the previous expression, as long as $A \sim \mathcal{O}(1)$. Keeping only the first two terms we find:

$$F(T,x) \sim -\frac{CV_p}{\beta_H}\int_\Lambda^\infty dt\, e^{-\pi(x^2-1)t}\left[t^{\frac{p-9}{2}} - \pi\left(2\alpha' A^2\left(T^4-4T^2+1\right)+T^2\right)t^{\frac{p-11}{2}}\right] \tag{5.41}$$

In the case in which p = 9 this integral can be easily done and the result is

$$F(T,x) \sim -\frac{CV_p}{\beta_H}\left[\frac{1}{\pi\left(x^2-1\right)} - \pi\left(2\alpha' A^2\left(T^4-4T^2+1\right)+T^2\right)\Gamma\left(0,\pi\left(x^2-1\right)\Lambda\right)\right] \tag{5.42}$$

We may fix the cutoff scale Λ by comparison with the free energy computed in the microcanonical ensemble with $A = 0$, [106]. In particular, if we set $\Lambda = (2\pi)^{-1}$, the two results agree. We have now all the ingredients to write the effective potential in eq. (5.15) for the D9-$\overline{\text{D9}}$ pair with constant Wilson line A, in order to study the phase transitions.

The critical temperature β_{cr} and the value of the tachyon T_{cr} at which the phase transition occurs can be found by finding the solutions of the equation:

$$\frac{\partial V_{eff}(T,\beta)}{\partial T} = V' = 0 \tag{5.43}$$

$$\frac{\partial^2 V_{eff}(T,\beta)}{\partial T^2} = V'' = 0 \tag{5.44}$$

We have:

$$\begin{aligned} V' &= T_9\, e^{-T^2} T\left(8A^2\alpha' - 4\left(2A^2\alpha' T^2+1\right)\right) + \\ &\quad \frac{C\pi}{\beta_H}\left(2\left(4T^3-8T\right)\alpha' A^2 + 2T\right)\Gamma\left(0,\pi\left(x^2-1\right)\Lambda\right) \end{aligned} \tag{5.45}$$

A clear critical point is $T_{cr} = 0$. Substituting this value in $V''_{eff} = 0$ gives the following condition

$$\Gamma\left(0,\pi\left(x_{cr}^2-1\right)\Lambda\right) = \frac{2\beta_H T_9\left(2A^2\alpha'-1\right)}{C\pi\left(8A^2\alpha'-1\right)} \tag{5.46}$$

This equation is important, because it allows us to compute an approximate expression for the critical temperature at the point $T_{cr} = 0$.[3] However, we note that

[3] The divergence in the rhs of eq.(5.46) coming from the vanishing of the denominator is only apparent since it is due to the truncation to the second order term in the expansion of eq. (5.39) around large t. The full expression of the free energy (5.39) is not divergent for any value of A.

whereas the lhs of eq. (5.46) is positive definite, the rhs is positive definite only when $0 \leq A \leq \frac{A_{cr}}{2}$ and $A > A_{cr}$. *Therefore there is no phase transition at* $T = 0$ *for* $\frac{A_{cr}}{2} \leq A \leq A_{cr}$.

When $0 \leq A \leq \frac{A_{cr}}{2}$ or $A > A_{cr}$ we can expand the gamma function in eq.(5.46) near $x = 1$ using the fact that

$$\Gamma(0,t) = -\gamma - \log t + \mathcal{O}(t)$$

and we find

$$\beta_{cr} \sim \beta_H \left[1 + \exp\left(-\frac{16}{\pi\, g_s}\frac{\left(2A^2\alpha' - 1\right)}{\left(8A^2\alpha' - 1\right)} - \gamma\right)\right]. \tag{5.47}$$

where we have set $\Lambda = \frac{1}{2\pi}$. For weak coupling, g_s needs to be small, therefore, the argument of the exponential in the previous equation is large and negative which means that the critical temperature is very close the the Hagedorn temperature. (The limit of $A \to 0$ of this expression gives the results that Hotta found in [106].) Let us try now to find other solutions for the system of equations (5.43) and (5.44). Isolating the gamma-function from the first equation and substituting it into the second one gives the following condition for the presence of critical points:

$$\frac{8e^{-T^2}T^2T_9\left(8\left(T^4 - 3T^2 + 3\right)\alpha'^2A^4 + 2\left(3T^2 - 4\right)\alpha'A^2 + 1\right)}{4\left(T^2 - 2\right)\alpha'A^2 + 1} = 0 \tag{5.48}$$

Except for the point $T_{cr} = 0$, [4] other possible solutions to the previous equation are

$$T_\pm^2 = \frac{12\alpha'^2A^4 - 3\alpha'A^2 \pm \alpha'\,A^2\sqrt{-48\alpha'^2A^4 - 8\alpha'A^2 + 1}}{8A^4\alpha'^2} \tag{5.49}$$

The argument of the square root is positive definite only for $0 < A < \frac{1}{2\sqrt{3\alpha'}}$, but for these values of A one can verify that $T_\pm^2$ is negative, giving an imaginary T.
We conclude then that there is only a second order phase transition at $T = 0$.

5.4.3 Phase Structure

In order to study and understand the phase transitions within a system consisting of a D9-$\overline{\text{D9}}$ -pair at high temperature, standard thermal field theory reasoning can be very useful: the minima of the effective potential at high temperature are located around those values of T which minimize the tachyon mass at zero temperature and

[4] The point $T = +\infty$ solves the equation (5.48) but it is out the range of our approximation, namely, we have expanded the free energy around $T = 0$.

hence increase the entropy of the tachyon gas.
Recall that the mass of the tachyon in the presence of a Wilson line was given in eq. (5.12) which we rewrite here for our convenience in terms of real T:

$$M^2 = \frac{\partial^2 V(\phi)}{\partial \phi^2} = \frac{1}{\alpha'}\left[\frac{T^2-1}{2} + \alpha' A^2\left(T^4 - 4T^2 + 1\right)\right] \tag{5.50}$$

The extrema of $M^2(T)$ above are given by

$$T_1 = 0 \tag{5.51}$$

and

$$T_2 = \pm\frac{\sqrt{8\alpha' A^2 - 1}}{2A\sqrt{\alpha'}} \tag{5.52}$$

The second derivative of eq. (5.50) evaluated at T_1 is $(1-8\alpha' A^2)/\alpha'$ which is positive for $A < \frac{1}{2}A_{cr}$. Therefore, for $A < \frac{1}{2}A_{cr}$ we expect that at high temperatures, $T = 0$ is a minimum of the effective potential. If instead $A > \frac{1}{2}A_{cr}$, the point $T = 0$ is a local maximum, the minimum being $T_2 \neq 0$.

We will now investigate the phase structure of our system in the 3 cases where $0 \leq A \leq \frac{1}{2}A_{cr}$, $\frac{A_{cr}}{2} < A < A_{cr}$ or $A > A_{cr}$ respectively.

$\mathbf{0 \leq A \leq \frac{1}{2}A_{cr}}$

In this case, we know that there is a phase transition at $T = 0$ which is also a minimum at high temperature. Referring to Figure 5.2, we find that:
1. When the temperature is slightly above to the critical temperature and close to the Hagedorn temperature, i.e. $x \sim 1$, we expect that the system will be at the minimum at $T = 0$. Therefore, for these temperatures and for $0 \leq A \leq \frac{1}{2}A_{cr}$ the open string vacuum is stable.
We also see in Figure 5.2 that $T = 0$ is actually a global minimum of the effective potential and the latter is negative around this point. To understand why this is the case, consider for example when $A = 0$. The zero temperature potential becomes $V_0|_{\{T=0,A=0\}} = 2T_9$ and the finite temperature contribution can be obtained from eq. (5.42)

$$F(0,x)|_{A=0} \sim -\frac{C\,V_9}{\pi\,\beta_H\,(x^2-1)} \tag{5.53}$$

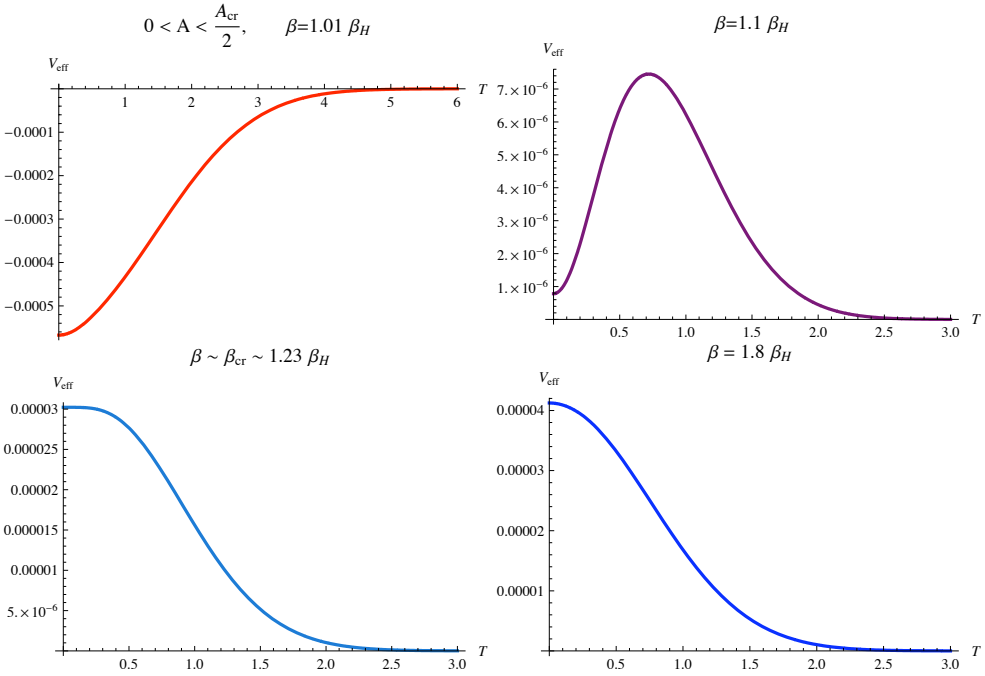

Figure 5.2: Phase Transition for temperatures close to the Hagedorn temperature and separation, $0 < A < \frac{A_{cr}}{2}$. The plots show the effective potential as derived from eq. (5.6) and eq. (5.38) using numerical integration, for various values of the temperature. We chose the values $A = 0.3\,A_{cr}$, $g_s = 0.1$, $\alpha' = 1/2$, $\Lambda = \frac{1}{2\pi}$, p = 9, $d = 8$, $D = 1$ in these plots.

At the critical temperature, this expression can be rewritten using eq. (5.47) as

$$F(0, x_{cr}) \sim -\frac{2C\,V_9}{\pi\beta_H}\exp\left(\frac{16}{\pi\,g_s} - \gamma\right) \tag{5.54}$$

At weak coupling, g_s is small and consequently the value of the free energy is much larger than the zero temperature piece, resulting in the effective potential becoming negative around $T = 0$.

2. When the temperature is equal to the critical temperature given by (5.46) the minimum at $T = 0$ becomes flat and is uplifted so that the potential energy becomes positive.

3. For temperatures lower than this critical temperature the point $T = 0$ is a global maximum and the tachyon field will start rolling towards $T = \infty$ and the system will undergo tachyon condensation.

Moreover, we find that the value of the critical temperature for a second order phase transition at the point $T = 0$ is proportional to the value of the Wilson line A:

the greater the value of A, the closer the critical temperature β_{cr} is to the Hagedorn temperature. It therefore requires more energy to produce a separated D8-$\overline{\text{D8}}$ than a coincident one.

$\frac{\mathbf{A_{cr}}}{\mathbf{2}} < \mathbf{A} < \mathbf{A_{cr}}$

In this case, we know from eq. (5.46) that there is no phase transition at $T = 0$, in fact there is no second order phase transition at all. At high temperatures, thermodynamic reasoning tells us that the system is in a global minimum of the effective potential which is located at $T^\star \sim T_2$ given in eq. (5.52) while the point $T = 0$ is a local maximum. Then, when the temperature decreases this minimum is uplifted and becomes shallower and shallower until it disappears at lower temperatures giving the zero temperature potential as the effective potential. (See Figure 5.3.)

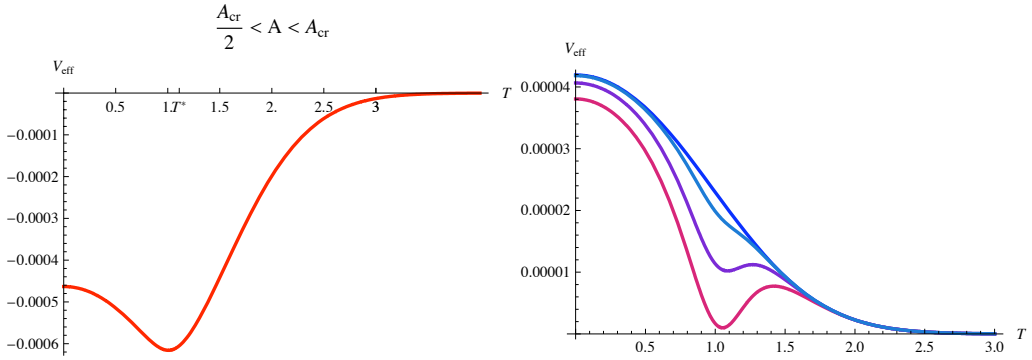

Figure 5.3: Phase Transition for temperatures close to the Hagedorn temperature and separation, $\frac{A_{cr}}{2} < A < A_{cr}$. The plots show the effective potential as derived from eq. (5.6) and eq. (5.38) using numerical integration, for various values of the temperature and for the choice $A = 0.7\,A_{cr}$, $g_s = 0.1$, $\alpha' = 1/2$, $\Lambda = \frac{1}{2\pi}$, p = 9, $d = 8$, $D = 1$. The temperatures are the following: in the left hand plot, $\beta = 1.01\,\beta_H$; In the right hand plot, $\beta = (1.2, 1.3, 1.6, 2.8)\,\beta_H$ for the sequence of curves displayed from left to right.

$\mathbf{A} > \mathbf{A_{cr}}$

In this case, referring to Figure 5.4 we find that:

1. At temperatures very close to the Hagedorn temperature, the system is in a global and deep minimum of the effective potential, say $T^\star$, which is not at the origin of the tachyon space. The point $T = 0$ is a local maximum at this temperature.

2. When the temperature approaches the critical temperature, given by eq. (5.46), the point $T = 0$ becomes flat and there is a second order phase transition in this

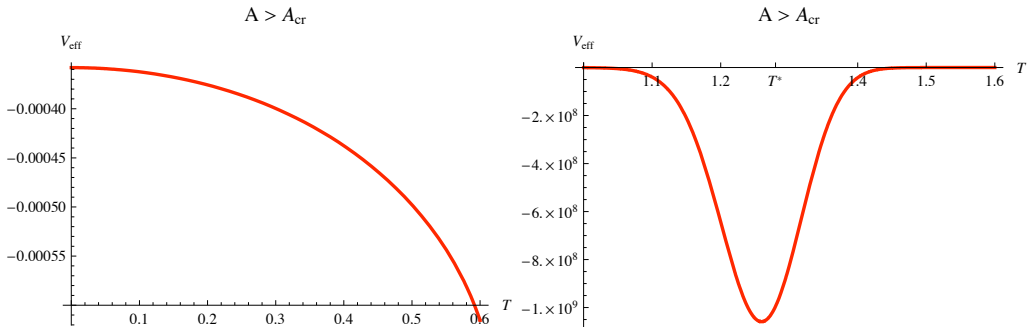

Figure 5.4: Phase Transition for temperatures close to the Hagedorn temperature and separation, $A > A_{cr}$. The plots show the effective potential as derived from eq. (5.6) and eq. (5.38) using numerical integration and the following parameters choices : $A = 1.1\, A_{cr}$, $g_s = 0.1$, $\alpha' = 1/2$, $\Lambda = 1/2\pi$, p = 9, $d = 8$, $D = 1$. The temperature is the same in both plots: $\beta = 1.01\, \beta_H$. The left plot is a zoom on the region of the effective potential close to $T = 0$ whereas the right one shows the deep minimum at $T = T^\star$.

point. (see left plot of Figure 5.5). However, the second minimum continues to exist and it is still deep.

3. For temperatures below this critical temperature, we have two minima $T = 0$ and $T = T^\star$. (See right plot of Figure 5.5). As the temperature continues to decrease the minimum $T^\star$ becomes shallow and eventually will disappear.

4. Eventually, close to zero temperature, the minimum $T^\star$ has disappeared and the system will undergo tachyon condensation.

From our findings, it seems unlikely that at zero temperature the system will be in the open string minimum $T = 0$ but rather in the closed string minimum at $T = \infty$. This is because, unless finite temperature tunneling effects happen between the two minima when the separation barrier is short, the system will likely find itself in the minimum $T = T^\star$ at high temperature and as the temperature decreases, this minimum will become shallower and the tachyon field will eventually undergo tachyon condensation in the closed string vacuum.

5.5 Conclusions

In this chapter we have investigated the phase structure of a Dp-$\overline{\text{Dp}}$ pair at finite temperature, including a constant Wilson line A wrapping a spatial circle S^1. By T-dualizing along the S^1, this system is mapped to a D(p-1)-$\overline{\text{D}}(p-1)$ pair where the branes are parallel but separated by a distance d along the dual circle S^1 with

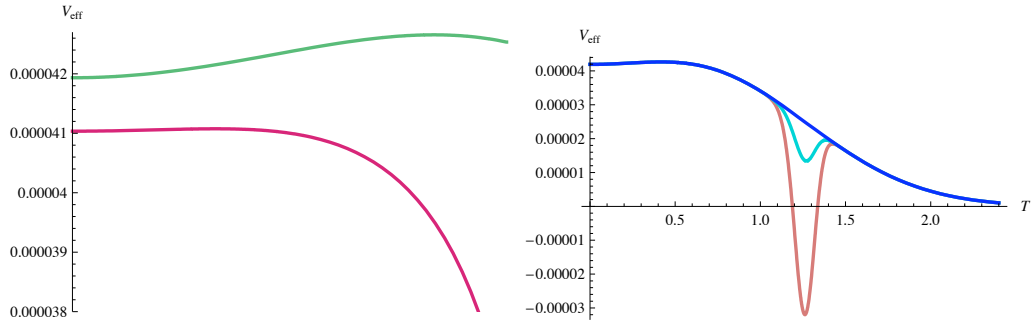

Figure 5.5: Phase transition for temperatures below the critical temperature and separation, $A > A_{cr}$. The plots show the effective potential as derived from eq. (5.6) and eq. (5.38) using numerical integration, with the following parameter choices: $A = 1.1\, A_{cr}$, $g_s = 0.1$, $\alpha' = 1/2$, $\Lambda = \frac{1}{2\pi}$, p = 9, $d = 8$, $D = 1$. The temperatures are the followings: in the left plots $\beta = (1.199,\, 2.4,\,)\beta_H$ for the lower and upper curves; in the right hand plot $\beta = (7.8,\, 8.0,\, 8.6)\,\beta_H$ for the three curves starting from the lower.

$d \sim |A|$. Due to the limitations of the canonical ensemble as we take the temperatures close to the Hagerdorn transition, our results are mainly focused on the p = 9 case. The extension to all other values of 'p' can be found by extending the microcanonical ensemble calculations of [106, 107] with the inclusion of a non-vanishing Wilson line A.

We found that the inclusion of A makes the effective potential acquire two minima at finite temperature if $A > A_{cr}$ compared to the situation with $A < A_{cr}$ (which includes the case $A = 0$ of coincident Dp-$\overline{\text{Dp}}$ branes studied in [105, 106]). This raised the question concerning which of the two minima our system is likely to be found. If we consider the case where we are at high temperatures, close to but below the Hagedorn temperature, then there is a single minimum with $T \neq 0$, indicating the open string vacuum is unstable. As the temperature drops a second order phase transition occurs at the origin $T = 0$ where a new minimum develops which one can interpret as a meta-stable open string vacuum. However unless there are very special initial conditions it is unlikely that the system can be found in this metastable state but rather the second minimum at $T \neq 0$. The latter coincides with the closed string vacuum $T \to \infty$ as the temperature approaches zero.

If instead, $A \leq A_{cr}$, then we showed that there is a phase transition in $T = 0$ only for $0 \leq A \leq \frac{A_{cr}}{2}$. In particular if this condition is satisfied, $T = 0$ is a global minimum of the effective potential which is negative at high temperature and the system of a D9-$\overline{\text{D9}}$ pair is stable. Then as the temperature decreases this minimum is uplifted

and a second order phase transition occurs.

Notice that in the dual picture, this implies that the separated D8-$\overline{\text{D8}}$ pairs undergo a phase transition, even in the case that the branes become coincident. This might appear at odds with the results of [106], where it was found that no phase transition occurred in a coincident Dp-$\overline{\text{Dp}}$ pair with p < 9. However, recall that in the dual system the D8-$\overline{\text{D8}}$ pair have one perpendicular spatial direction compactified on a circle, the branes span all non-compact directions. In [107], phase transitions for a Dp-$\overline{\text{Dp}}$ pair were considered when some spatial dimensions are compactified on a torus and it was shown that a phase transition will occur for a coincident Dp-$\overline{\text{Dp}}$ pair even with p < 9 as long as the branes span all the non-compact directions. Thus our results are consistent with those in [107].

For $\frac{A_{cr}}{2} < A \leq A_{cr}$ we showed that there is no phase transition near $T = 0$. At high temperature the system is in a minimum away from the origin. As the temperature decreases this minimum eventually disappears.

Our analysis in this paper is directed mainly at separated D8-$\overline{\text{D8}}$ pairs because of the limitations of the canonical ensemble for high temperatures. To properly study the case of separated Dp-$\overline{\text{Dp}}$ pairs with p ≤ 7 (where we assume separation along a single compact direction) will require use of the microcanonical ensemble and extension of the complex temperature techniques used in the case of coincident Dp-$\overline{\text{Dp}}$ pairs, considered in [106].

Finally, even if the D8-$\overline{\text{D8}}$ system were to find itself in the metastable minimum at $T = 0$ as the temperature decreases, one should then consider the possibility that quantum tunneling effects can lead to the nucleation of closed string vacua at $T \neq 0$. In the zero temperature case, [131] considered the possibility of tachyon tunnelling between the two minima of the effective potential when $A > A_{cr}$. It would be interesting to extend this analysis in the case of finite temperature since then the barrier height and width between the two minima becomes a function of temperature so that it is not a priori obvious if tunnelling effects will be suppressed or not.

Bibliography

[1] L. Anguelova and V. Calò, *O'KKLT at Finite Temperature*, *Nucl. Phys.* **B801** (2008) 45–69 [0708.4159].

[2] L. Anguelova and V. Calò, *Finite Temperature Behaviour of O'KKLT Model*, *Fortsch. Phys.* **56** (2008) 901–907 [0804.0770].

[3] L. Anguelova, V. Calò and M. Cicoli, *LARGE Volume String Compactifications at Finite Temperature*, *JCAP* **10** (2009) 025 [0904.0051].

[4] V. Calò and S. Thomas, *Phase Transitions in Separated D_{p-1} and anti-D_{p-1} Branes at Finite Temperature*, *JHEP* **06** (2008) 093 [0802.2453].

[5] P. Candelas, M. Lynker and R. Schimmrigk, *Calabi-Yau Manifolds in Weighted P(4)*, *Nucl. Phys.* **B341** (1990) 383–402.

[6] B. R. Greene and M. R. Plesser, *DUALITY IN CALABI-YAU MODULI SPACE*, *Nucl. Phys.* **B338** (1990) 15–37.

[7] A. Strominger and C. Vafa, *Microscopic Origin of the Bekenstein-Hawking Entropy*, *Phys. Lett.* **B379** (1996) 99–104 [hep-th/9601029].

[8] E. Witten, *Phases of $N = 2$ theories in two dimensions*, *Nucl. Phys.* **B403** (1993) 159–222 [hep-th/9301042].

[9] P. S. Aspinwall, B. R. Greene and D. R. Morrison, *Multiple mirror manifolds and topology change in string theory*, *Phys. Lett.* **B303** (1993) 249–259 [hep-th/9301043].

[10] A. Strominger, *Massless black holes and conifolds in string theory*, *Nucl. Phys.* **B451** (1995) 96–108 [hep-th/9504090].

[11] B. R. Greene, D. R. Morrison and A. Strominger, *Black hole condensation and the unification of string vacua*, *Nucl. Phys.* **B451** (1995) 109–120 [hep-th/9504145].

[12] J. M. Maldacena, *The large N limit of superconformal field theories and supergravity*, *Adv. Theor. Math. Phys.* **2** (1998) 231–252 [hep-th/9711200].

[13] M. Grana, *Flux compactifications in string theory: A comprehensive review*, *Phys. Rept.* **423** (2006) 91–158 [hep-th/0509003].

[14] M. R. Douglas and S. Kachru, *Flux compactification*, *Rev. Mod. Phys.* **79** (2007) 733–796 [hep-th/0610102].

[15] J. P. Conlon, *Moduli stabilisation and applications in IIB string theory*, *Fortsch. Phys.* **55** (2007) 287–422 [hep-th/0611039].

[16] M. Cicoli, *String Loop Moduli Stabilisation and Cosmology in IIB Flux Compactifications*, 0907.0665.

[17] A. Sen, *Tachyon dynamics in open string theory*, *Int. J. Mod. Phys.* **A20** (2005) 5513–5656 [hep-th/0410103].

[18] E. Fischbach and C. Talmadge, *Ten years of the fifth force*, hep-ph/9606249.

[19] O. Bertolami, J. Paramos and S. G. Turyshev, *General theory of relativity: Will it survive the next decade?*, gr-qc/0602016.

[20] T. Kaluza, *On the Problem of Unity in Physics*, *Sitzungsber. Preuss. Akad. Wiss. Berlin (Math. Phys.)* **1921** (1921) 966–972.

[21] O. Klein, *Quantum theory and five-dimensional theory of relativity*, *Z. Phys.* **37** (1926) 895–906.

[22] S. Gukov, C. Vafa and E. Witten, *CFT's from Calabi-Yau four-folds*, *Nucl. Phys.* **B584** (2000) 69–108 [hep-th/9906070].

[23] K. Dasgupta, G. Rajesh and S. Sethi, *M theory, orientifolds and G-flux*, *JHEP* **08** (1999) 023 [hep-th/9908088].

[24] S. B. Giddings, S. Kachru and J. Polchinski, *Hierarchies from fluxes in string compactifications*, *Phys. Rev.* **D66** (2002) 106006 [hep-th/0105097].

[25] P. G. O. Freund and M. A. Rubin, *Dynamics of Dimensional Reduction*, *Phys. Lett.* **B97** (1980) 233–235.

[26] J. M. Maldacena and C. Nunez, *Supergravity description of field theories on curved manifolds and a no go theorem*, *Int.J.Mod.Phys.* **A16** (2001) 822–855 [hep-th/0007018].

[27] E. Witten, *Dimensional Reduction of Superstring Models*, *Phys. Lett.* **B155** (1985) 151.

[28] C. P. Burgess, A. Font and F. Quevedo, *Low-Energy Effective Action for the Superstring*, *Nucl. Phys.* **B272** (1986) 661.

[29] S. P. de Alwis, *On integrating out heavy fields in SUSY theories*, *Phys. Lett.* **B628** (2005) 183–187 [hep-th/0506267].

[30] J. P. Conlon, F. Quevedo and K. Suruliz, *Large-volume flux compactifications: Moduli spectrum and D3/D7 soft supersymmetry breaking*, *JHEP* **08** (2005) 007 [hep-th/0505076].

[31] K. Becker, M. Becker, M. Haack and J. Louis, *Supersymmetry breaking and alpha'-corrections to flux induced potentials*, *JHEP* **06** (2002) 060 [hep-th/0204254].

[32] M. Berg, M. Haack and E. Pajer, *Jumping Through Loops: On Soft Terms from Large Volume Compactifications*, *JHEP* **09** (2007) 031 [0704.0737].

[33] M. Cicoli, J. P. Conlon and F. Quevedo, *Systematics of String Loop Corrections in Type IIB Calabi- Yau Flux Compactifications*, *JHEP* **01** (2008) 052 [0708.1873].

[34] M. Berg, M. Haack and B. Kors, *On volume stabilization by quantum corrections*, *Phys. Rev. Lett.* **96** (2006) 021601 [hep-th/0508171].

[35] S. Kachru, R. Kallosh, A. Linde and S. P. Trivedi, *De Sitter vacua in string theory*, *Phys. Rev.* **D68** (2003) 046005 [hep-th/0301240].

[36] C. P. Burgess, R. Kallosh and F. Quevedo, *de Sitter string vacua from supersymmetric D-terms*, *JHEP* **10** (2003) 056 [hep-th/0309187].

[37] K. Choi, A. Falkowski, H. P. Nilles and M. Olechowski, *Soft supersymmetry breaking in KKLT flux compactification*, *Nucl. Phys.* **B718** (2005) 113–133 [hep-th/0503216].

[38] S. P. de Alwis, *Effective potentials for light moduli*, *Phys. Lett.* **B626** (2005) 223–229 [hep-th/0506266].

[39] A. Achucarro, B. de Carlos, J. A. Casas and L. Doplicher, *de Sitter vacua from uplifting D-terms in effective supergravities from realistic strings*, *JHEP* **06** (2006) 014 [hep-th/0601190].

[40] M. Haack, D. Krefl, D. Lust, A. Van Proeyen and M. Zagermann, *Gaugino condensates and D-terms from D7-branes*, *JHEP* **01** (2007) 078 [hep-th/0609211].

[41] K. Intriligator, N. Seiberg and D. Shih, *Dynamical SUSY breaking in meta-stable vacua*, *JHEP* **04** (2006) 021 [hep-th/0602239].

[42] E. Dudas, C. Papineau and S. Pokorski, *Moduli stabilization and uplifting with dynamically generated F-terms*, *JHEP* **02** (2007) 028 [hep-th/0610297].

[43] S. A. Abel and V. V. Khoze, *Metastable SUSY breaking within the standard model*, hep-ph/0701069.

[44] O. Aharony and N. Seiberg, *Naturalized and simplified gauge mediation*, *JHEP* **02** (2007) 054 [hep-ph/0612308].

[45] A. Amariti, L. Girardello and A. Mariotti, *Non-supersymmetric meta-stable vacua in SU(N) SQCD with adjoint matter*, *JHEP* **12** (2006) 058 [hep-th/0608063].

[46] A. Amariti, L. Girardello and A. Mariotti, *On meta-stable SQCD with adjoint matter and gauge mediation*, *Fortsch. Phys.* **55** (2007) 627–632 [hep-th/0701121].

[47] T. Banks, *Remodeling the pentagon after the events of 2/23/06*, hep-ph/0606313.

[48] C. Csaki, Y. Shirman and J. Terning, *A simple model of low-scale direct gauge mediation*, *JHEP* **05** (2007) 099 [hep-ph/0612241].

[49] M. Dine, J. L. Feng and E. Silverstein, *Retrofitting O'Raifeartaigh models with dynamical scales*, *Phys. Rev.* **D74** (2006) 095012 [hep-th/0608159].

[50] M. Dine and J. Mason, *Gauge mediation in metastable vacua*, *Phys. Rev.* **D77** (2008) 016005 [hep-ph/0611312].

[51] R. Kitano, H. Ooguri and Y. Ookouchi, *Direct mediation of meta-stable supersymmetry breaking*, *Phys. Rev.* **D75** (2007) 045022 [hep-ph/0612139].

[52] H. Murayama and Y. Nomura, *Gauge mediation simplified*, *Phys. Rev. Lett.* **98** (2007) 151803 [hep-ph/0612186].

[53] H. Ooguri and Y. Ookouchi, *Landscape of supersymmetry breaking vacua in geometrically realized gauge theories*, *Nucl. Phys.* **B755** (2006) 239–253 [hep-th/0606061].

[54] O. Lebedev, H. P. Nilles and M. Ratz, *de Sitter vacua from matter superpotentials*, *Phys. Lett.* **B636** (2006) 126–131 [hep-th/0603047].

[55] R. Kallosh and A. Linde, *Landscape, the scale of SUSY breaking, and inflation*, *JHEP* **12** (2004) 004 [hep-th/0411011].

[56] N. J. Craig, P. J. Fox and J. G. Wacker, *Reheating metastable O'Raifeartaigh models*, *Phys. Rev.* **D75** (2007) 085006 [hep-th/0611006].

[57] S. A. Abel, C.-S. Chu, J. Jaeckel and V. V. Khoze, *SUSY breaking by a metastable ground state: Why the early universe preferred the non-supersymmetric vacuum*, *JHEP* **01** (2007) 089 [hep-th/0610334].

[58] W. Fischler, V. Kaplunovsky, C. Krishnan, L. Mannelli and M. A. C. Torres, *Meta-Stable Supersymmetry Breaking in a Cooling Universe*, *JHEP* **03** (2007) 107 [hep-th/0611018].

[59] L. Anguelova, R. Ricci and S. Thomas, *Metastable SUSY breaking and supergravity at finite temperature*, *Phys. Rev.* **D77** (2008) 025036 [hep-th/0702168].

[60] C. Papineau, *Finite temperature behaviour of the ISS-uplifted KKLT model*, 0802.1861.

[61] R. Kallosh and A. Linde, *O'KKLT*, *JHEP* **02** (2007) 002 [hep-th/0611183].

[62] V. Balasubramanian, P. Berglund, J. P. Conlon and F. Quevedo, *Systematics of moduli stabilisation in Calabi-Yau flux compactifications*, *JHEP* **03** (2005) 007 [hep-th/0502058].

[63] L. Dolan and R. Jackiw, *Symmetry Behavior at Finite Temperature*, *Phys. Rev.* **D9** (1974) 3320–3341.

[64] R. Jackiw, *Functional evaluation of the effective potential*, *Phys. Rev.* **D9** (1974) 1686.

[65] P. Binetruy and M. K. Gaillard, *Temperature corrections, supersymmetric effective potential and inflation*, *Nucl. Phys.* **B254** (1985) 388.

[66] P. Binetruy and M. K. Gaillard, *Temperature corrections in the case of derivative interactions*, *Phys. Rev.* **D32** (1985) 931.

[67] K. Enqvist and J. Sirkka, *Chemical equilibrium in QCD gas in the early universe*, *Phys. Lett.* **B314** (1993) 298–302 [hep-ph/9304273].

[68] B. de Carlos, J. A. Casas, F. Quevedo and E. Roulet, *Model independent properties and cosmological implications of the dilaton and moduli sectors of 4-d strings*, *Phys. Lett.* **B318** (1993) 447–456 [hep-ph/9308325].

[69] D. H. Lyth and E. D. Stewart, *Cosmology with a TeV mass GUT Higgs*, *Phys. Rev. Lett.* **75** (1995) 201–204 [hep-ph/9502417].

[70] D. H. Lyth and E. D. Stewart, *Thermal inflation and the moduli problem*, *Phys. Rev.* **D53** (1996) 1784–1798 [hep-ph/9510204].

[71] B. S. Acharya, K. Bobkov, G. Kane, J. Shao and S. Watson, *Non-thermal Dark Matter and the Moduli Problem in String Frameworks*, *JHEP* **06** (2008) 064 [0804.0863].

[72] J. J. Heckman, A. Tavanfar and C. Vafa, *Cosmology of F-theory GUTs*, 0812.3155.

[73] T. Barreiro, B. de Carlos, E. J. Copeland and N. J. Nunes, *Moduli evolution in the presence of thermal corrections*, 0712.2394.

[74] Z. Chacko, M. A. Luty and E. Ponton, *Calculable dynamical supersymmetry breaking on deformed moduli spaces*, *JHEP* **12** (1998) 016 [hep-th/9810253].

[75] K. A. Intriligator and S. D. Thomas, *Dynamical Supersymmetry Breaking on Quantum Moduli Spaces*, *Nucl. Phys.* **B473** (1996) 121–142 [hep-th/9603158].

[76] K.-I. Izawa and T. Yanagida, *Dynamical Supersymmetry Breaking in Vector-like Gauge Theories*, *Prog. Theor. Phys.* **95** (1996) 829–830 [hep-th/9602180].

[77] J. J. Blanco-Pillado, R. Kallosh and A. D. Linde, *Supersymmetry and stability of flux vacua*, *JHEP* **05** (2006) 053 [hep-th/0511042].

[78] W. Buchmuller, K. Hamaguchi, O. Lebedev and M. Ratz, *Maximal temperature in flux compactifications*, *JCAP* **0501** (2005) 004 [hep-th/0411109].

[79] W. Buchmuller, K. Hamaguchi, O. Lebedev and M. Ratz, *Dilaton destabilization at high temperature*, *Nucl. Phys.* **B699** (2004) 292–308 [hep-th/0404168].

[80] R. Barbieri and S. Cecotti, *Radiative Corrections to the Effective Potential in N=1 Supergravity*, *Z. Phys.* **C17** (1983) 183.

[81] J. W. Burton, M. K. Gaillard and V. Jain, *Effective one loop scalar lagrangian in no scale supergravity models*, *Phys. Rev.* **D41** (1990) 3118–3148.

[82] M. K. Gaillard, A. Papadopoulos and D. M. Pierce, *A String inspired supergravity model at one loop*, *Phys. Rev.* **D45** (1992) 2057–2065.

[83] M. K. Gaillard and V. Jain, *Supergravity coupled to chiral matter at one loop*, *Phys. Rev.* **D49** (1994) 1951–1965 [hep-th/9308090].

[84] M. K. Gaillard, *Pauli-Villars regularization of supergravity coupled to chiral and Yang-Mills matter*, *Phys. Lett.* **B342** (1995) 125–131 [hep-th/9408149].

[85] M. K. Gaillard, V. Jain and K. Saririan, *Supergravity coupled to chiral and Yang-Mills matter at one loop*, *Phys. Lett.* **B387** (1996) 520–528 [hep-th/9606135].

[86] M. Srednicki and S. Theisen, *Supergravitational Radiative Corrections to the Gauge Hierarchy*, *Phys. Rev. Lett.* **54** (1985) 278.

[87] S. Weinberg, *Anthropic Bound on the Cosmological Constant*, *Phys. Rev. Lett.* **59** (1987) 2607.

[88] M. Tegmark and M. J. Rees, *Why is the CMB fluctuation level* 10^{-5}*?*, *Astrophys. J.* **499** (1998) 526–532 [astro-ph/9709058].

[89] S. M. Barr and A. Khan, *Anthropic tuning of the weak scale and of m(u)/m(d) in two-Higgs-doublet models*, *Phys. Rev.* **D76** (2007) 045002 [hep-ph/0703219].

[90] N. Arkani-Hamed, S. Dimopoulos and S. Kachru, *Predictive landscapes and new physics at a TeV*, hep-th/0501082.

[91] M. Cicoli, J. P. Conlon and F. Quevedo, *General Analysis of LARGE Volume Scenarios with String Loop Moduli Stabilisation*, 0805.1029.

[92] J. P. Conlon and F. Quevedo, *Astrophysical and Cosmological Implications of Large Volume String Compactifications*, *JCAP* **0708** (2007) 019 [0705.3460].

[93] A. Saltman and E. Silverstein, *The scaling of the no-scale potential and de Sitter model building*, *JHEP* **11** (2004) 066 [hep-th/0402135].

[94] R. Blumenhagen, S. Moster and E. Plauschinn, *Moduli Stabilisation versus Chirality for MSSM like Type IIB Orientifolds*, *JHEP* **01** (2008) 058 [0711.3389].

[95] R. Blumenhagen, V. Braun, T. W. Grimm and T. Weigand, *GUTs in Type IIB Orientifold Compactifications*, *Nucl. Phys.* **B815** (2009) 1–94 [0811.2936].

[96] A. Collinucci, M. Kreuzer, C. Mayrhofer and N.-O. Walliser, *Four-modulus 'Swiss Cheese' chiral models*, 0811.4599.

[97] M. Cicoli, C. P. Burgess and F. Quevedo, *Fibre Inflation: Observable Gravity Waves from IIB String Compactifications*, 0808.0691.

[98] J. P. Conlon, S. S. Abdussalam, F. Quevedo and K. Suruliz, *Soft SUSY breaking terms for chiral matter in IIB string compactifications*, *JHEP* **01** (2007) 032 [hep-th/0610129].

[99] J. I. Kapusta, *Finite Temperatue Field Theory*. Cambridge University Press, 1989.

[100] G. Weidenspointner and al., *An asymmetric distribution of positrons in the galactic disk revealed by gamma-rays*, 2008.

[101] J. P. Conlon, D. Cremades and F. Quevedo, *Kaehler potentials of chiral matter fields for Calabi-Yau string compactifications*, *JHEP* **01** (2007) 022 [hep-th/0609180].

[102] S. Kachru *et. al.*, *Towards inflation in string theory*, *JCAP* **0310** (2003) 013 [hep-th/0308055].

[103] L. McAllister and E. Silverstein, *String Cosmology: A Review*, *Gen. Rel. Grav.* **40** (2008) 565–605 [0710.2951].

[104] R. Kallosh, *On Inflation in String Theory*, *Lect. Notes Phys.* **738** (2008) 119–156 [hep-th/0702059].

[105] U. H. Danielsson, A. Guijosa and M. Kruczenski, *Brane-antibrane systems at finite temperature and the entropy of black branes*, *JHEP* **09** (2001) 011 [hep-th/0106201].

[106] K. Hotta, *Brane-antibrane systems at finite temperature and phase transition near the Hagedorn temperature*, *JHEP* **12** (2002) 072 [hep-th/0212063].

[107] K. Hotta, *Finite temperature systems of brane-antibrane on a torus*, *JHEP* **09** (2003) 002 [hep-th/0303236].

[108] K. Hashimoto, *Dynamical decay of brane-antibrane and dielectric brane*, *JHEP* **07** (2002) 035 [hep-th/0204203].

[109] W.-H. Huang, *Boundary string field theory approach to high temperature tachyon potential*, hep-th/0106002.

[110] A. Bagchi and A. Sen, *Tachyon Condensation on Separated Brane-Antibrane System*, arXiv:0801.3498 [hep-th].

[111] E. Witten, *On background independent open string field theory*, *Phys. Rev.* **D46** (1992) 5467–5473 [hep-th/9208027].

[112] E. Witten, *Some computations in background independent off-shell string theory*, *Phys. Rev.* **D47** (1993) 3405–3410 [hep-th/9210065].

[113] S. L. Shatashvili, *Comment on the background independent open string theory*, *Phys. Lett.* **B311** (1993) 83–86 [hep-th/9303143].

[114] A. Sen and B. Zwiebach, *Tachyon condensation in string field theory*, *JHEP* **03** (2000) 002 [hep-th/9912249].

[115] V. A. Kostelecky and S. Samuel, *On a Nonperturbative Vacuum for the Open Bosonic String*, *Nucl. Phys.* **B336** (1990) 263.

[116] N. Moeller and W. Taylor, *Level truncation and the tachyon in open bosonic string field theory*, *Nucl. Phys.* **B583** (2000) 105–144 [hep-th/0002237].

[117] W. Taylor, *A perturbative analysis of tachyon condensation*, *JHEP* **03** (2003) 029 [hep-th/0208149].

[118] P. Kraus and F. Larsen, *Boundary string field theory of the DD-bar system*, *Phys. Rev.* **D63** (2001) 106004 [hep-th/0012198].

[119] T. Takayanagi, S. Terashima and T. Uesugi, *Brane-antibrane action from boundary string field theory*, *JHEP* **03** (2001) 019 [hep-th/0012210].

[120] M. R. Garousi, *D-brane anti-D-brane effective action and brane interaction in open string channel*, *JHEP* **01** (2005) 029 [hep-th/0411222].

[121] T. Suyama, *Tachyon condensation and spectrum of strings on D- branes*, *Prog. Theor. Phys.* **106** (2001) 1017–1025 [hep-th/0102192].

[122] M. Alishahiha, *One-loop correction of the tachyon action in boundary superstring field theory*, *Phys. Lett.* **B510** (2001) 285–294 [hep-th/0104164].

[123] K. Bardakci and A. Konechny, *Tachyon condensation in boundary string field theory at one loop*, hep-th/0105098.

[124] B. Craps, P. Kraus and F. Larsen, *Loop corrected tachyon condensation*, *JHEP* **06** (2001) 062 [hep-th/0105227].

[125] G. Arutyunov, A. Pankiewicz and J. Stefanski, B., *Boundary superstring field theory annulus partition function in the presence of tachyons*, *JHEP* **06** (2001) 049 [hep-th/0105238].

[126] D. Nemeschansky and V. Yasnov, *Tachyon condensation at one loop*, hep-th/0408157.

[127] O. Andreev and T. Ott, *On one-loop approximation to tachyon potentials*, *Nucl. Phys.* **B627** (2002) 330–356 [hep-th/0109187].

[128] J. A. Minahan and B. Zwiebach, *Effective tachyon dynamics in superstring theory*, *JHEP* **03** (2001) 038 [hep-th/0009246].

[129] J. A. Minahan and B. Zwiebach, *Field theory models for tachyon and gauge field string dynamics*, *JHEP* **09** (2000) 029 [hep-th/0008231].

[130] A. A. Gerasimov and S. L. Shatashvili, *On exact tachyon potential in open string field theory*, *JHEP* **10** (2000) 034 [hep-th/0009103].

[131] M. R. Garousi and K. B. Fadafan, *Tachyon Tunnelling in D-brane-anti-D-brane*, *JHEP* **04** (2006) 005 [hep-th/0506055].